SYMPOSIUM ON RESEARCH RESULTS FROM THE 2007 SUMMER INSTITUTE ON ATMOSPHERIC, BIOSPHERIC, AND HYDROSPHERIC SCIENCES

Friday, August 17, 2007

Building 33, Conference Room A128

9:30a	Opening remarks -- Per Gloersen
9:45a	Neutral Particle Detection in Low Energy Levels -- Kaylan Orben, Kutztown University (Keith Oglivie/612.2, mentor)
10:00a	A Study of Rainfall Triggered Landslides on a Global Scale -- Stephanie Hill, Salisbury University (Yang Hong/ 613.1, mentor)
10:15a	The Effect of Aerosol on Stratocumulus Clouds in the Eastern-North Pacific -- Cody Fritz, University of Missouri (Eric Wilcox/613.2, mentor)
10:30a	An Examination of the Olympus Mons Aureoles -- Annie Griswold, Case Western Reserve University (Mark Bulmer/JCET (698), mentor)
10:45a	Retrieval of global aerosol and water properties: Validation and climatology from MODIS -- Natalia A. Rodriguez, Universidat de Puerto Rico (Rob Levy/ 613.2, mentor)
11:00a	Compiling a Climatology of Smoke Plume Injection Heights from Satellite Measurements -- Shawn Gindhart, Millersville University (Charles Ichoku/613.2, mentor)
11:15a	Aerosol Effects on Surface Insolation and Skin Temperatures -- Krista Romita, Vassar College (Menling Jin/ 613.2, & Lorraine Remer, mentors)
11:30a	Snow and ICESat: Techniques for Satellite-Based Snow Depth Measurement -- Rachel Mauk, Ohio State University. (Mike Jasinski and Jordan Borak/614.3, mentors)
11:45p	Using NASA Products to Help Improve Water Forecasting: : A study of Irrigated Alfalfa along the Middle Rio Grande -- Alvin Rentsch University of Louisville (David Toll, Kristi Arsenault, & Jiarui Dong/ 614.3, mentors)

12:00 LUNCH BREAK

01:00p	Comparison of GRACE Data with Modeled and In-Situ Data -- Erik Jensen, Pacific University (Matt Rodell/614.3, mentor)
01:15p	Hurricane Intensity and Ocean Vertical Structure -- Lisha Roubert, Universidat de Puerto Rico . (Paolo de Matthaeis/ 614.6, mentor)
01:30p	Modeled and Microwave Observations of Variation of Snow Depth on Greenland -- Ashley Welty, North Carolina State University.(Per Gloersen/614.1, mentor)
01:45p	ADJOURN

Neutral Particle Detection

Kaylan Orben, Kutztown University

Keith Ogilvie, NASA, GSFC

Michael Coplan, Patrick Hughes, University of Maryland

Goal:

- To identify surfaces that efficiently convert neutral particles to negative ions.

Application:

- The purpose of an efficient surface can apply to neutral atom imaging of plasma structures in space.

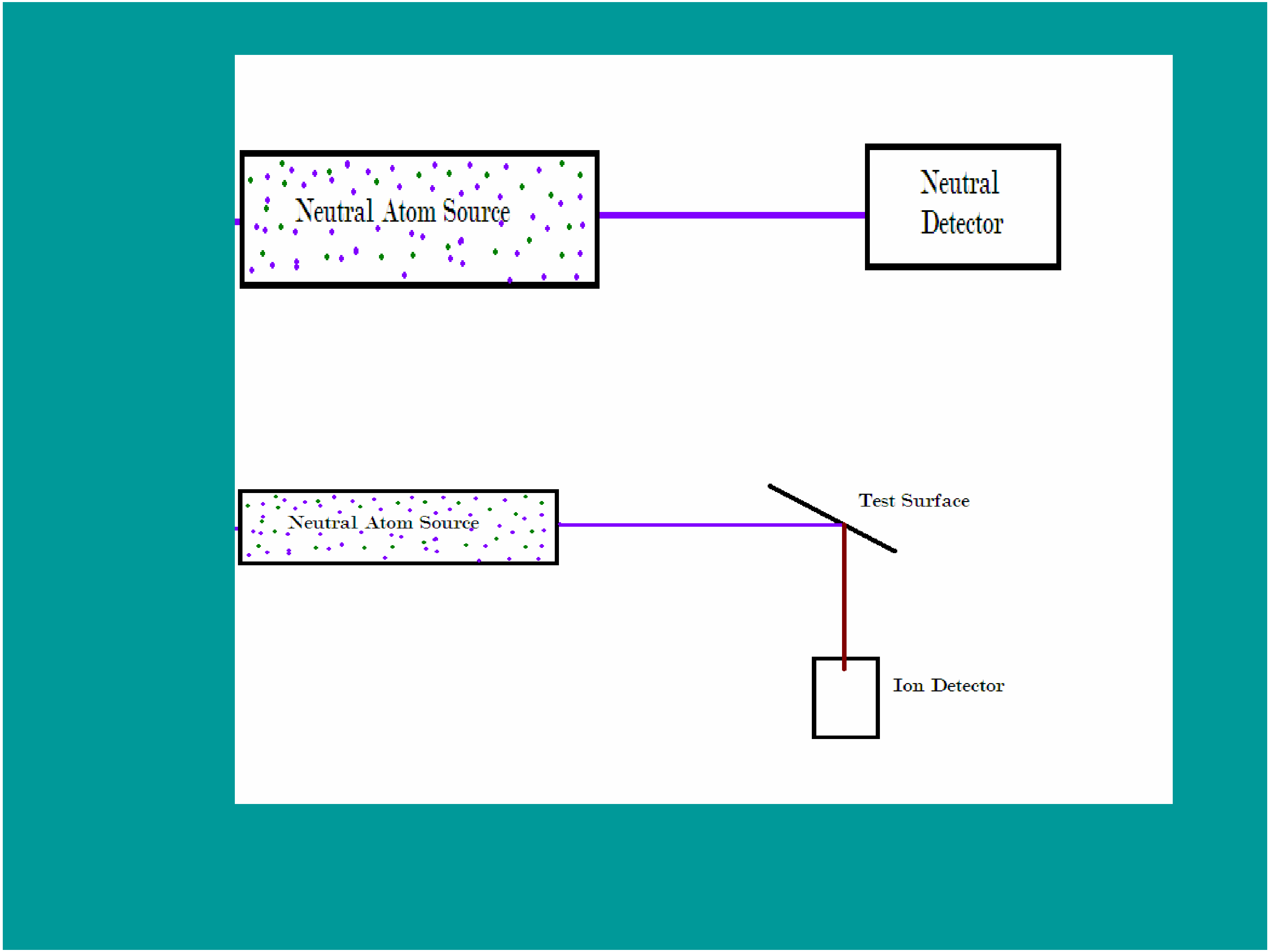
Neutral Atom Source
Neutral
Detector
Neutral Atom Source
Test Surface
Ion Detector

Efficiency Ratio:

$$\left[\frac{\text{Negative Ions From Surface}}{\text{Neutral Atoms Incident}}\right]$$

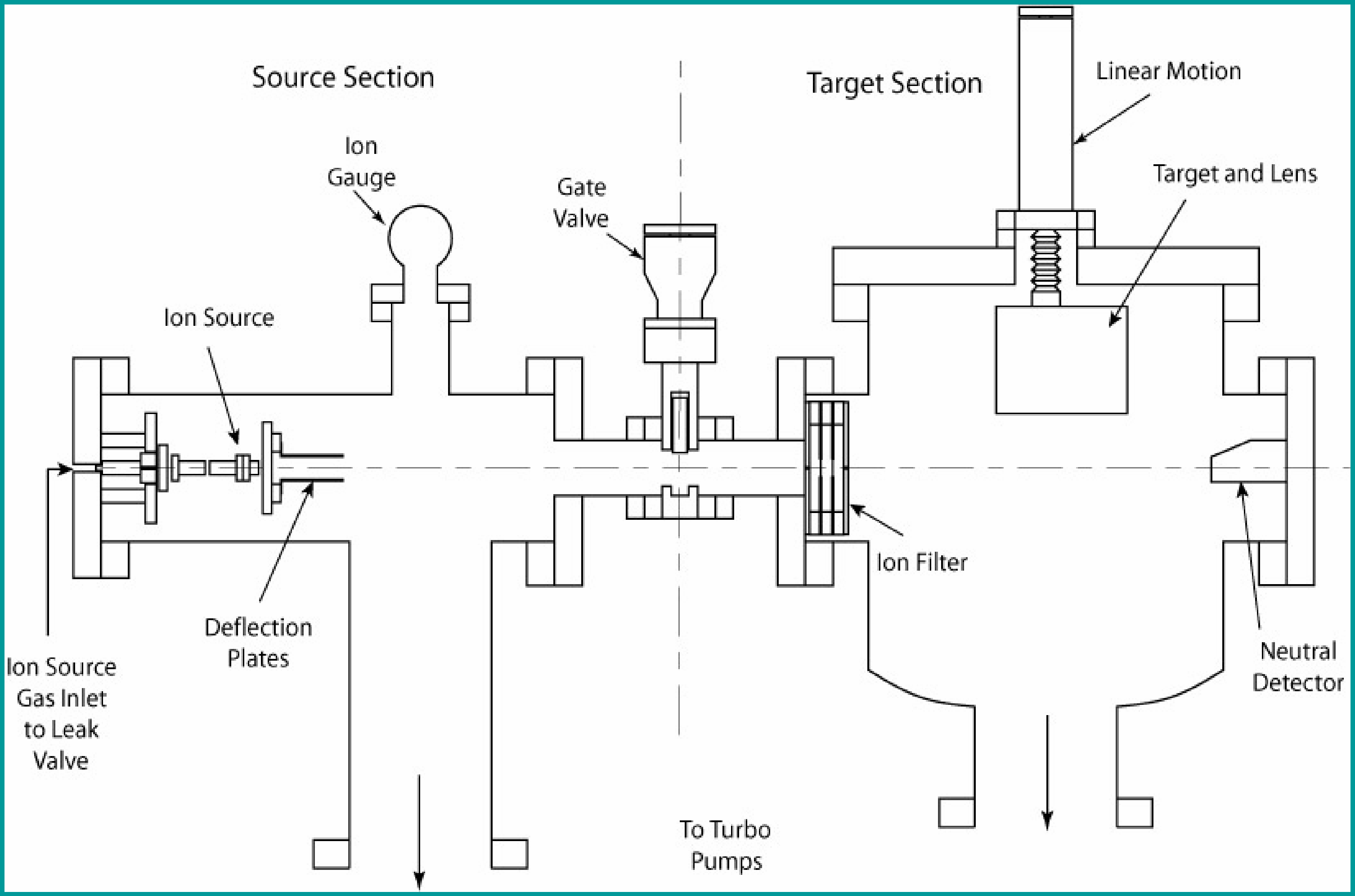
Source Section
Target Section
Linear Motion
Ion
Gauge
Gate
Valve
Target and Lens
Ion Source
Ion Filter
Deflection
Plates
Ion Source
Gas Inlet
to Leak
Valve
Neutral
Detector
To Turbo
Pumps

The Apparatus

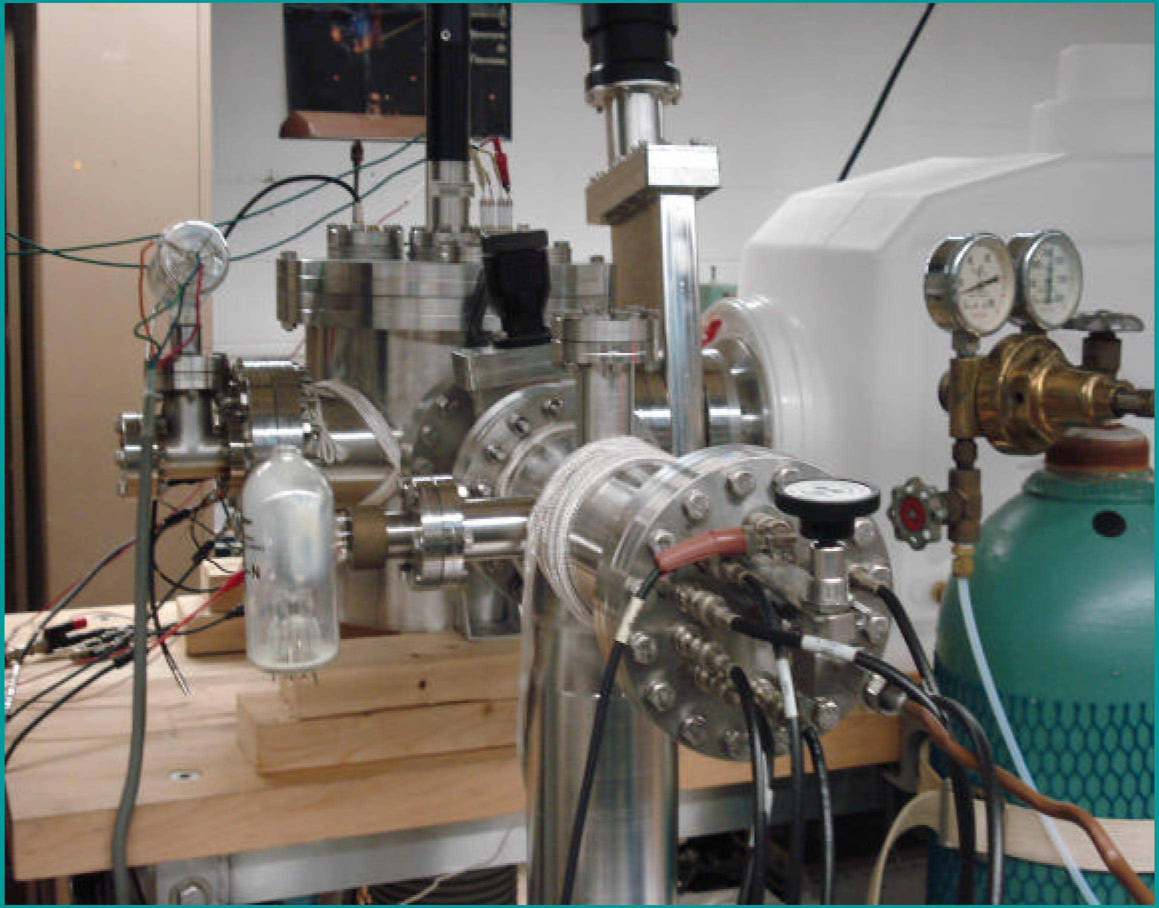

Improvements

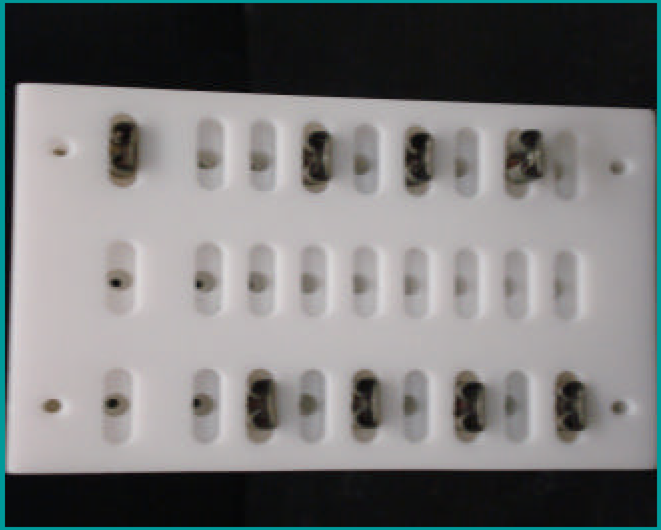

- To improve the design of the neutral ion detecting system, I designed a connector that increased the possible voltage

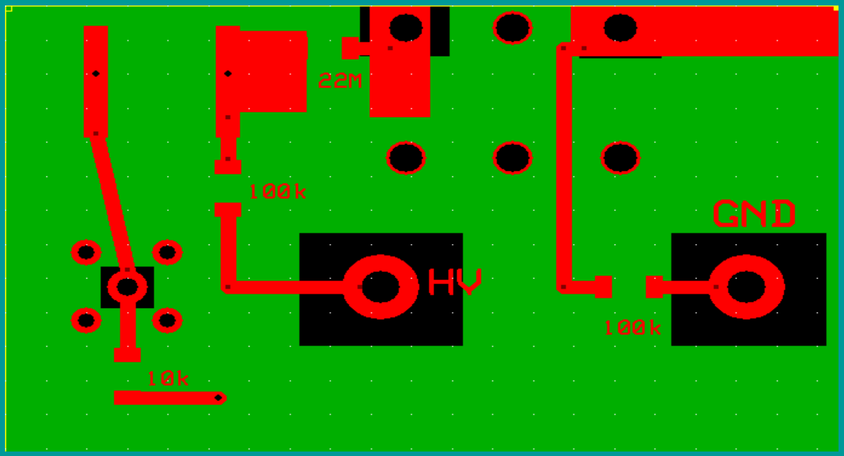

- I improved the circuit board that holds the channel electron multiplier, which detects the negative ions.
  - The circuit board provides a way to mount the detector
  - To provide the proper voltage to the apparatus,
  - To transport the signal to the electronics.
- To do this I had to learn about circuit board design and the different types of circuit board that exist.

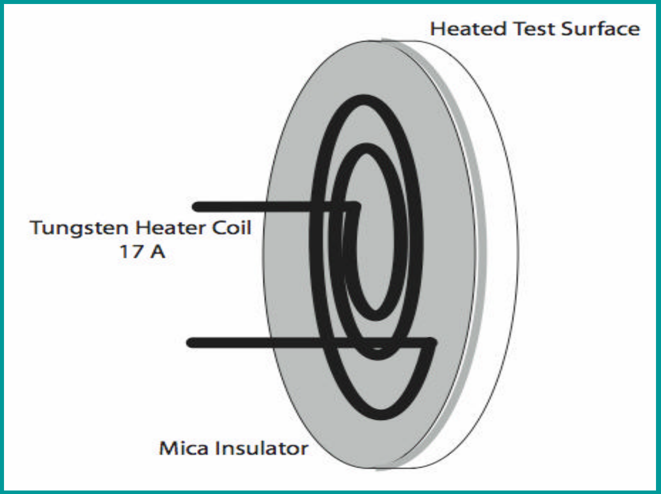

- Some of the samples are heated
- I helped to improve the heater assembly, which required the use of a CAD program.

Summary

- This summer I gained many skills including:
  - designing
  - mechanical
  - electric
  - minor machining
- I improved skills including:
  - analytical
  - precision
  - data collection

Acknowledgements

- Dr. Keith Ogilvie, NASA
- Dr. Michael Coplan, University of Maryland
- Patrick Hughes, University of Maryland
- Dr. Paul Quinn Sr., Kutztown University of Pennsylvania

A Study of Rainfall Triggered Landslides on a Global Scale

Stephanie Hill
Salisbury University
Graduate Student: Dalia Bach, Columbia University
Mentors: Bob Adler and Yang Hong
NASA Goddard Space Flight Center

Summer Research

- **Problem**:
- Landslides are one of the most widespread natural hazards on Earth, responsible for thousands of deaths and billions of dollars in property damage.

- In U.S. alone landslides can occur in any state, and they cause an estimated $2 billion in damages and 25–50 deaths each year (FEMA).

- Currently, no system exists at regional or global scale to **detect landslides triggered by heavy rainfall.**

- **Goals**:
- Compile a database of all 2003 global landslides
- Complete case studies for a better understanding of specific events
- Calculate and examine the Probability of Detection (POD) and susceptibility
- Compare 2003 events with algorithm predicted events for validation
- Compile a database for summer of 2007 global landslides and compare to algorithm predicted landslides

Prototyping: Global Flood Landslide Prediction System

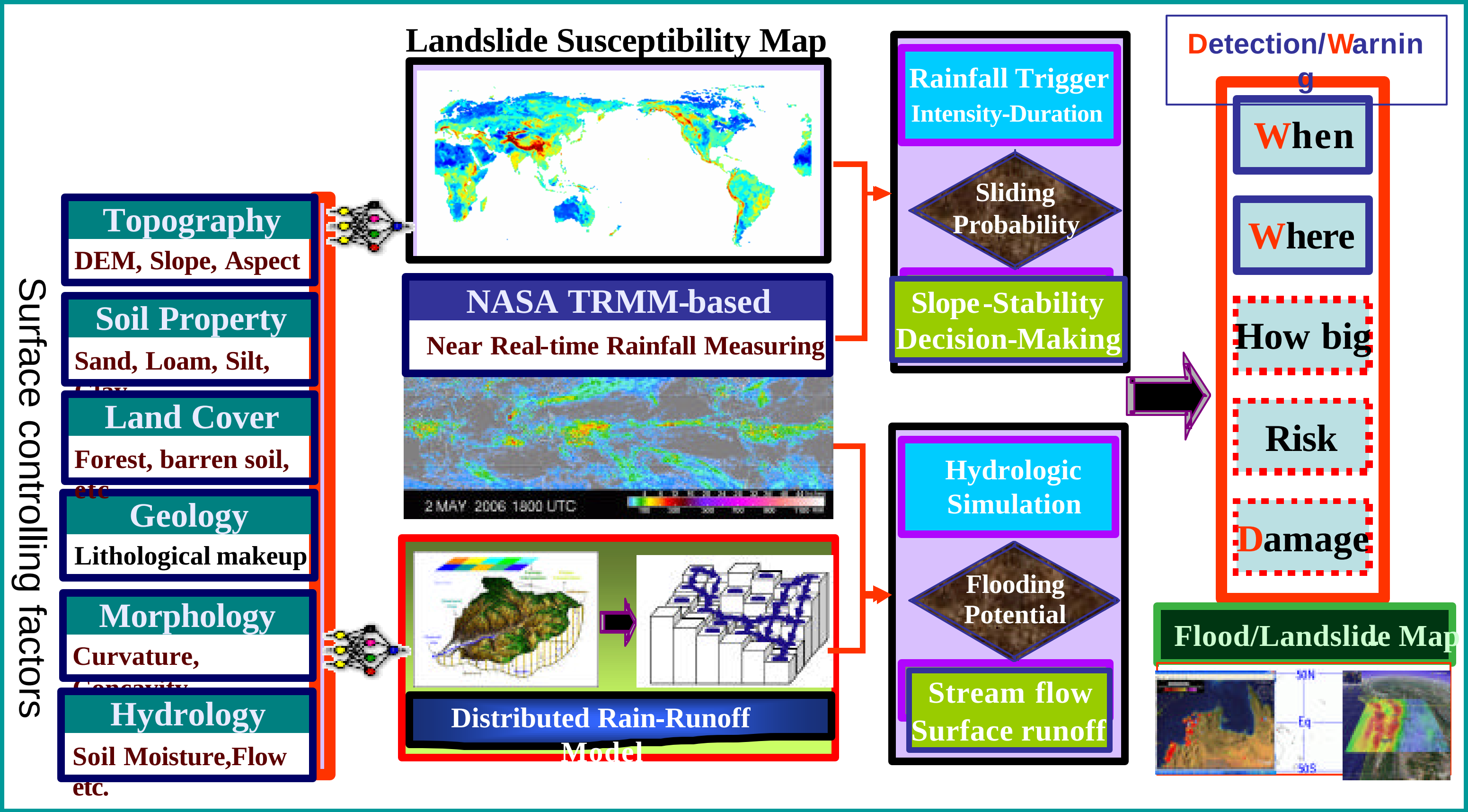

First-cut Experimental Global Flood Landslide Operational System

1. Landslide:
2. Flood:

Hong et al. (2006, 2007)

Huffman et al. (2007)

The Algorithm

- Takes into consideration:
  - Susceptibility of the landslide site (topography, soil properties, land cover)
  - the rainfall Intensity-Duration threshold equation
- Applications:
  - Used to create a global landslide susceptibility map
  - Predicting future landslide locations

Intensity-Duration Rainfall Thresholds Relationships at Different Spatial Scales

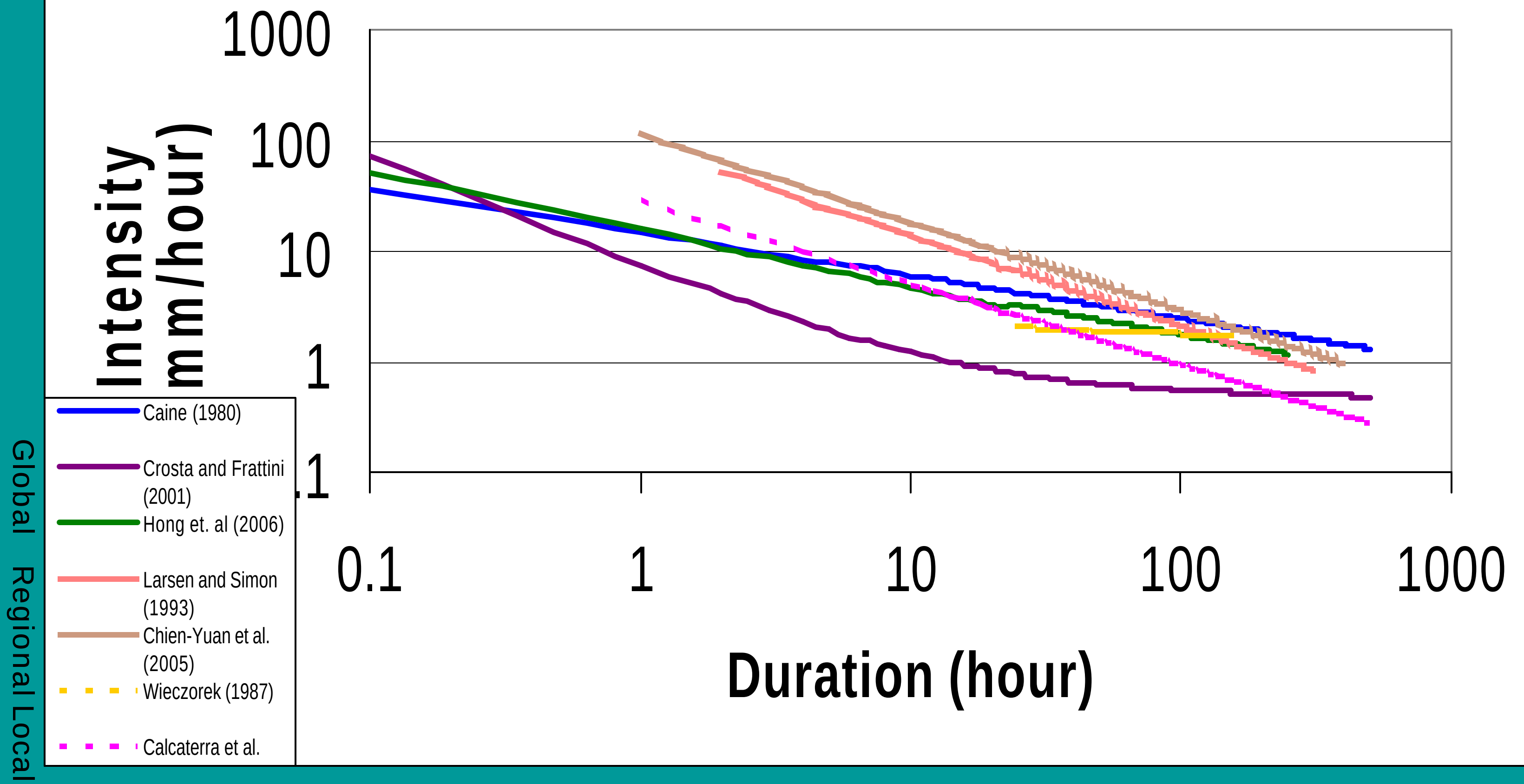

2003 Global Landslide Inventory

Microsoft Excel - TRMM sheet

P223 Is info

	ID	Month	Day	Year	other/to different date	Continent	Country	Location	Latitude	Longitude	Death toll	EM-DAT estimates (dead-affected)
174	173	9	19	2003		Europe	Ireland	Mayo County, Pollothomas	54.2235	-9.799565		
175	174	9	20	2003		S Asia	Nepal	Tehrathum	27.1167	87.5333	2	
176	175	9	20	2003		SE Asia	Indonesia	Lengkong hamlet, Pasir Buncir village, Caringin subdistrict	-6.5888	106.7918	5	
177	176	9	23	2003		E Asia	China	Liangjiagou, Shaanxi province	37.6308	109.9936	12	
178	177	9	24	2003		S Asia	India	Varunavat Parvat LS in Uttarkashi town, Uttaranchal Himalayas	30.7368	78.4380	affected 2000 and caused rupees 500 million rupees in damage	
179	178	9	26	2003		N America	USA	Georgetown, Denver	39.7061	-105.6969	1	
180	179	9	28	2003		E Asia	Philippines	Antipolo City	14.6000	121.1680	1	
181	180	10	1	2003		S Asia	Sri Lanka	Kudagala	6.2905	80.1782	1	
182	181	10	1	2003		S Asia	Sri Lanka	Elpitiya	6.2719	80.1987	2	
183	182	10	1	2003		S asia	Sri Lanka	Yakkalamulla	6.1124	80.3661	8	
184	183	10	1	2003		S Asia	India	Malad, N. Mumbai	19.1560	72.8000	3	
185	184	10	2	2003		E Asia	Malaysia	Ringlet, Cameron Highlands	4.4116	101.3844	1	
186	185	10	5	2003	6/10/2003	SE Asia	Indonesia	Tanjung Jabung Bar, Jambi, Sumatra	-1.6040	103.6060	5	
187	186	10	6	2003		Caribbean	Haiti	Port-au-Prince	18.5180	-72.3488	13	
188	187	10	6	2003		SE Asia	Malaysia	Bukit Besar, Kulim	5.9500	100.4167	2	
189	188	10	7	2003		S Asia	India	Vetaltekdi hill, near Chatuhshrungi, Pune	18.5381	73.8238	4	
190	189	10	7	2003		S Asia	India	West Bengal, Sewak Road connecting Sikkim to Darjeeling	27.1588	88.4920	17 dead, 8 missing	
191	190	10	7	2003		C. America	El Salvadore	Highway in Central El Salvadore	13.8414	-88.8491	1	
192	191	10	9	2003		SE Asia	Indonesia	Dawuhan village, Trenggalek district, East Java	-7.9108	112.5894	2	
193	192	10	10	2003		S Asia	India	Likhuvir, Kalimpong sub-division	27.0736	88.4778	1	
194	193	10	11	2003		E Asia	China	Near Yima City	34.72	111.86		
195	194	10	14	2003		SE Asia	Malaysia	Jalan Gunung Raya, Langkawi	6.3668	99.8167	1	
196	195	10	16	2003		E Asia	Vietnam	Quang Nam	15.6011	107.9658	1	
197	196	10	16	2003		S America	Brazil	Vila Cruzeiro slum, Rio	-22.8484	-43.2814	5	
198	197	10	17	2003		SE Asia	Indonesia	Semangkung village, Pejawaran district, Banjarnegara	-7.3833	109.6833	1	
199	198	10	18	2003		N America	Guam	Tamuning, Guam	13.4803	144.7760		
200	199	10	18	2003		N america	Washington	Road 112	48.2575	-124.3		

trmm rainfall mean / Read ME / Total_adjusted / Total merged list / ICL Events 2003

Ready NUM

2003 Global Landslide Locations

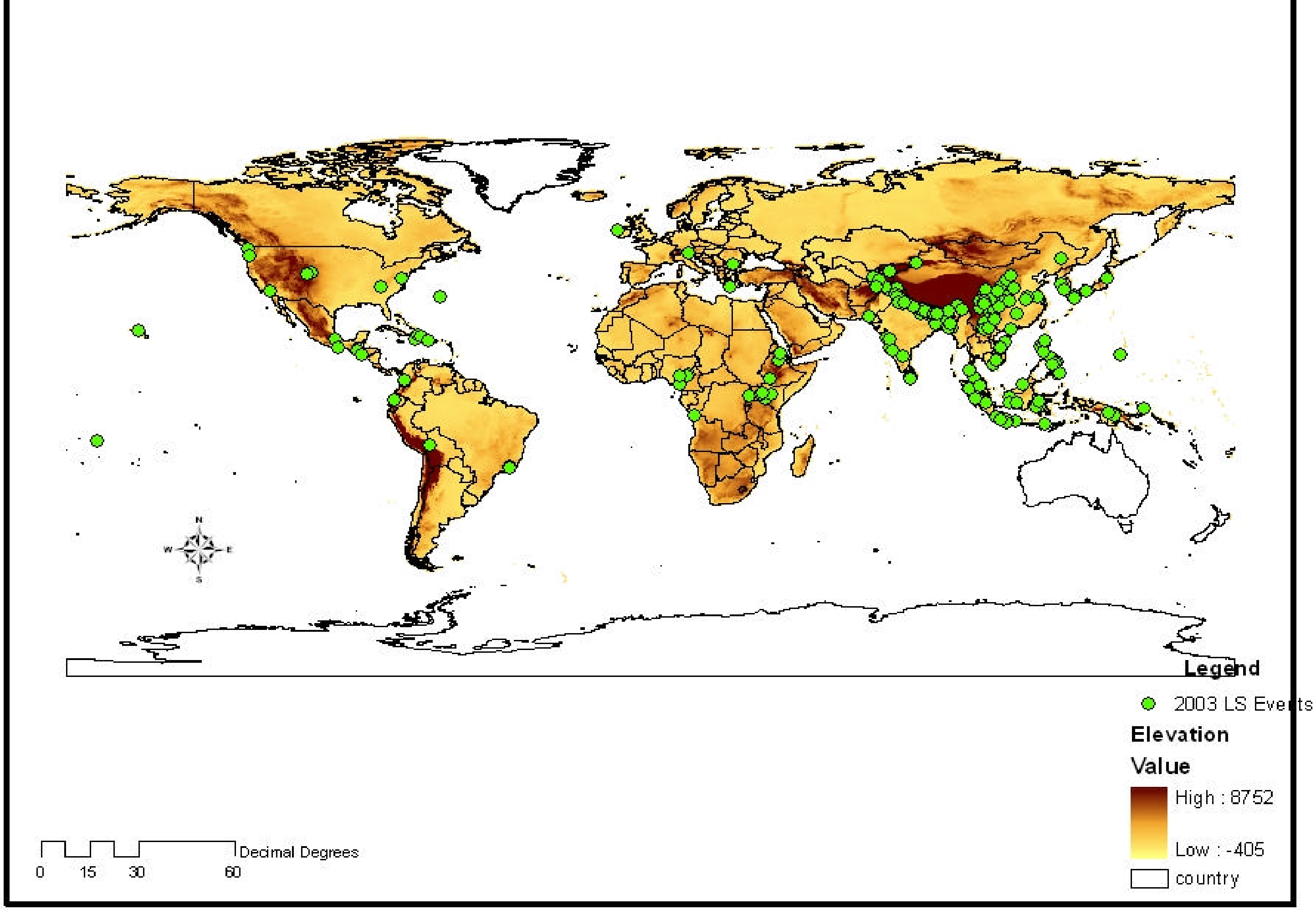

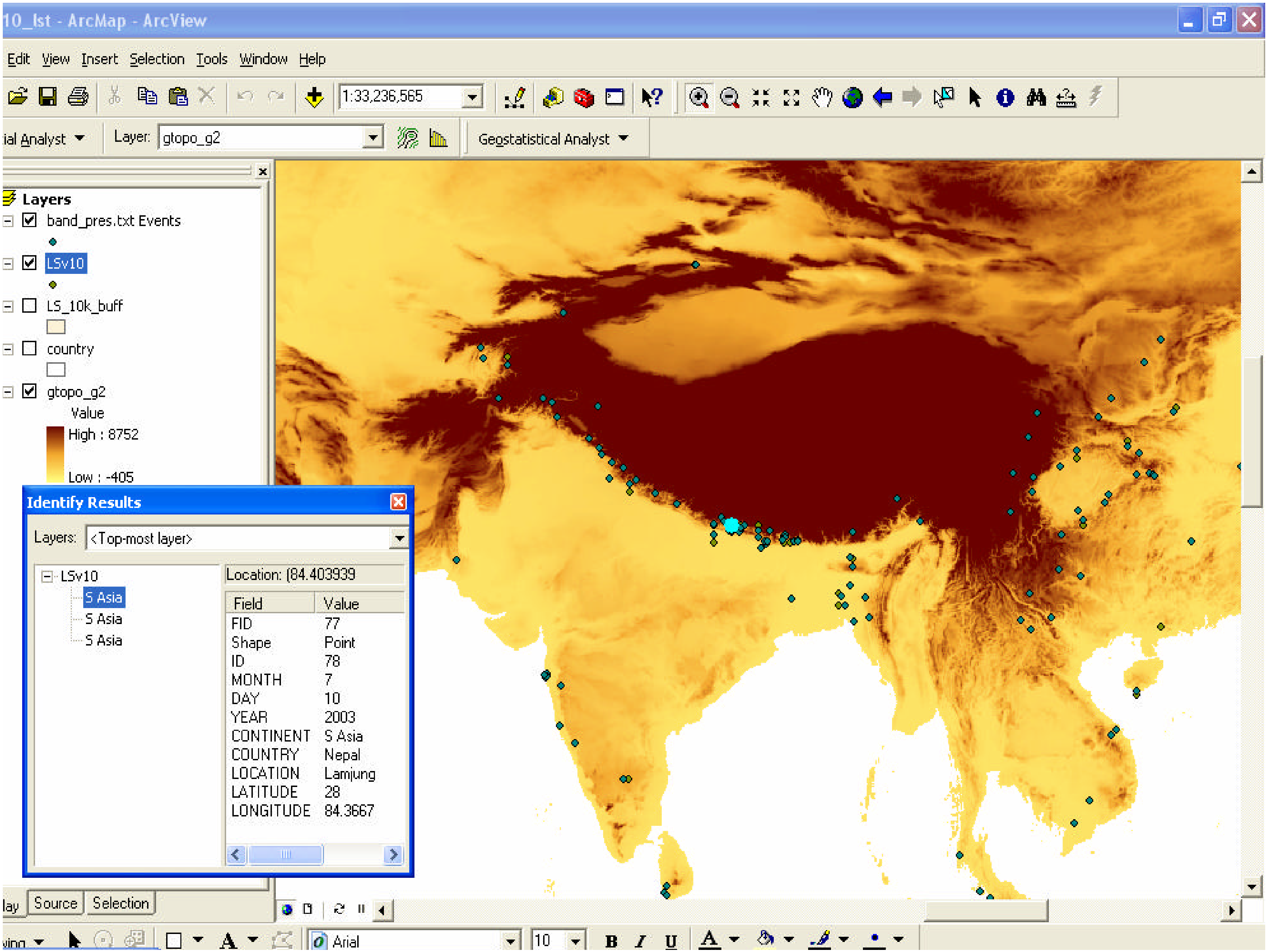
10_lst - ArcMap - ArcView
Edit View Insert Selection Tools Window Help
1:33,236,565
ial Analyst
Layer: gtopo_g2
Geostatistical Analyst
Layers
band_pres.txt Events
LSv10
LS_10k_buff
country
gtopo_g2
Value
High : 8752
Low : -405
Identify Results
Layers: <Top-most layer>
LSv10
S Asia
S Asia
S Asia
Location: (84.403939
Field Value
FID 77
Shape Point
ID 78
MONTH 7
DAY 10
YEAR 2003
CONTINENT S Asia
COUNTRY Nepal
LOCATION Lamjung
LATITUDE 28
LONGITUDE 84.3667
Source Selection
Arial
10

Case Study

- Date: July 10, 2003
- Location: Lamjung, Nep
- Lat Lon: 28.2, 84.3667
- Elevation: 1279m
- Deaths: 2 killed
- Trigger: monsoon/heav rainfall
- Total Rainfall: 371.86m

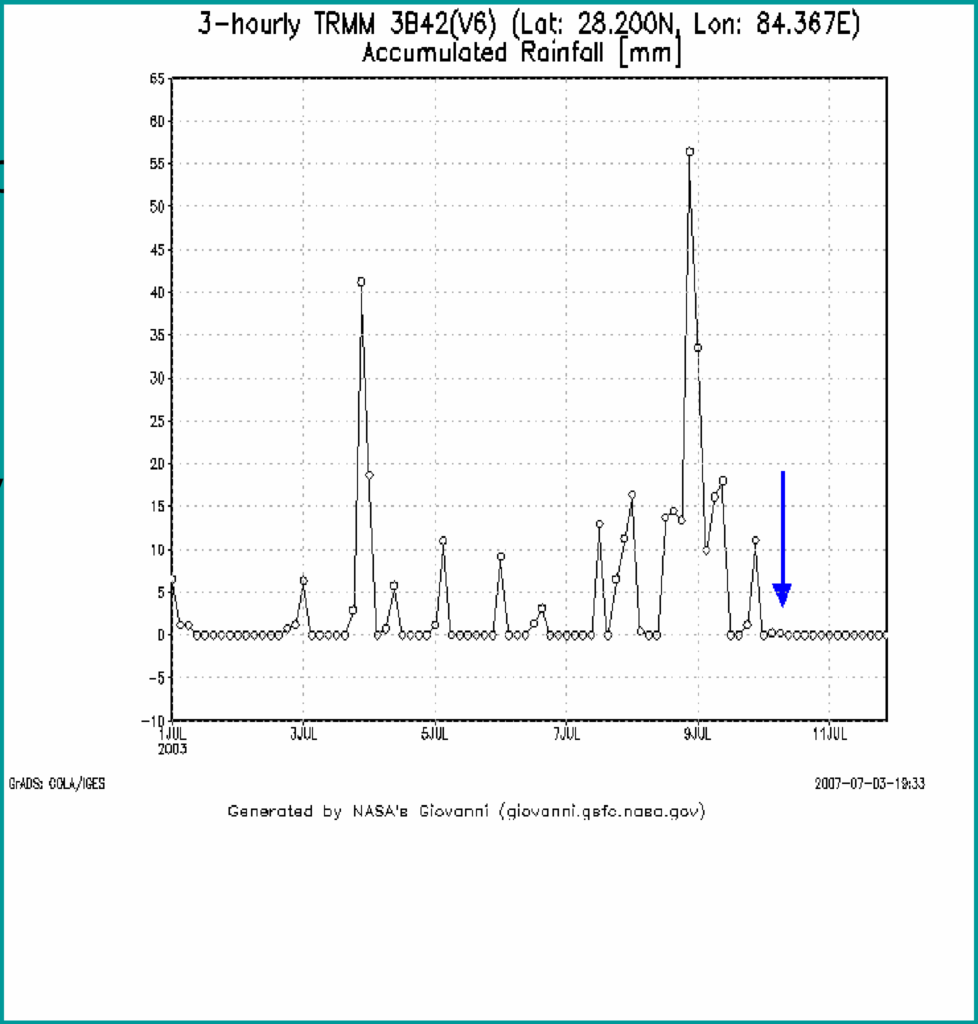

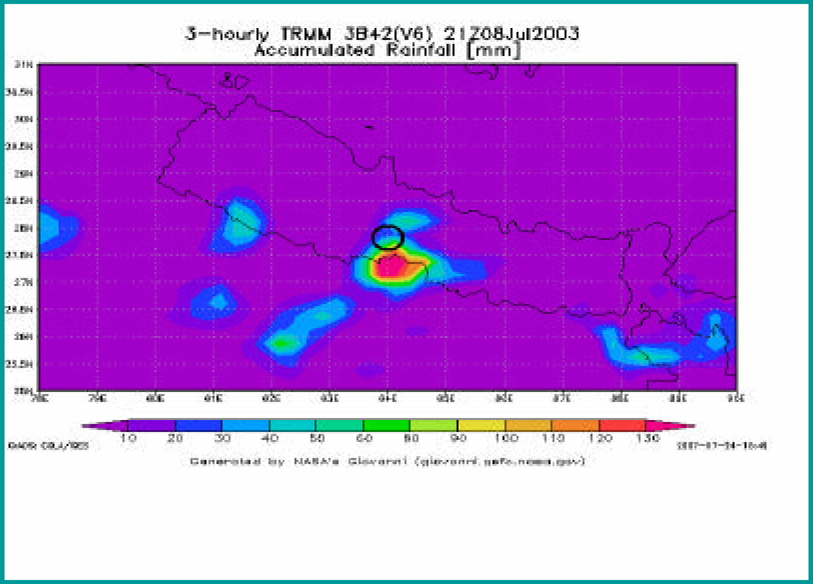
3-hourly TRMM 3B42(V6) 21Z08Jul2003
Accumulated Rainfall [mm]
10 20 30 40 50 60 80 90 100 110 120 130
Generated by NASA's Giovanni (giovanni.gsfc.nasa.gov)


3-hourly TRMM 3B42(V6) (Lat: 28.200N, Lon: 84.367E)
Rain Rate [mm/hr]
Generated by NASA's Giovanni (giovanni.gsfc.nasa.gov)

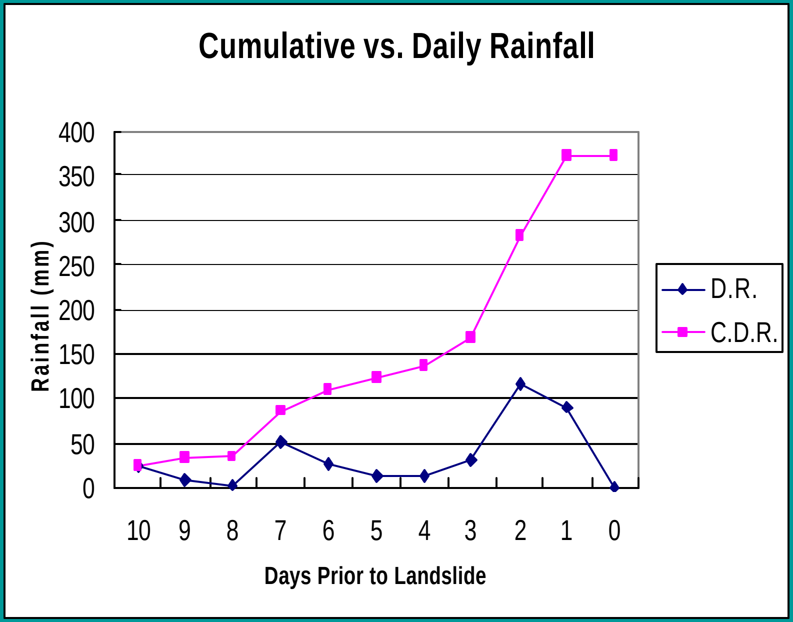
Cumulative vs. Daily Rainfall
Rainfall (mm)
400
350
300
250
200
150
100
50
0
10 9 8 7 6 5 4 3 2 1 0
Days Prior to Landslide
D.R.
C.D.R.

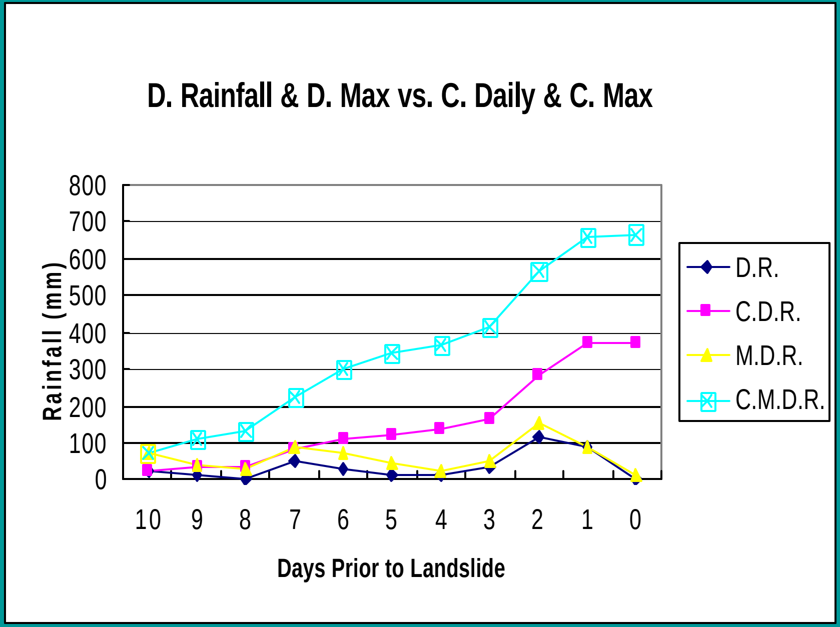
D. Rainfall & D. Max vs. C. Daily & C. Max
Rainfall (mm)
800
700
600
500
400
300
200
100
0
10 9 8 7 6 5 4 3 2 1 0
Days Prior to Landslide
D.R.
C.D.R.
M.D.R.
C.M.D.R.

2003 LS stat graphs

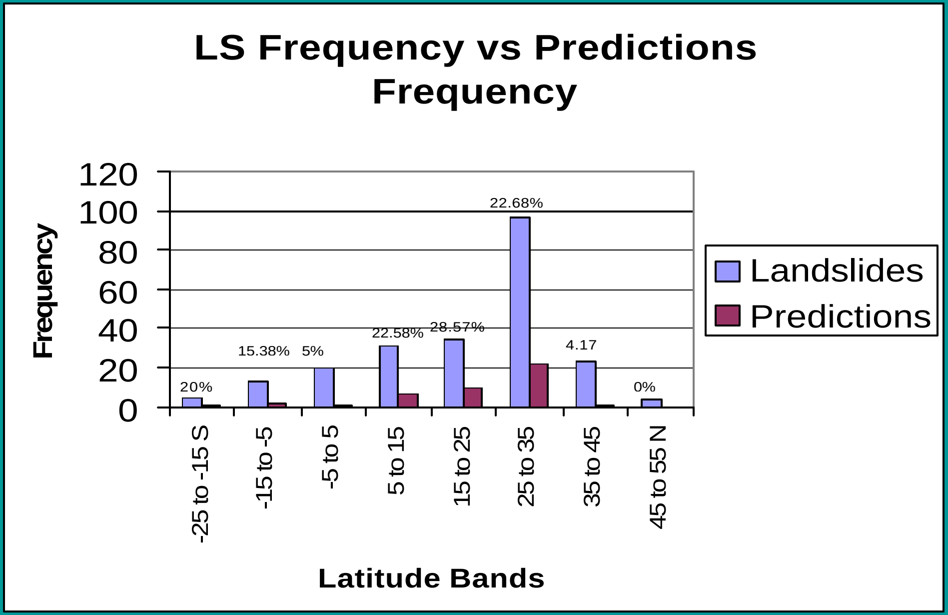

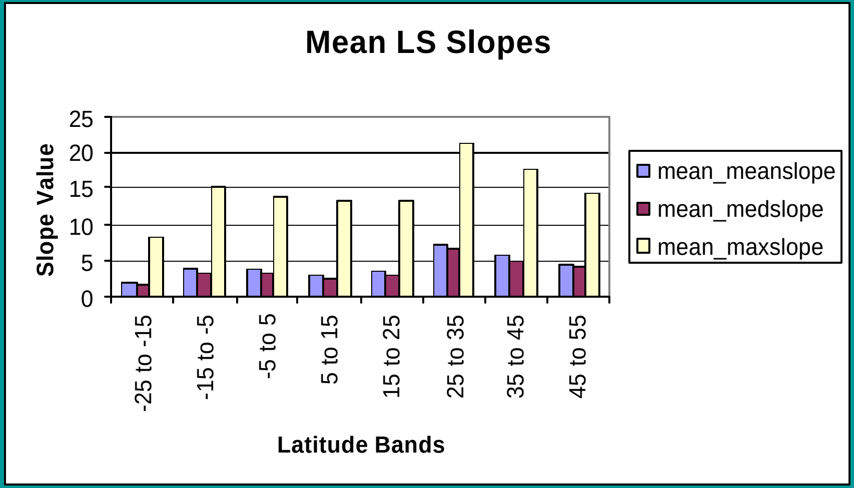

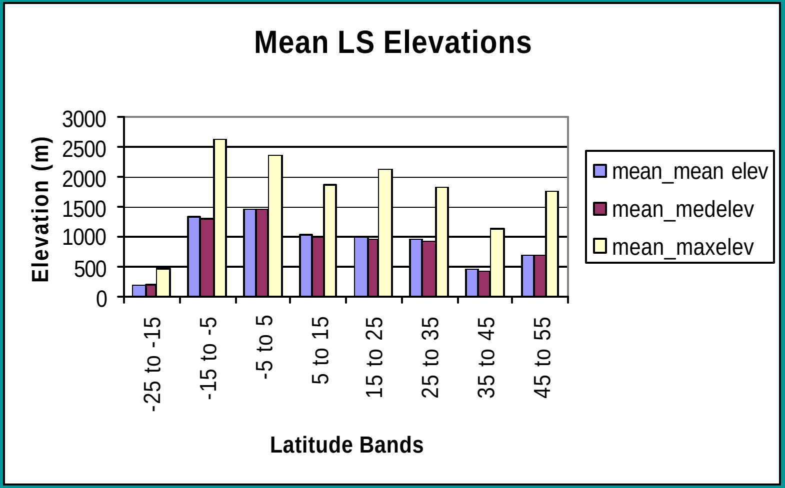

Global Landslide Susceptibility and 2003 Landslide events

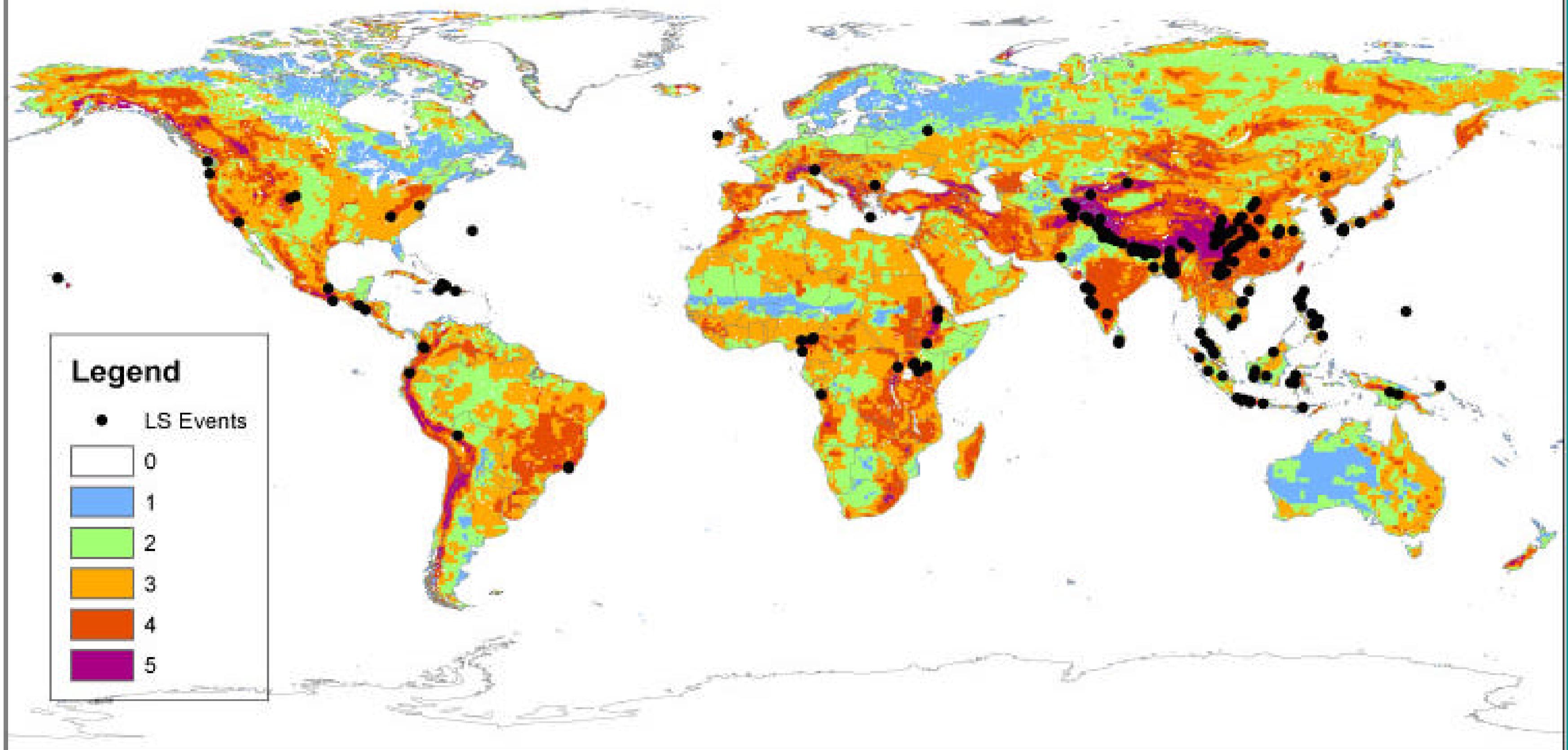

Weights: **0.4** – Slope, **0.2** – soil type and soil texture, **0.1** – elevation and land cover

Comparison of 2003 Landslide Inventory events and Landslide Susceptibility Algorithm predictions

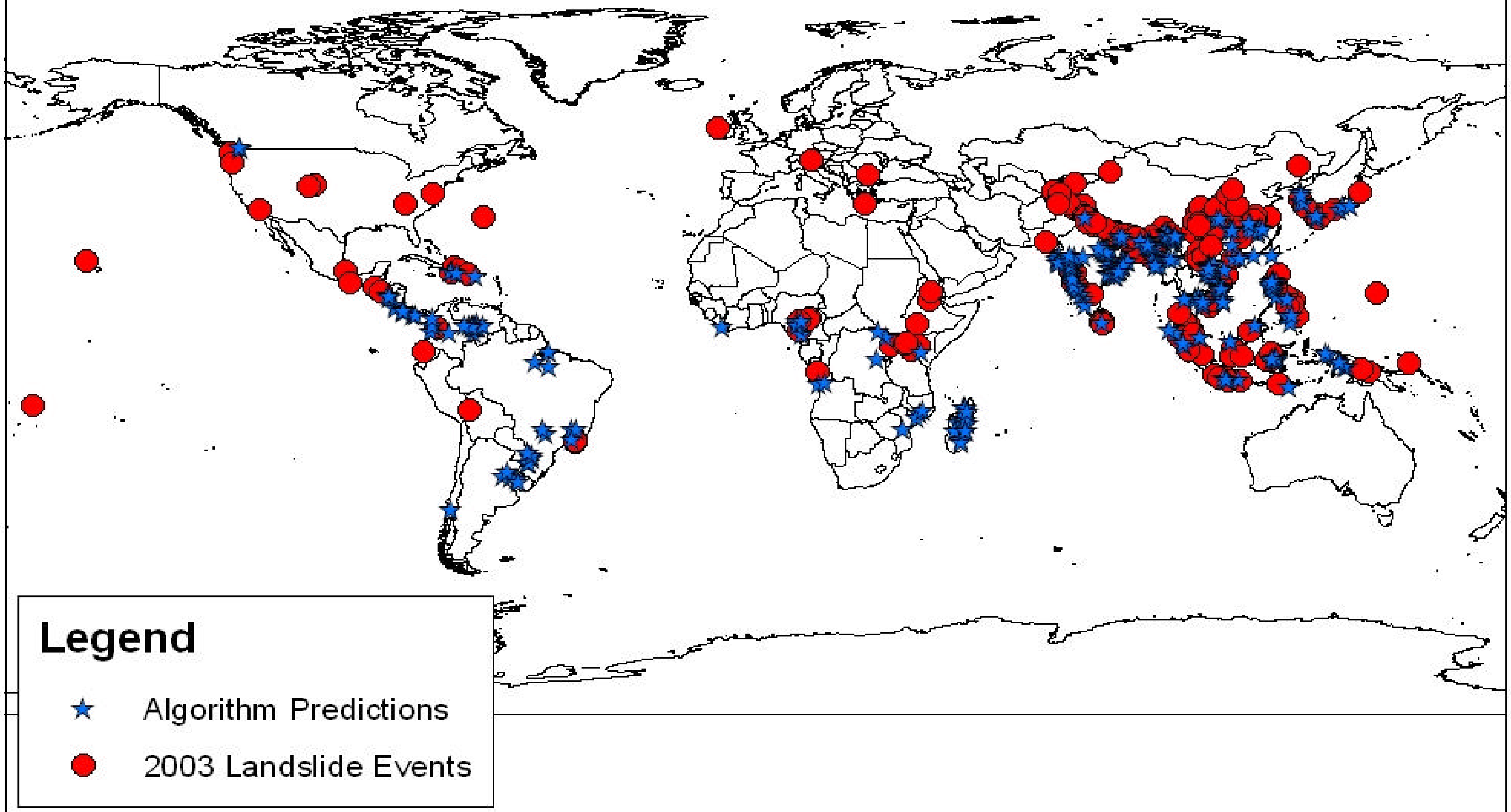

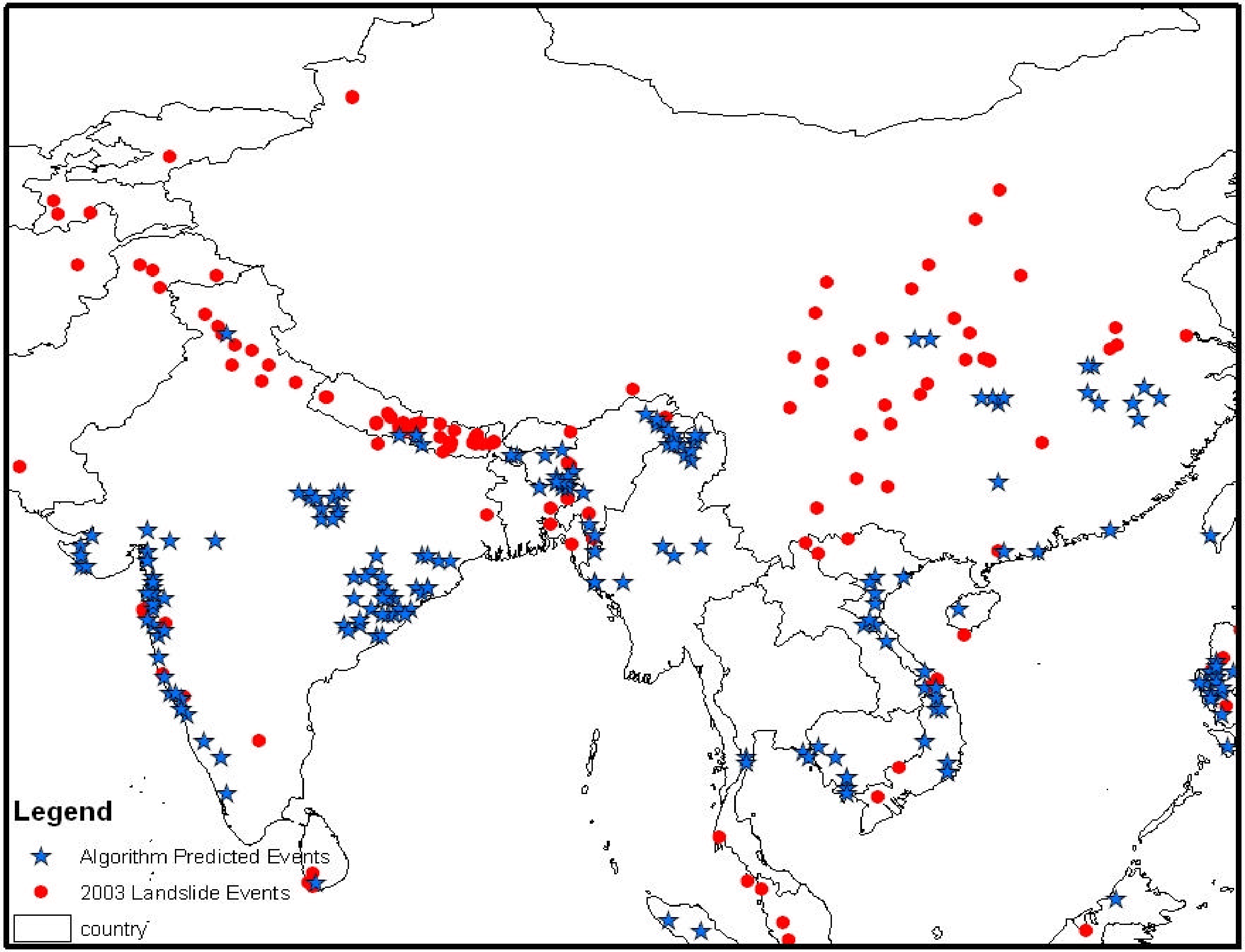
Legend
Algorithm Predicted Events
2003 Landslide Events
country

2003 LS POD's

- Susceptibility POD (cat 4 or 5): 73%

- Joint POD:

-Point (14.5%),

-Mean (11.9%),

-Max (46.1%)

2007 Real Time LS's vs. Algorithm Predicted LS's

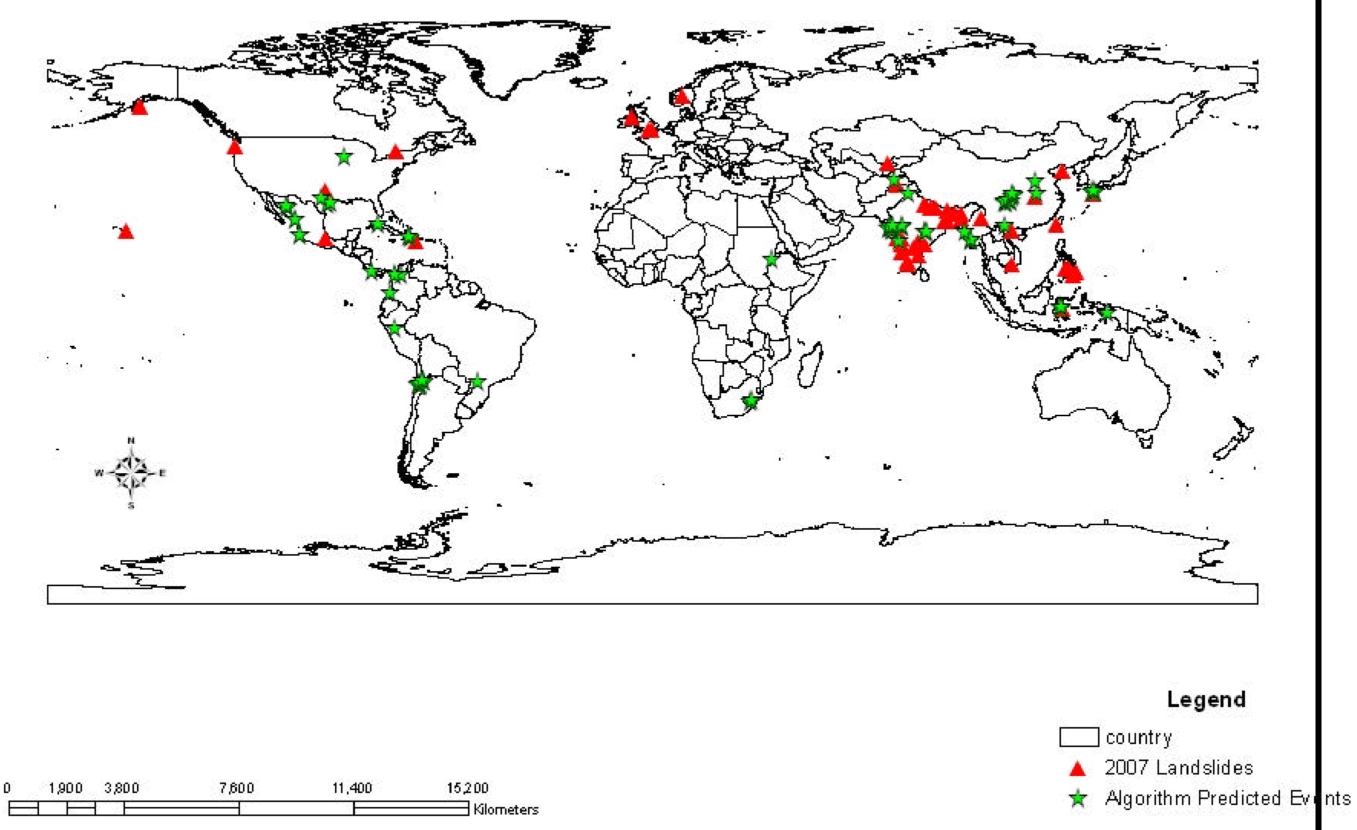

2007 Landslide Statistics

- Susceptibility POD: 60.98%

- Joint POD:

-Point (2.44%),

-Mean (2.44%),

-Max (12.20%)

Conclusions

- 2003 LS inventory is the first database to catalog global landslides
- In terms of the case studies, we found the LS occurred after the last peak of rainfall on the day of occurrence
- The majority of the 2003 LS’s were located in the 25N-35N latitude band surrounding the mountainous regions of northern India and central China
- Need to adjust the rainfall I-D threshold because of the low POD’s
- Better validation must be obtained

Future Work

- 2003 Global LS inventory is not complete, it needs to be improved in a stratified way
- Adjust the global Intensity-Duration equation and susceptibility map at the regional scale to better predict landslide locations
- Investigate why there aren’t high rain rates in the mountainous regions of northern India and central China; Could it be a limitation of satellite rainfall estimates?
- Continue to update the 2007 Global Landslide database for validation

1993 Tully Landslide, Tully Valley, NY
2007 Salisbury University Geomorph Class Trip

References

- Hong, Yang, Robert Adler, and George Huffman. "Evaluation of the Potential of NASA Multi-Satellite Precipitation Analysis in Global Landslide Hazard Assessment." Geophysical Research Letters 33 (2006): 1-5.
- Hong, Yang, Robert Adler, and George Huffman. "An Experimental Global Predicition System for Rainfall-Triggered Landslides Using Satellite Remote Sensing and Geospatial Datasets." IEEE Transactions on Geoscience and Remote Sensing 45 (2007): 1671-1680.
- The International Landslide Centre landslide fatality database, University of Durham:
- EM-DAT : the International Disaster Database:
-
- International Consortium on Landslides:
-
-
- http://disc2.nascom.nasa.gov/Giovanni/tovas/TRMM_V6.3B42.2.shtml

Thank You

- GSFC
- Bob Adler and Yang Hong
- Per Gloersen and Valerie Casasanto
- Dalia Bach
- Fellow Summer Institute interns

Failure Rates

- 10 km radius: 1 hit, 0.3%
- 50 km radius: 19 hits, 5.64%
- 100 km radius: 36 hits, 10.68%
- 150 km radius: 53 hits, 15.73%
- 200 km radius: 69 hits, 20.47%

WE NEED BETTER VALIDATION!

Effect of Aerosol on Stratocumulus Clouds in the Eastern-North Pacific

Cody L. Fritz (University of Missouri-Columbia, Atmospheric Science/Mathematics)

Dr. Eric Wilcox (NASA/Goddard Space Flight Center, Climate Division 613.2)

Overview

- Project Background
  - Cloud formation in a nut shell
  - Theory of aerosol in terms of its effect on cloud morphology
  - The pedestal to which this case study rests.
- Methodology
- Analysis
  - What was found and how it relates to our hypothesis.
  - Adoption to previous theory
- Conclusions

Cloud Formation 101

- Warm air rises (thermal less dense than environment).
- As the air cools it condenses on CCN (Cloud Condensation Nuclei, hygroscopic particles)
- Cloud droplets grow. Once fall drop velocity exceeds updraft velocity, drizzle/rain occurs.

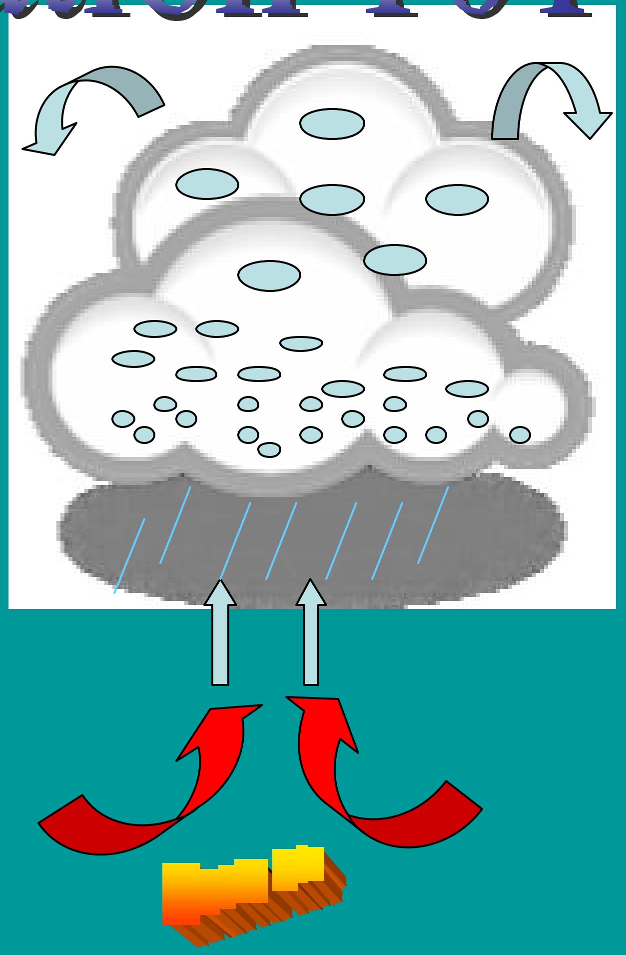

The Effect of Aerosol

- Entrainment of Aerosol
  - Increase # of CCN
- Cloud Deepens
  - Suppresses Rain
- Cooling Tendency Enabled
- Or Does it?

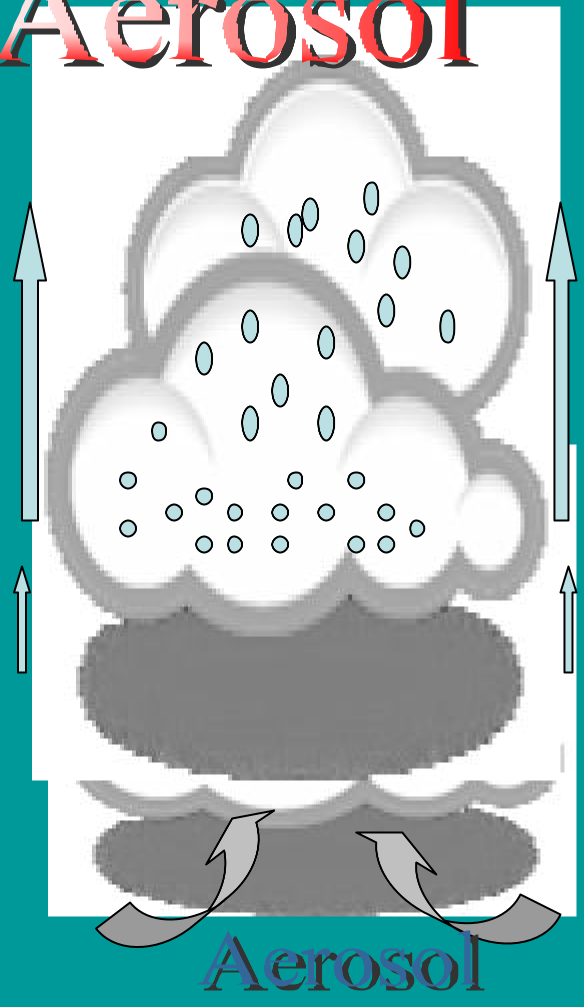

Background

- Clean/polluted clouds display systematic difference in cloud fraction with LWP of equal value.

- [redacted]

- Clouds in polluted environments must be thinner.

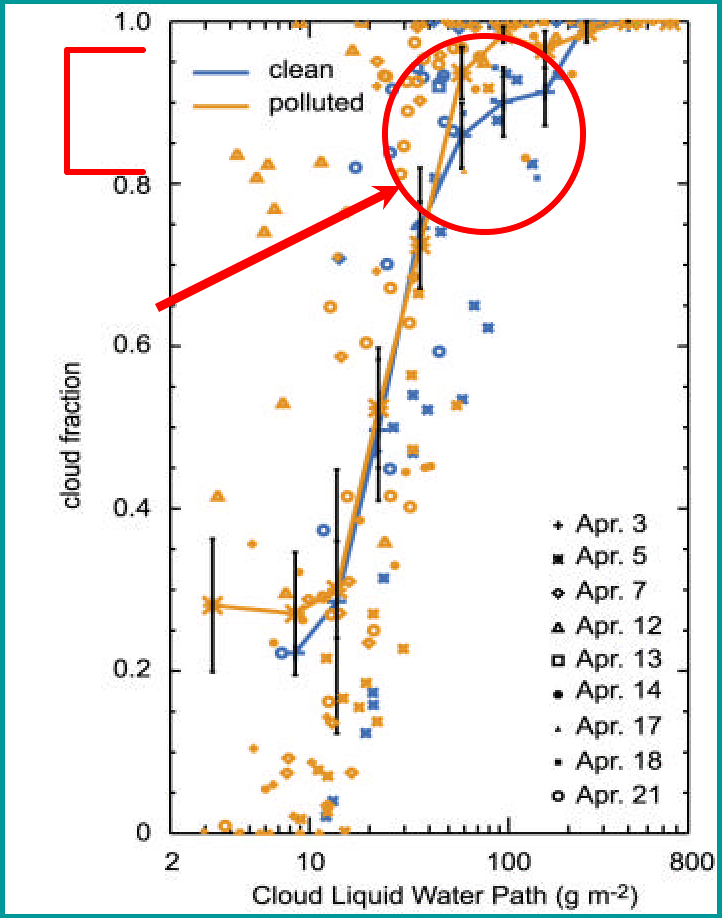

Wilcox, Eric unpublished

WCR


Wyoming KingAir Research Aircraft
Side/Up Antenna
Side-fore Antenna
N2UW
Nadir & Down-fore Antennas
NSF EC-130Q Hercules
WCR
MARSF
WCR scan set
21/31 GHz
RM

Cloud Radar

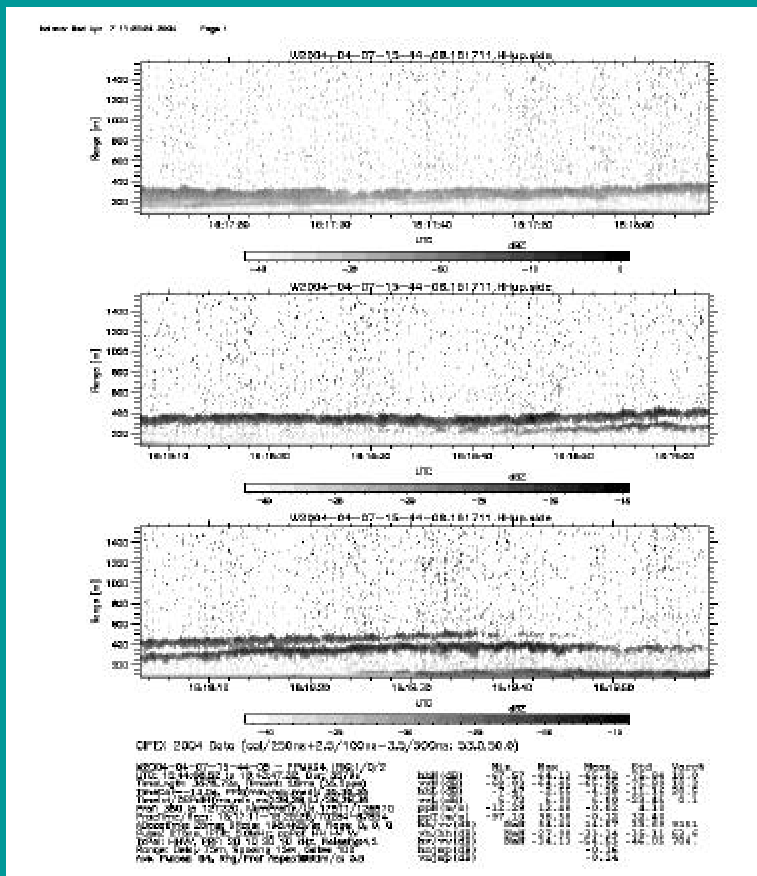

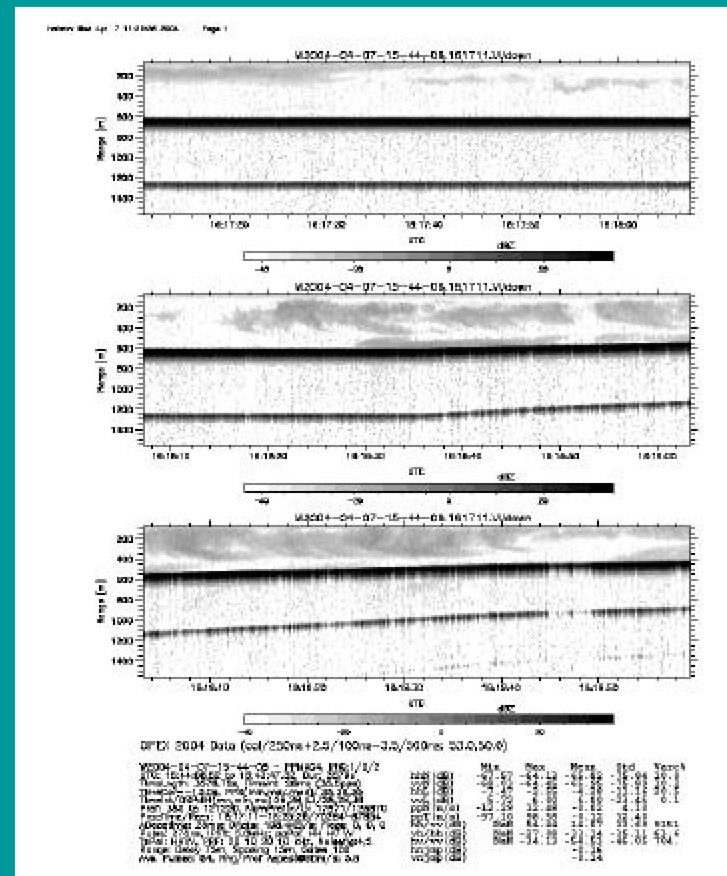

University of Wyoming-Atmospheric Science

WCR-CIFEXO4

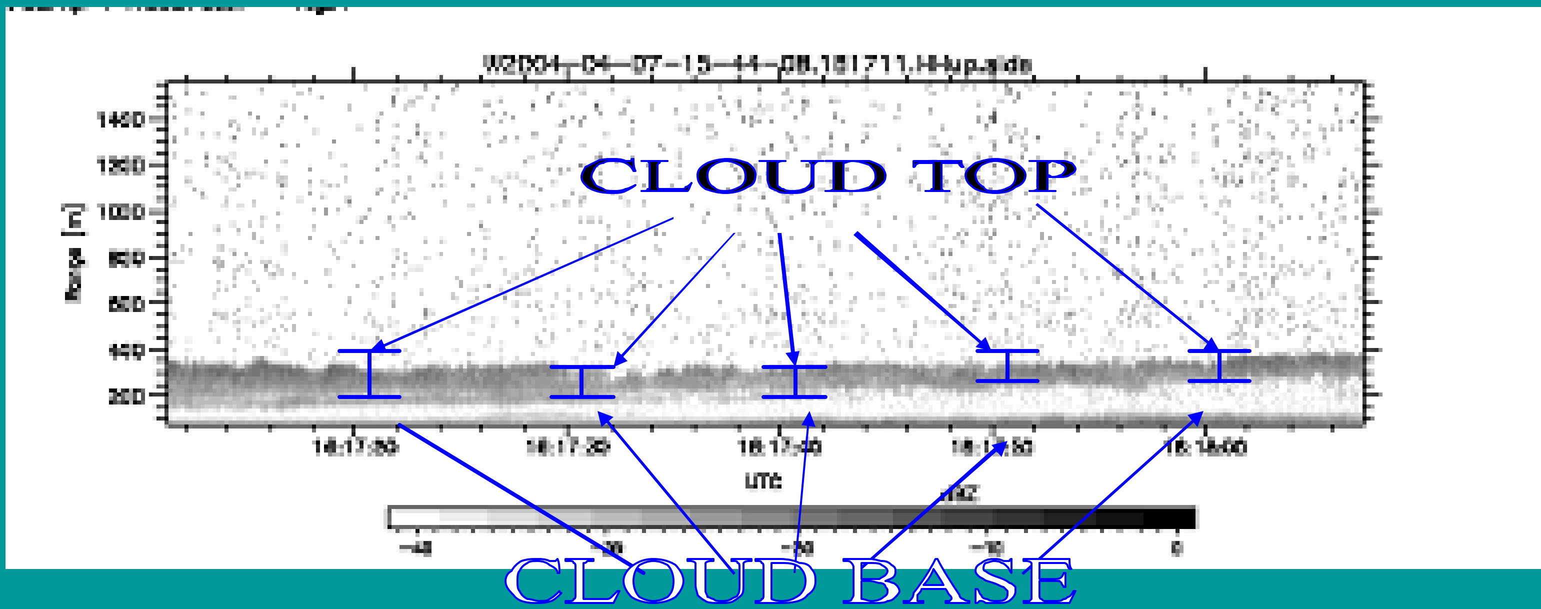
CLOUD TOP
CLOUD BASE
Range [m]
UTC
dBZ

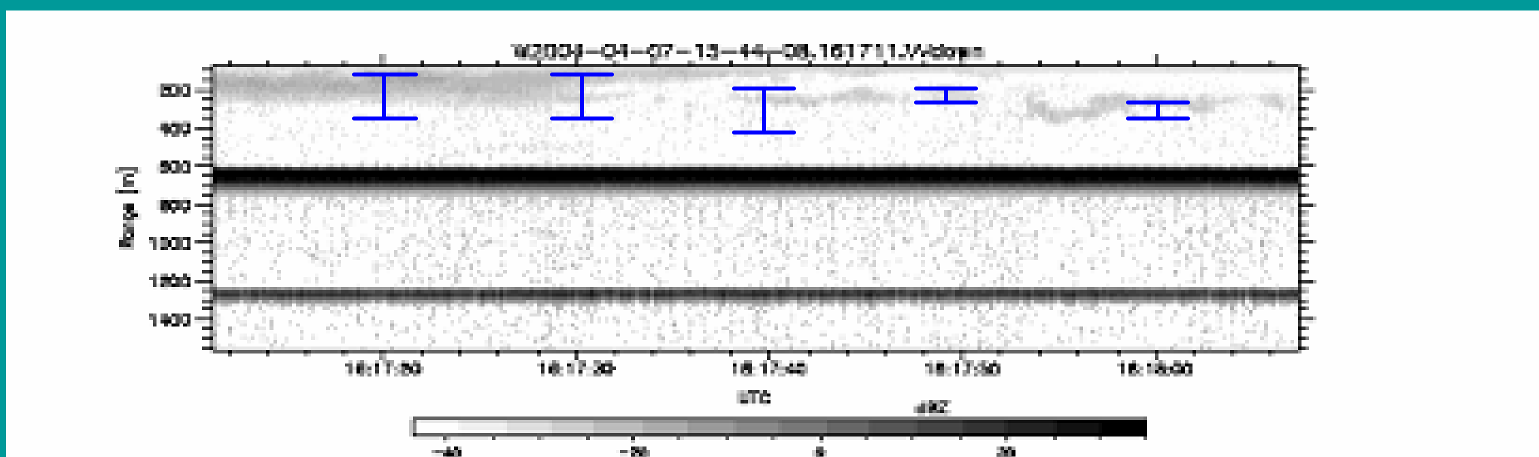
Range [m]
UTC
dBZ

RESULTS

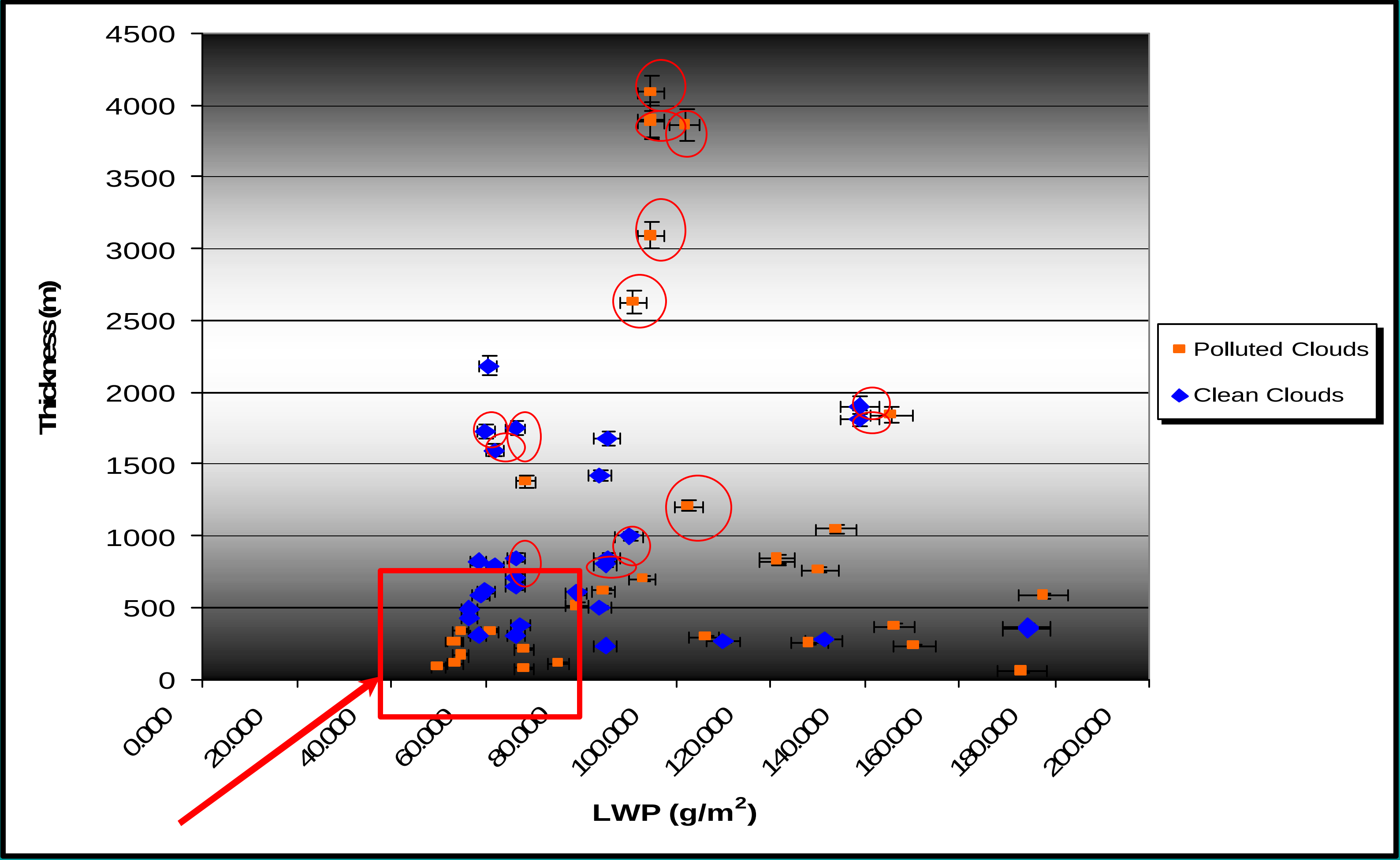

4500
4000
3500
3000
2500
2000
1500
1000
500
0
Thickness (m)
0.000
20.000
40.000
60.000
80.000
100.000
120.000
140.000
160.000
180.000
200.000
LWP (g/m2)
Polluted Clouds
Clean Clouds

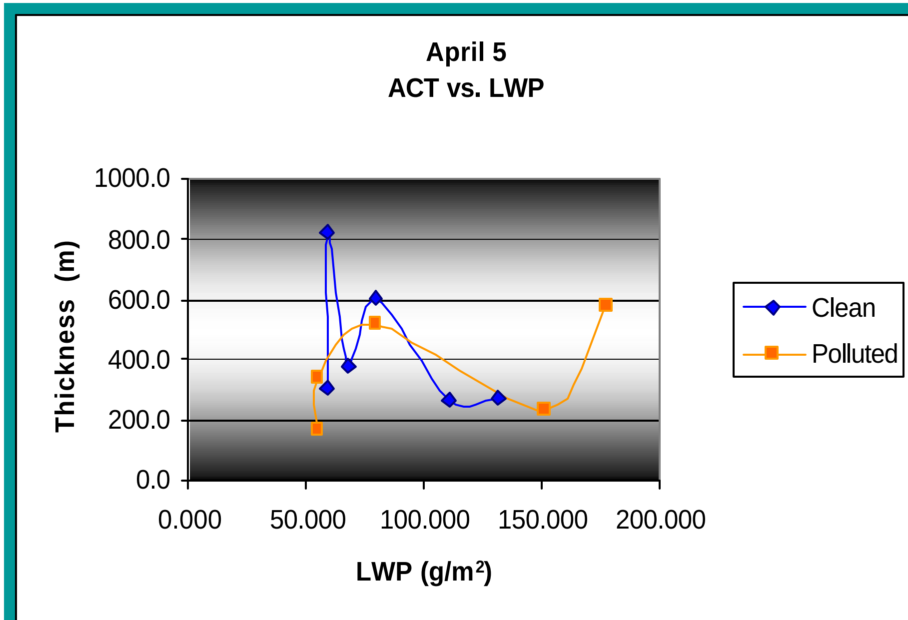
April 5
ACT vs. LWP
Thickness (m)
1000.0
800.0
600.0
400.0
200.0
0.0
0.000
50.000
100.000
150.000
200.000
LWP (g/m²)
Clean
Polluted

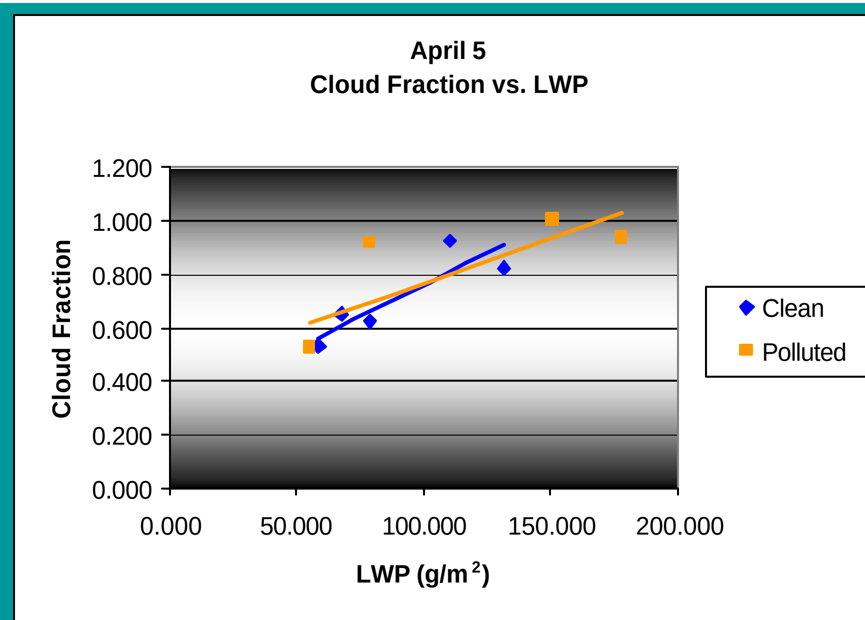
April 5
Cloud Fraction vs. LWP
Cloud Fraction
1.200
1.000
0.800
0.600
0.400
0.200
0.000
0.000
50.000
100.000
150.000
200.000
LWP (g/m²)
Clean
Polluted

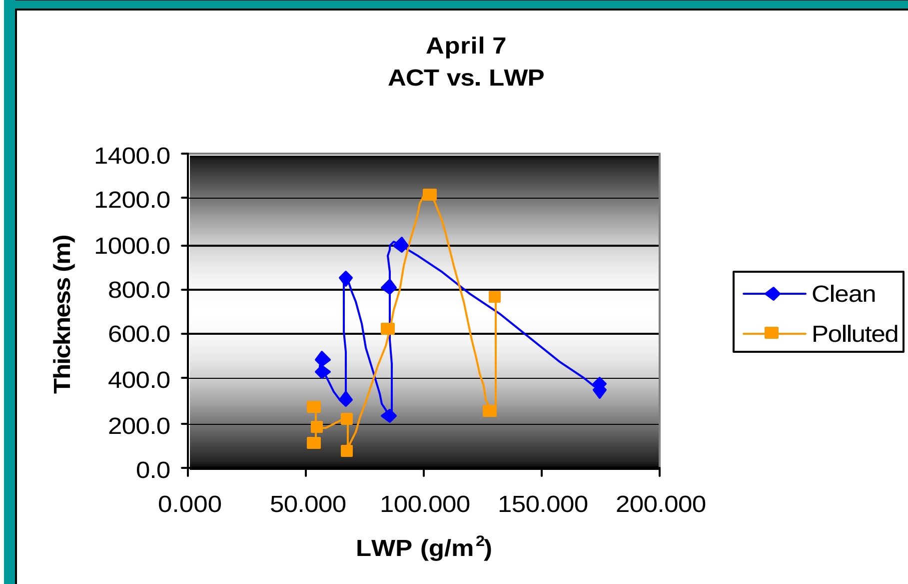
April 7
ACT vs. LWP
Thickness (m)
1400.0
1200.0
1000.0
800.0
600.0
400.0
200.0
0.0
0.000
50.000
100.000
150.000
200.000
LWP (g/m²)
Clean
Polluted

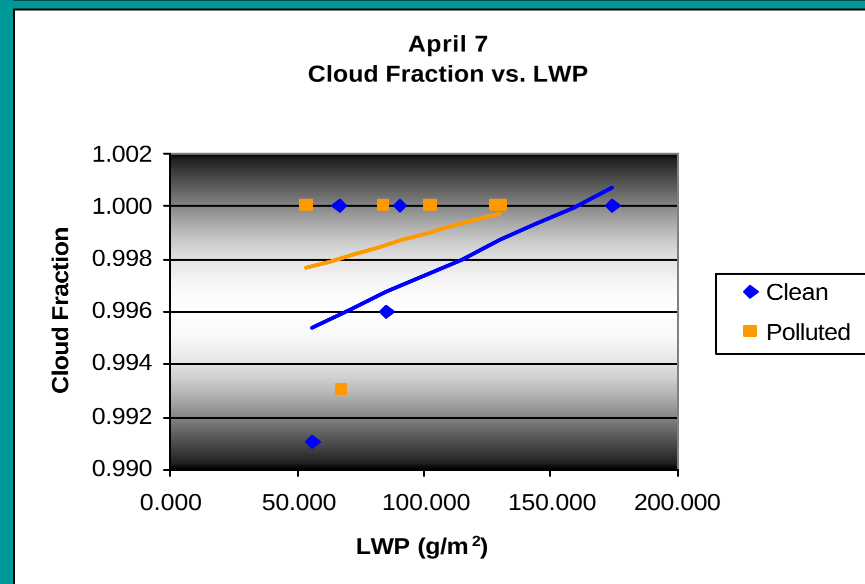
April 7
Cloud Fraction vs. LWP
Cloud Fraction
1.002
1.000
0.998
0.996
0.994
0.992
0.990
0.000
50.000
100.000
150.000
200.000
LWP (g/m²)
Clean
Polluted

Ackerman *et al.*

- Relationship b/t entrainment of aerosol and humidity in the overlying air above a cloud during its morphology

- Aerosol suppresses drizzle thus increasing entrainment

- Concentrations of aerosol held constant: ?RH-cloud deepens : ?RH cloud thins

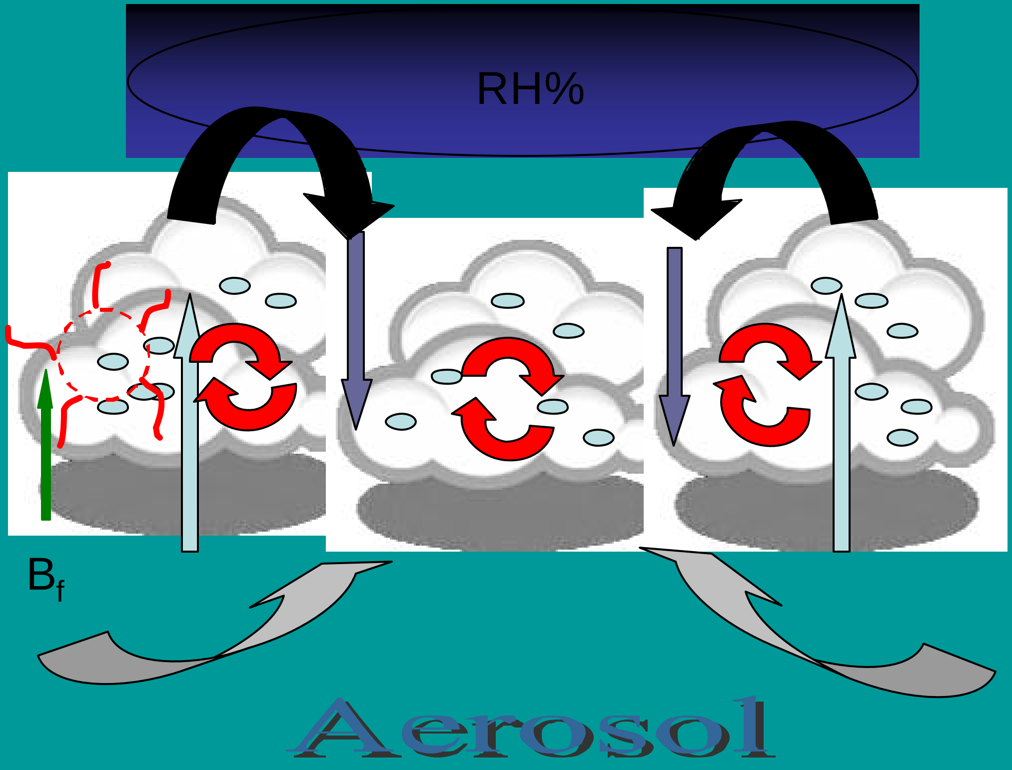

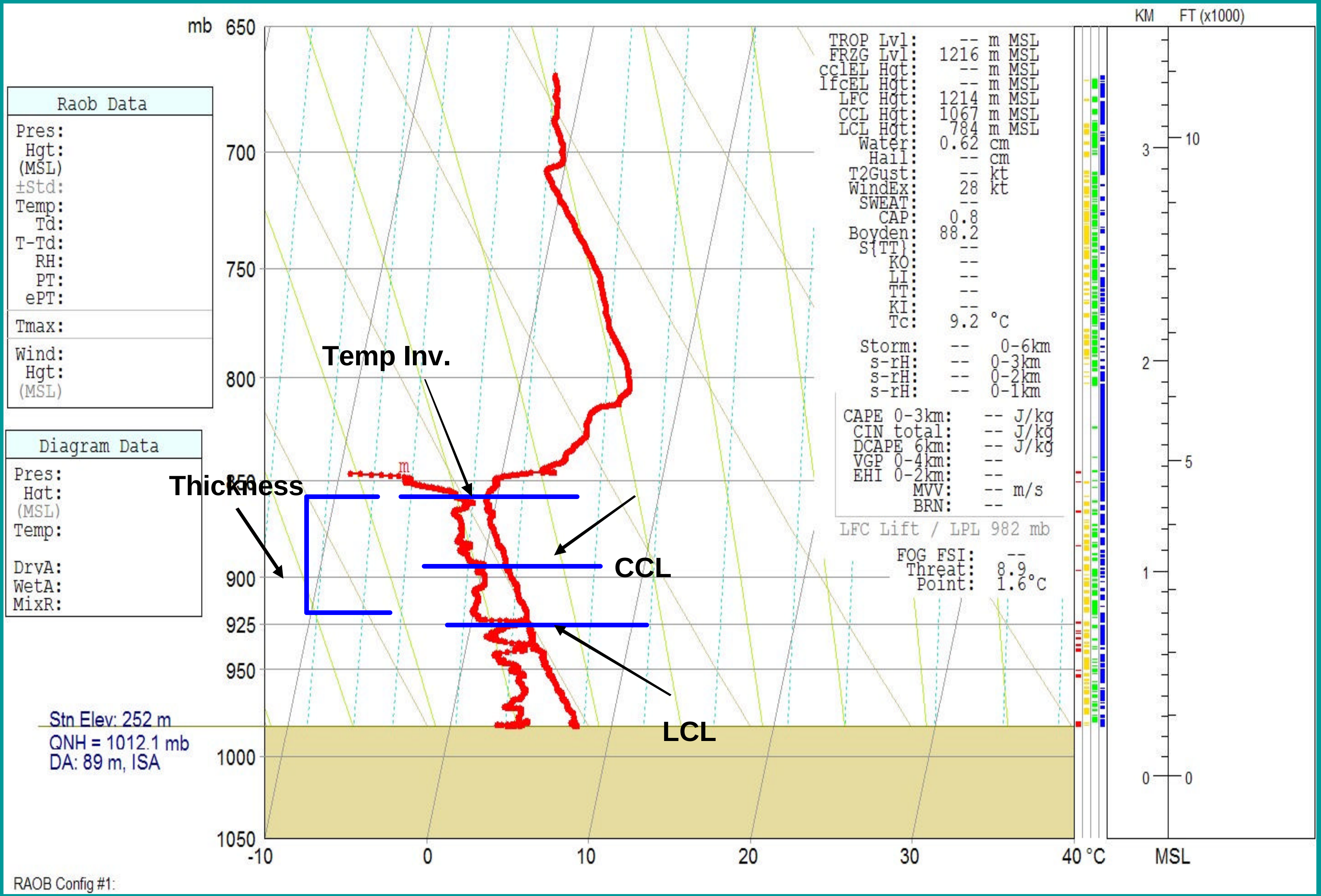

mb
650
700
750
800
850
900
925
950
1000
1050
-10
0
10
20
30
40 °C
KM
FT (x1000)
MSL
Raob Data
Pres:
Hgt:
(MSL)
±Std:
Temp:
Td:
T-Td:
RH:
PT:
ePT:
Tmax:
Wind:
Hgt:
(MSL)
Diagram Data
Pres:
Hgt:
(MSL)
Temp:
DryA:
WetA:
MixR:
TROP Lvl: -- m MSL
FRZG Lvl: 1216 m MSL
cclEL Hgt: -- m MSL
lfcEL Hgt: -- m MSL
LFC Hgt: 1214 m MSL
CCL Hgt: 1067 m MSL
LCL Hgt: 784 m MSL
Water: 0.62 cm
Hail: -- cm
T2Gust: -- kt
WindEx: 28 kt
SWEAT: --
CAP: 0.8
Boyden: 88.2
S{TT}: --
KO: --
LI: --
TT: --
KI: --
Tc: 9.2 °C
Storm: -- 0-6km
s-rH: -- 0-3km
s-rH: -- 0-2km
s-rH: -- 0-1km
CAPE 0-3km: -- J/kg
CIN total: -- J/kg
DCAPE 6km: -- J/kg
VGP 0-4km: --
EHI 0-2km: --
MVV: -- m/s
BRN: --
LFC Lift / LPL 982 mb
FOG FSI: --
Threat: 8.9
Point: 1.6°C
Temp Inv.
Thickness
CCL
LCL
Stn Elev: 252 m
QNH = 1012.1 mb
DA: 89 m, ISA
RAOB Config #1:

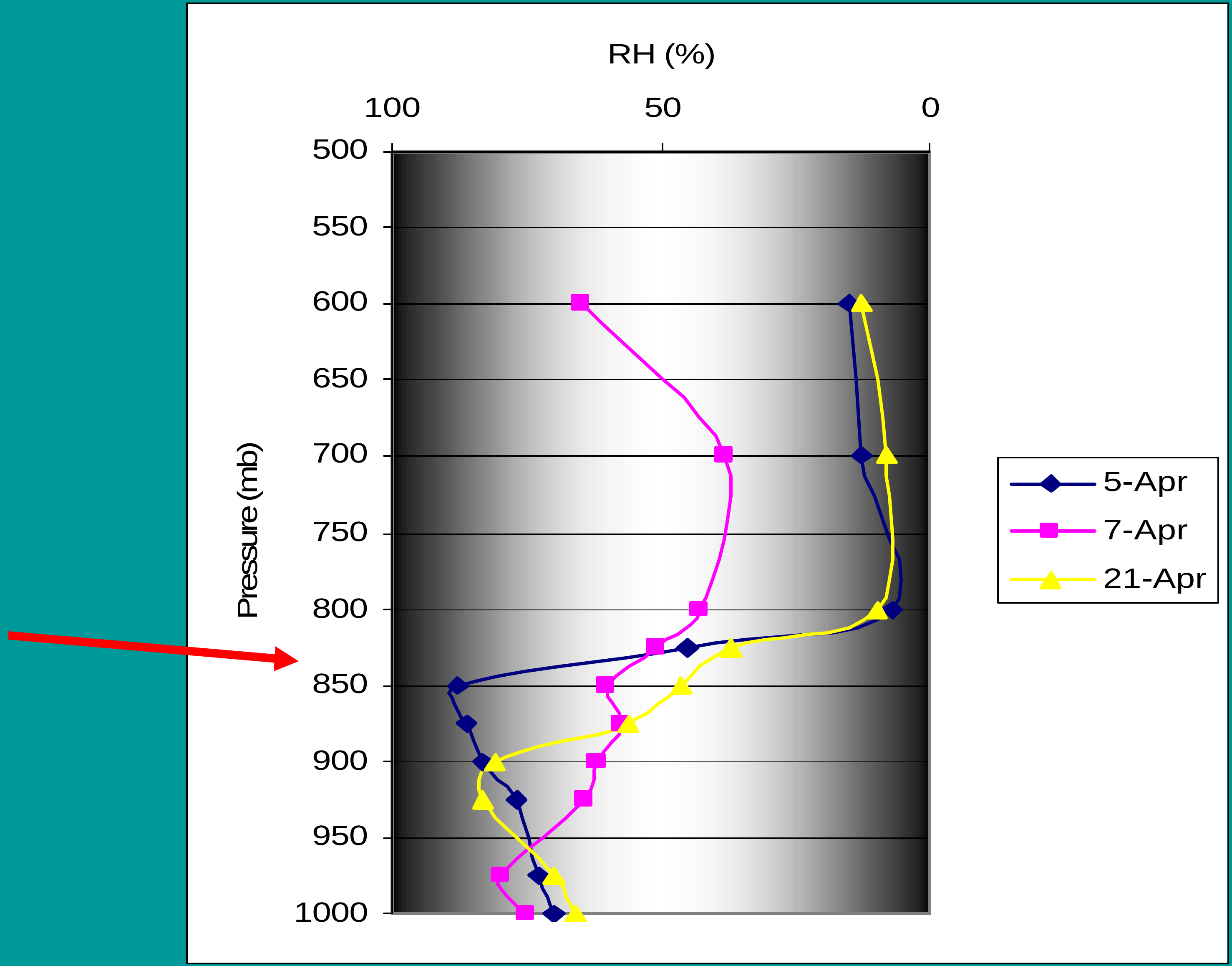
RH (%)
100
50
0
Pressure (mb)
500
550
600
650
700
750
800
850
900
950
1000
5-Apr
7-Apr
21-Apr

CONCLUSIONS

- Observations consistent with Ackerman *et al.*
- Not all cases, however, are in agreement.
- Many theories linger concerning the study of aerosol and its impact on stratiform convection over the Pacific region.
- Given our location or study of interest, we are left with a very dynamical pattern that in terms of large scale analysis provides a definite impact. Synoptic-scale systems are present during the entirety of this observation.
- Therefore, given the intricacy of this study our conclusions on the effects of aerosol on stratocum development over the Eastern-North Pacific are termed uncertain but in strong agreement to Ackerman *et al*.

REFERENCES:

- Andrew S. Ackerman, Michael P. Kirkpatrick, David E. Stevens & Owen B. Toon. The Impact of humidity above stratiform clouds on indirect aerosol climate forcing, letters to nature 432, 1014-1017 (2004).

- J. L. Breuguier, Parameterization of the Condensation Process: A Theoretical Approach Journal of the Atmospheric Sciences, vol. 48, No. 2, pp. 261-282m (1991).

Acknowledgements

Dr. Eric Wilcox

Dr. Per Gloersen

Valerie Casasanto

Summer Institute 2007

QUESTIONS???

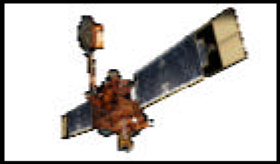

An Examination of the Olympus Mons Aureoles

Annie Griswold[1]

Mark Bulmer, Ph.D.[2], Daniel Beller[3], Patrick McGovern[4], Ph.D.

[1]Case Western Reserve University, Cleveland, OH; [2]Geophysical Flow Observatory, JCET, UMBC, MD; [3]Brandeis University, Waltham, MA; [4]Lunar and Planetary Institute, Houston, TX

Overview

- Motivation
- Questions to address
- Handling new data
- Geomorphic mapping
- Dimensional analysis
- Conclude
  - Volcanic history is long and dynamic
  - MOLA allows for new super-positional relationships to be deduced
  - Area and Volume calculations differ from Viking
  - Aureole units may be composed of multiple events
  - Data support mass movement origin to aureoles but the edifice has changed

Motivation

- Aureoles examined in detail using Viking images (1976)
- Based on observations, three emplacement models proposed
  - Volcanic Products [Morris, 1982; Carr, 1973; Morris and Tanaka, 1994]
  - Mass Movement [Lopes, et al., 1980, 1982; Francis and Wadge 1983]
  - Local emplacement [Morris, 1982]
- Limited resolution of Viking Orbiter meant no models could be conclusively validated

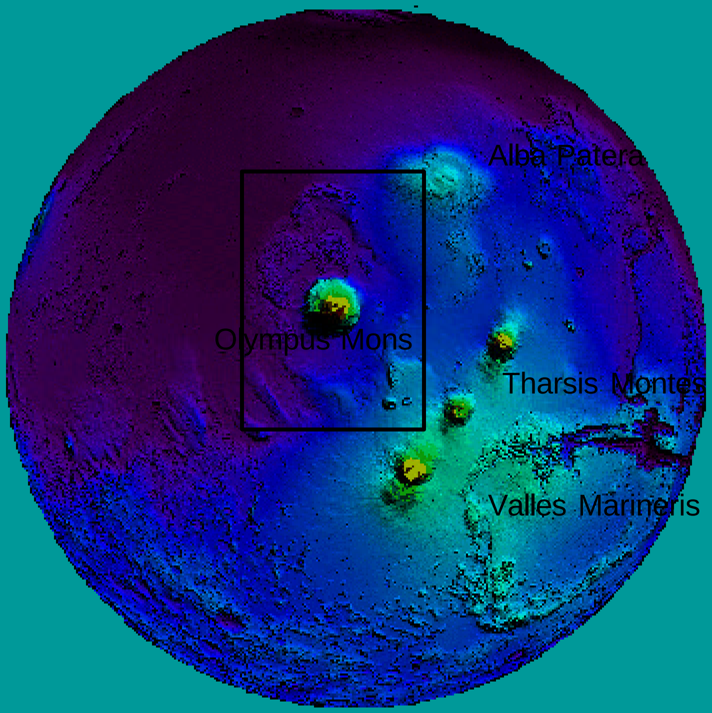

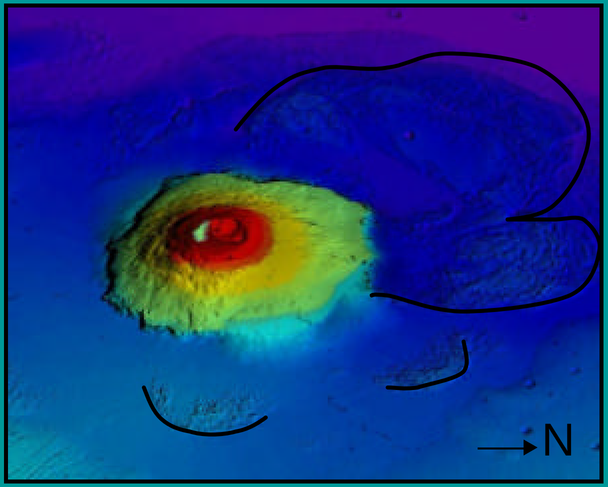

New Opportunities for Study

- Digital data
- Mars Global Surveyor
  - Mars Orbiter Laser Altimeter (MOLA)
    - PEDR data 150 m footprint shot at 300 m interval
    - Interpolated to global gridded dataset
  - Mars Orbiter Camera (MOC)
    - Visible spectrum
    - Narrow Angle: 1-10 m/pixel
    - Wide Angle: 230 m/pixel
- Mars Odyssey
  - Thermal Emission Imaging System (THEMIS)
    - Near and Far IR
    - 50-100 m/pixel
- Mars Express
  - High Resolution Stereo Camera (HRSC)
    - 10 m/pixel
    - Visible, Near IR, Stereo 20-50 m/pixel
- Mars Reconnaissance Orbiter
  - High Resolution Imaging Science Experiment (HiRISE)
    - Visible and IR
    - 30 cm/pixel
    - Limited stereo

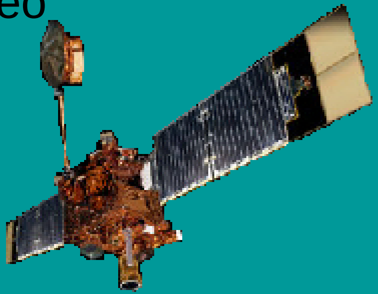

Mars Global Surveyor
Photo Credit: NASA

Questions

- How many aureole units exist and where are their boundaries?
- Are the dimensional characterization [length, width, slope, area, and volume] consistent with those from Viking?
- Is their topographic variability?
- Is the mapped geomorphology of area in need of revision?

Data Compilation in ArcGIS

- All mission data unique
- Not all georeferenced
- Utilize ArcGIS to assign all a cylindrical equal area projection and MOLA derived geographic coordinate system
- Geocorrection and rubber sheeting of THEMIS data
- Possible to overlay and relate topography with image data

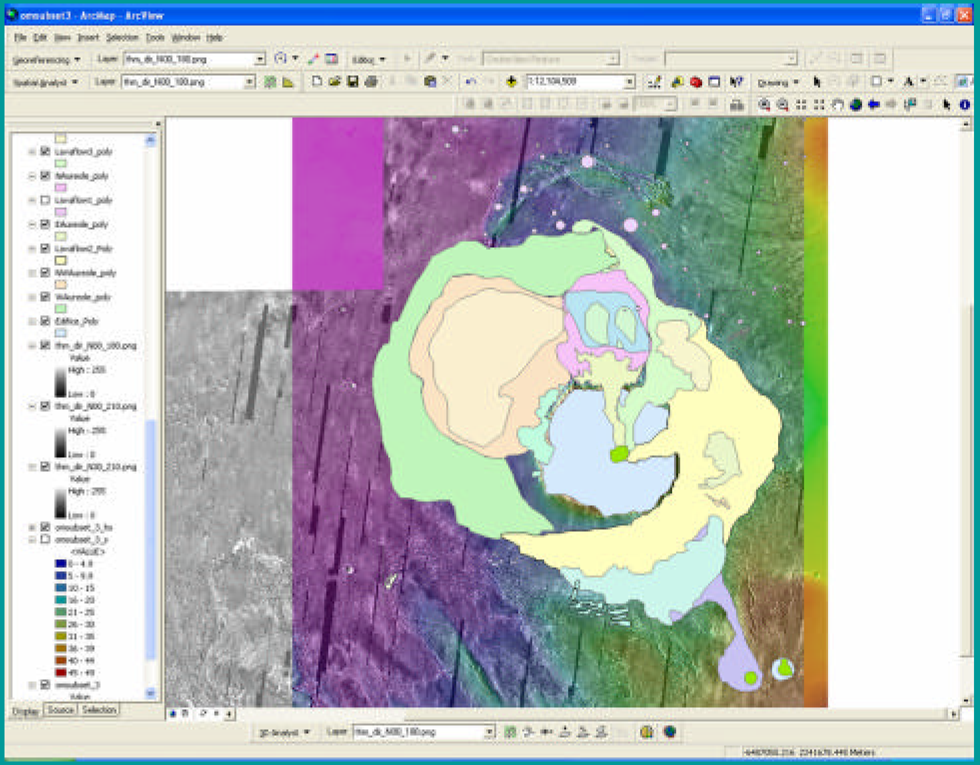

Geomorphic Mapping

- USGS mapping at 1:15M scale
- THEMIS Day IR provided complete coverage at 50-100 m/pixel
- Use MOC and HiRISE images and MOLA PEDR plus gridded topography to assist in the identification
- Identify:
  - Boundaries
  - Embayment and Superposition
  - Features

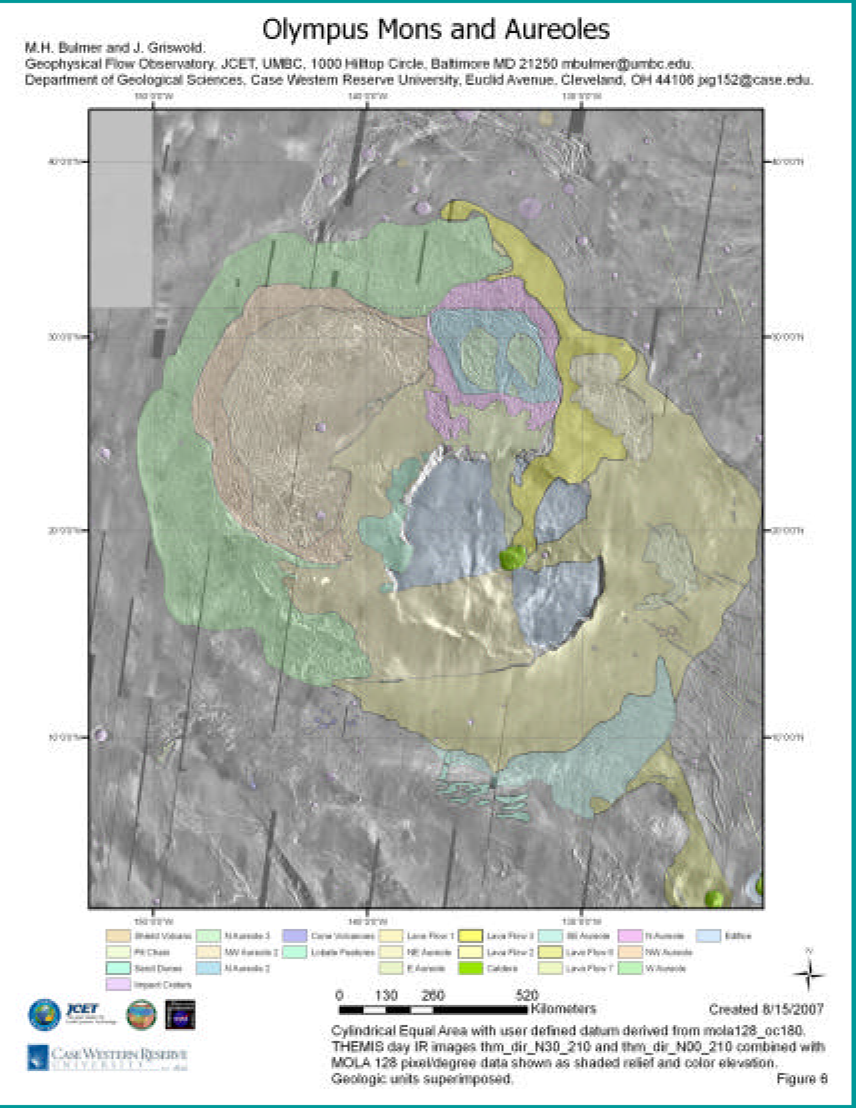

Identifying Aureole Boundaries

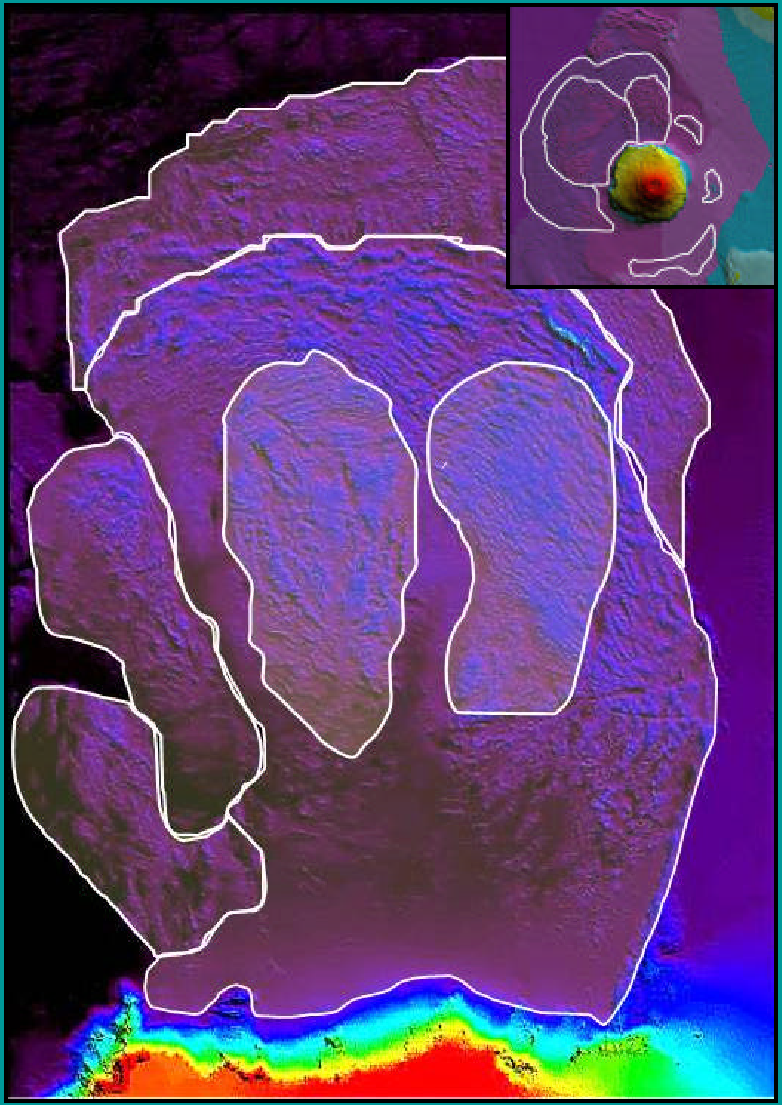

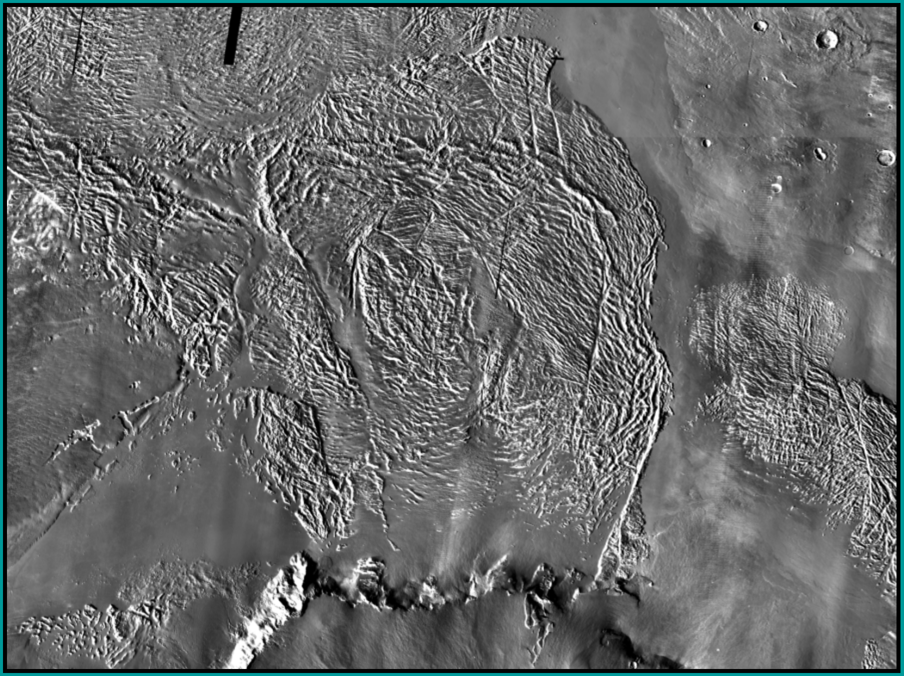

Super-positional relationships within boundaries

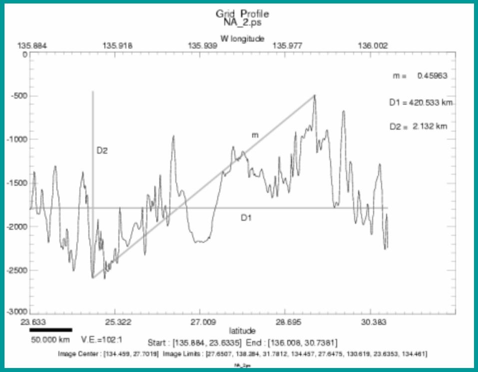

N. Aureole boundaries inferred from image analysis.

Color coded MOLA image gridded 128 ppd

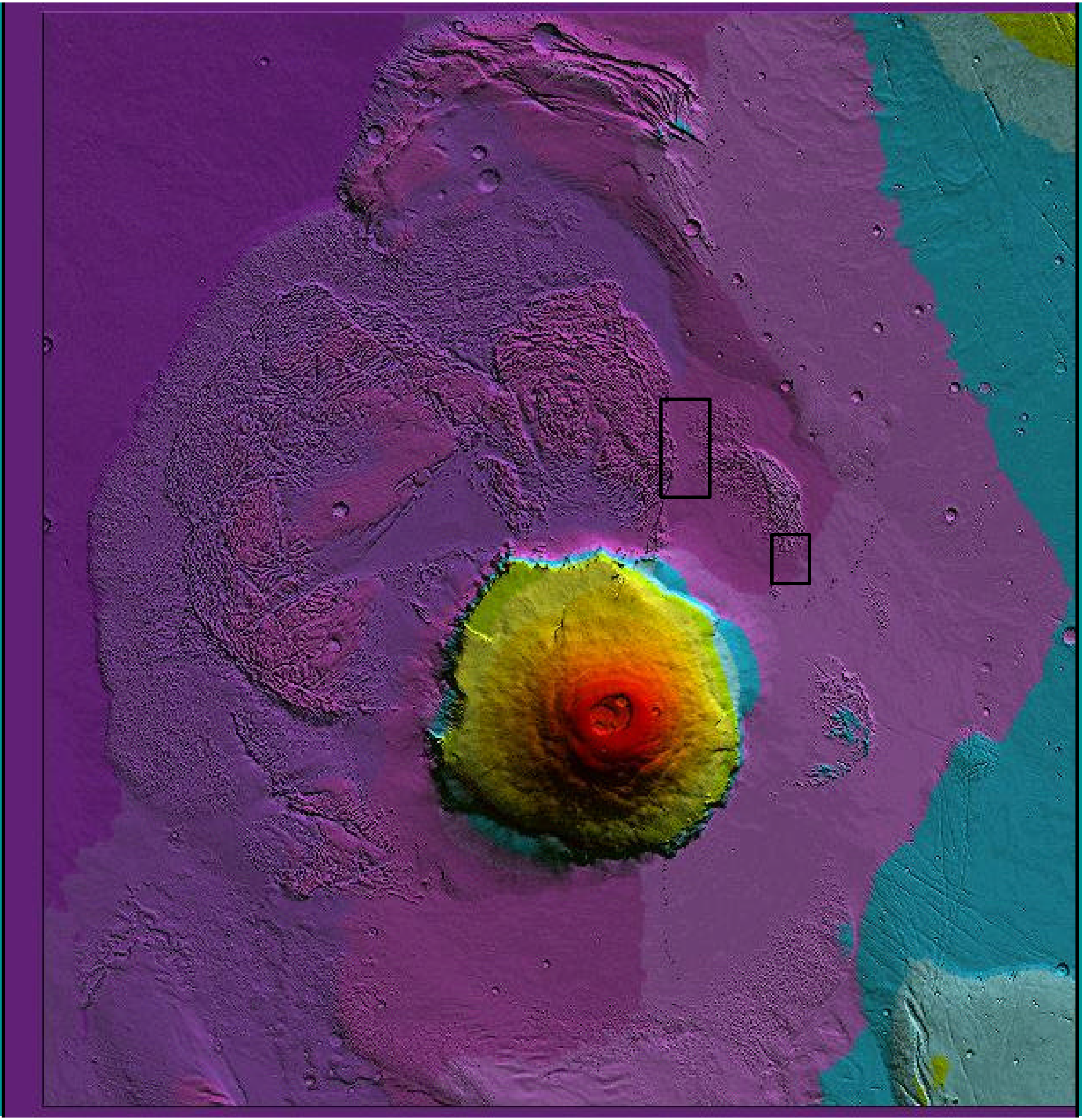

Embayment and Superposition Relations

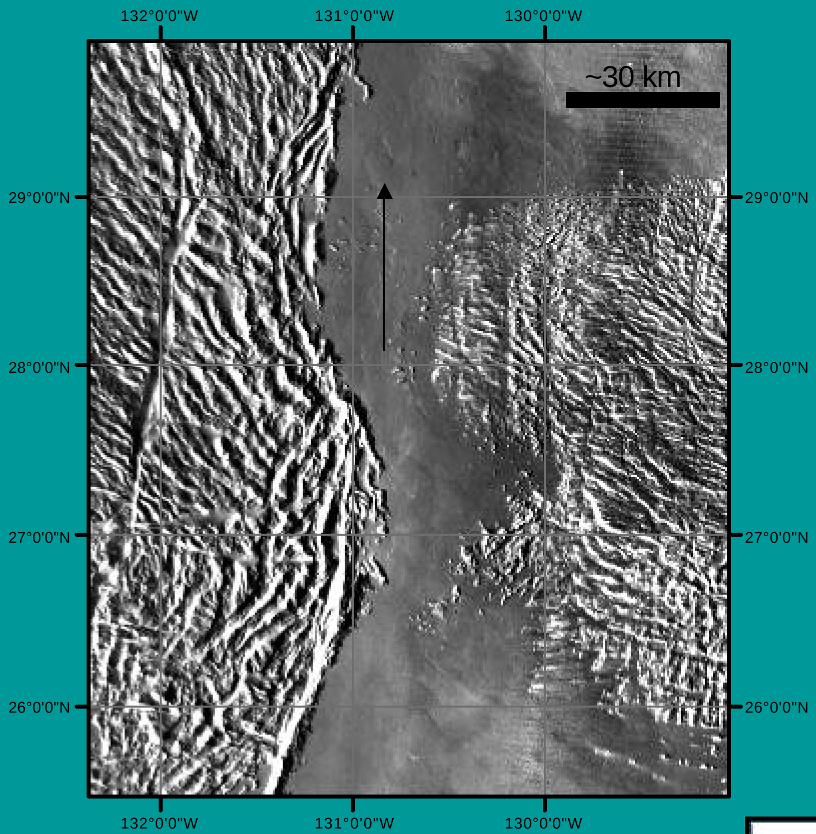

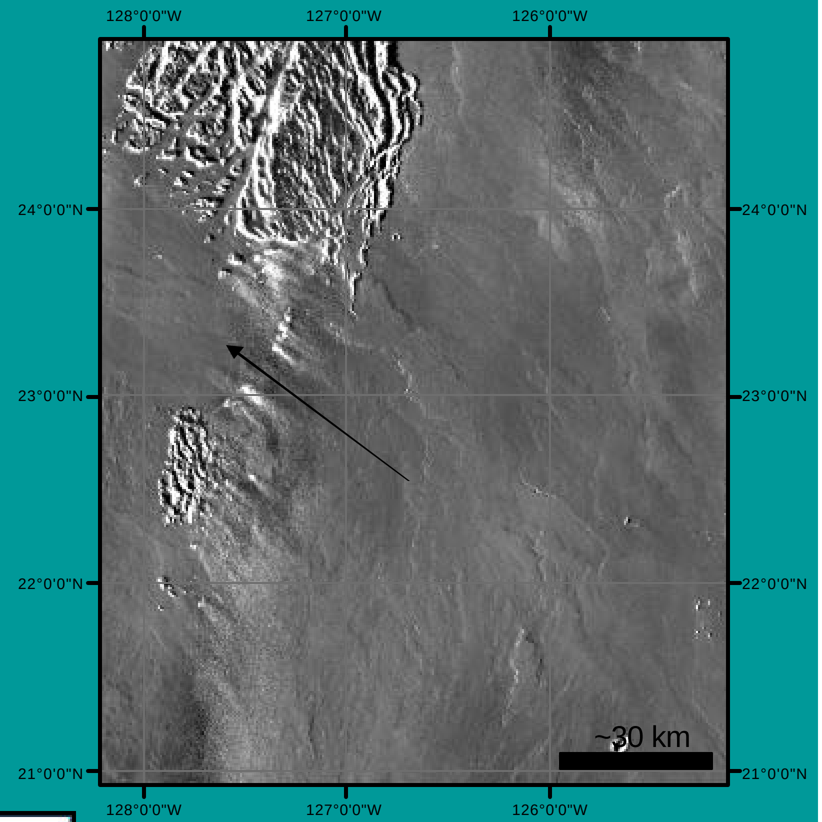

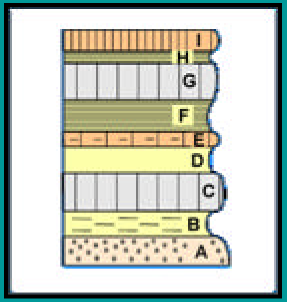

Super-positional relationships between aureole units

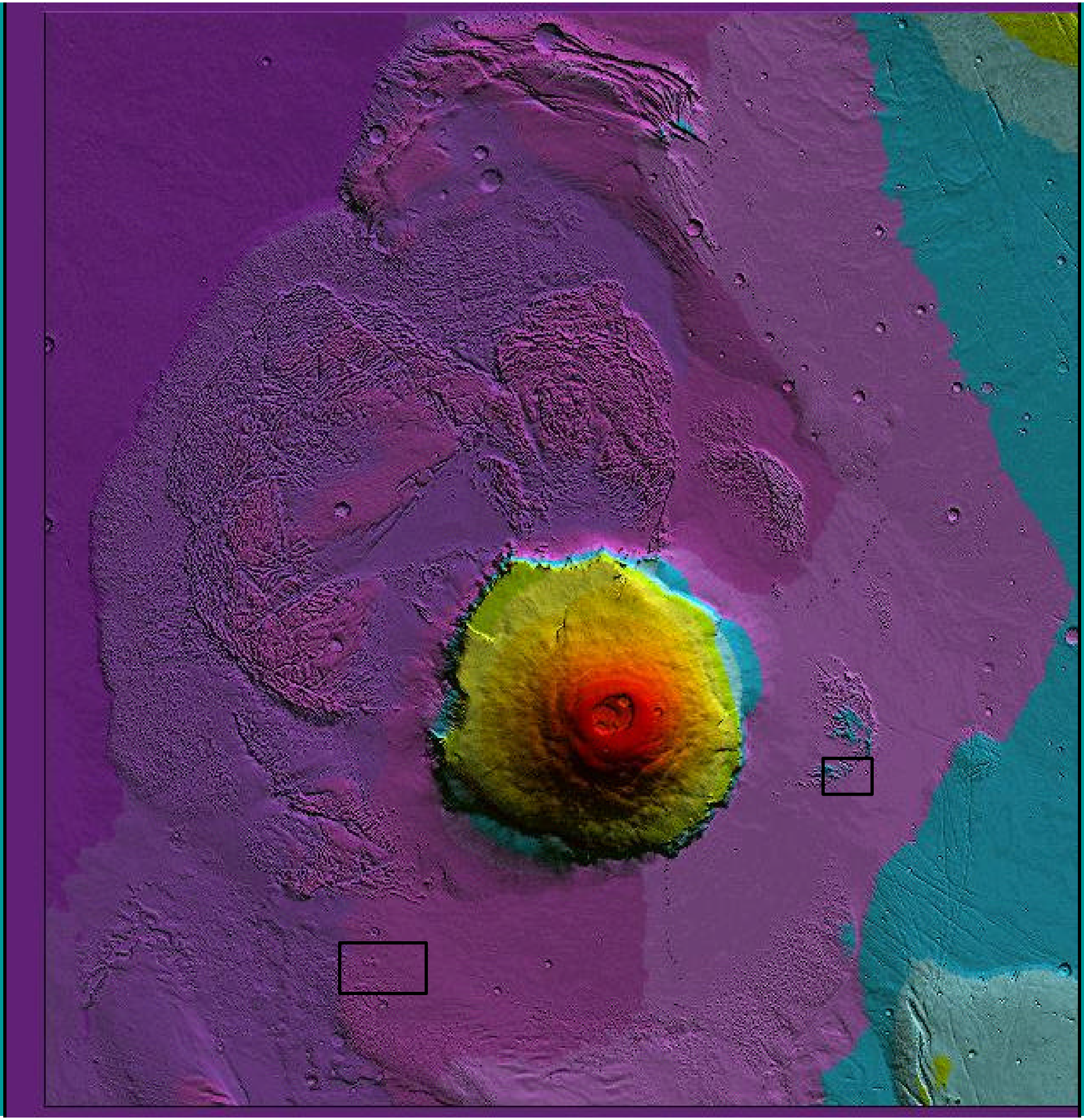

Identifying Features

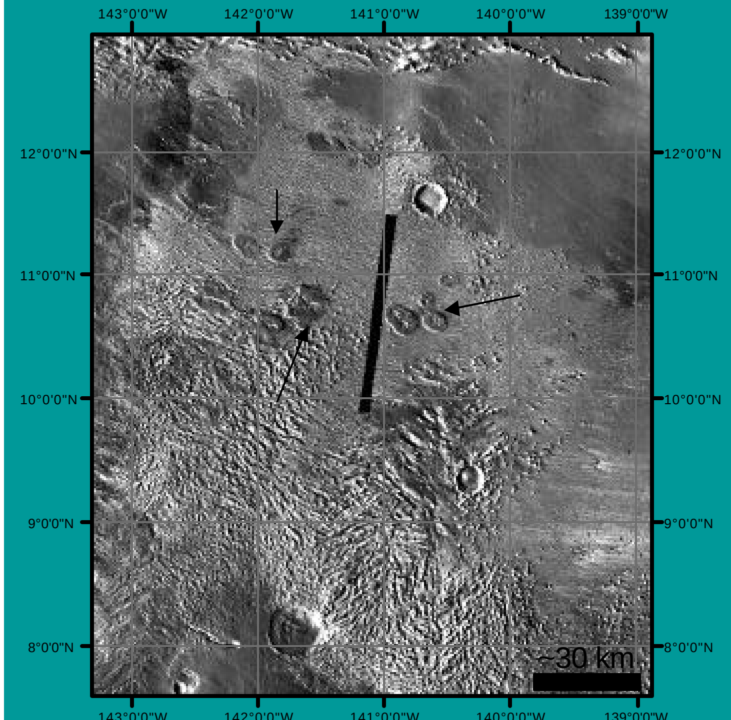

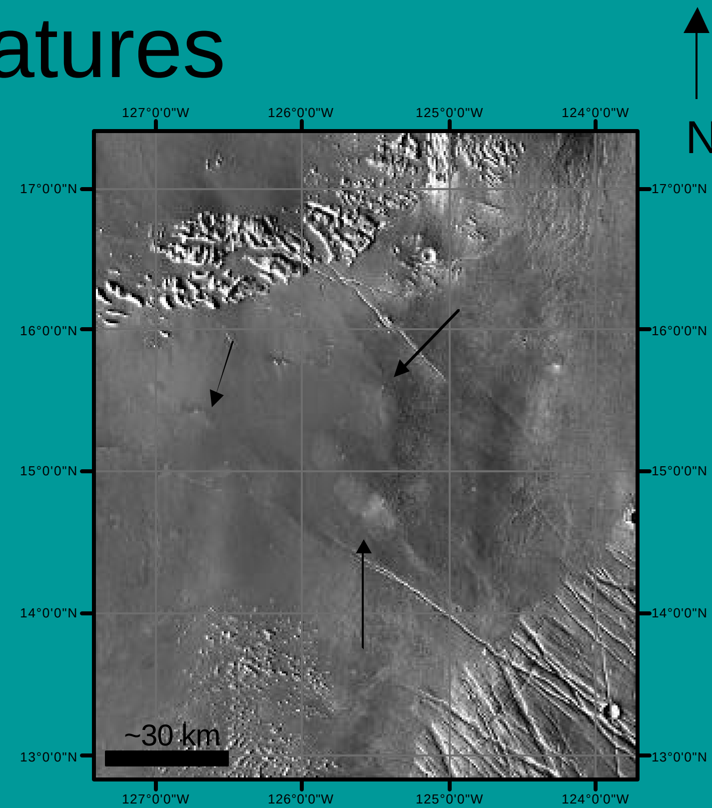

Volcanoes and windstreaks near southeast aureole material.

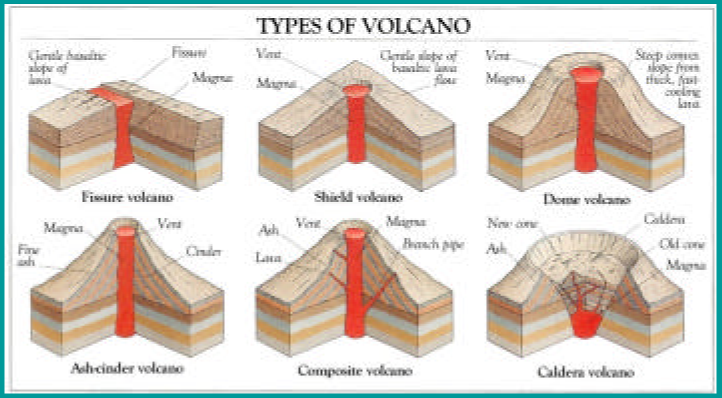

Field of shield volcanoes near east aureole.

Dimensional Analysis

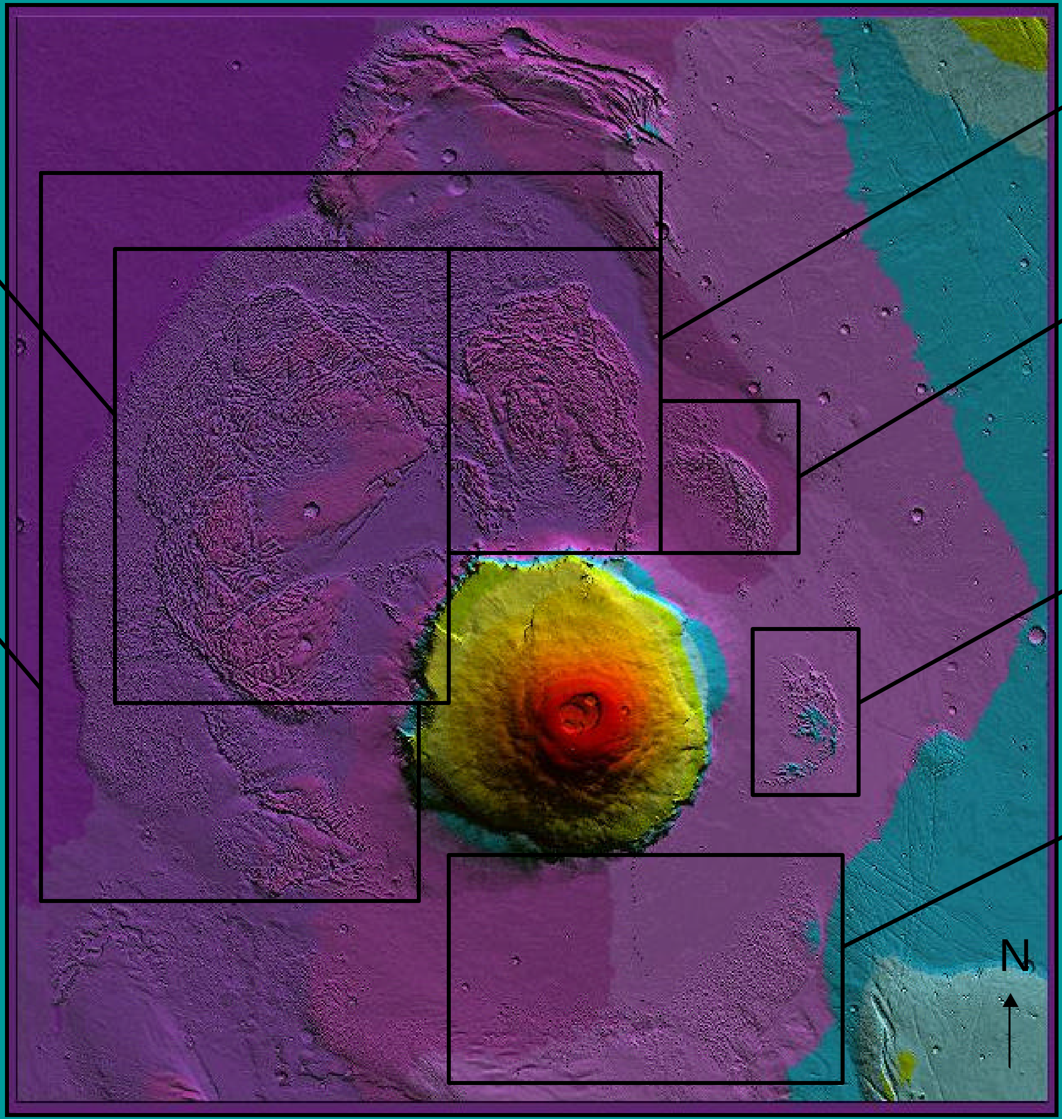

Color coded elevation MOLA image [128 pixel/degree gridded data]

MOLA Analysis Using Gridded Data

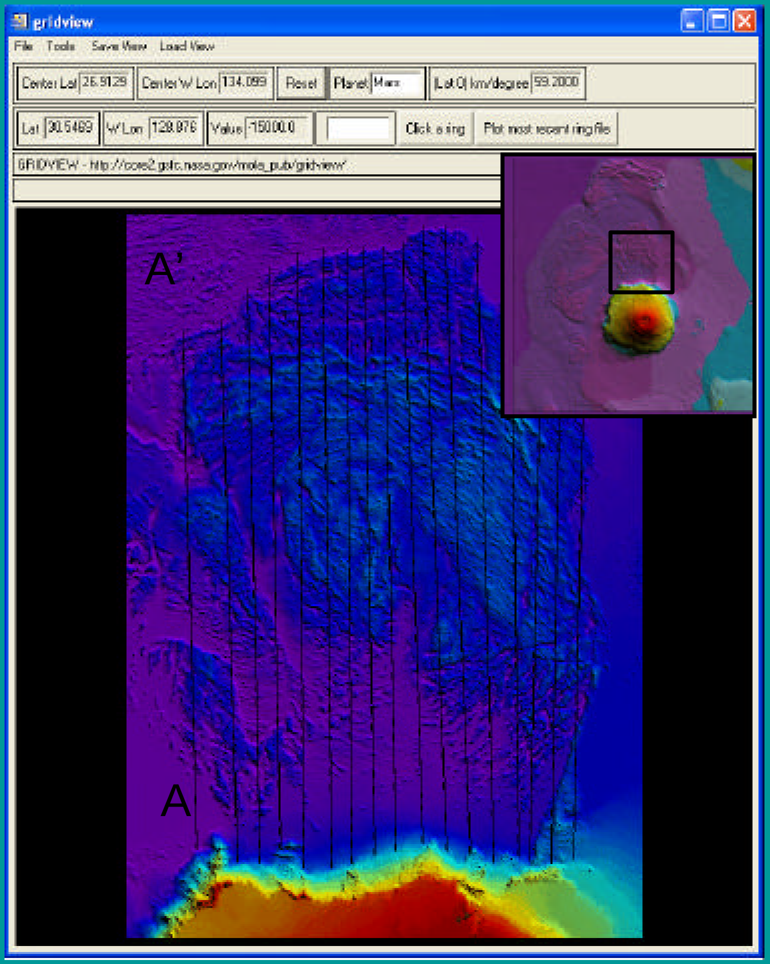

Color enhanced MOLA Image [128pixels/degree]

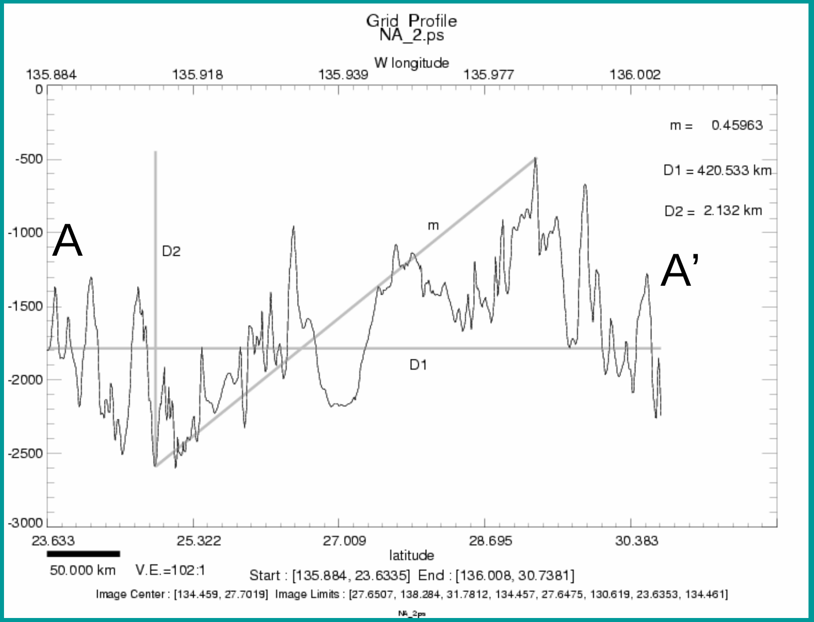

- Define area of interest based on geomorphic map
- Select profile using Profile function in Gridview
- Defined profiles trending E/W and N/S

Data Obtained from Profiles

Aureole Unit	Average Lengths (km)		Average Heights (km)		Average Slope (Degrees)	
	North/ South	East/ West	North/ South	East/ West	North/ South	East/ West
North	433.27	295.23	2.14	1.76	0.6	0.7
Northeast	136.3	115.73	1.2	1.55	0.79	1.19
East	118.32	251.25	1	1.52	0.6	0.51
Southeast	212.91	272.07	0.76	1.09	0.34	0.31
West	639.17	303.21	1.2	1.54	0.12	0.35
Northwest	653.15	461.78	1.79	1.87	0.21	0.77

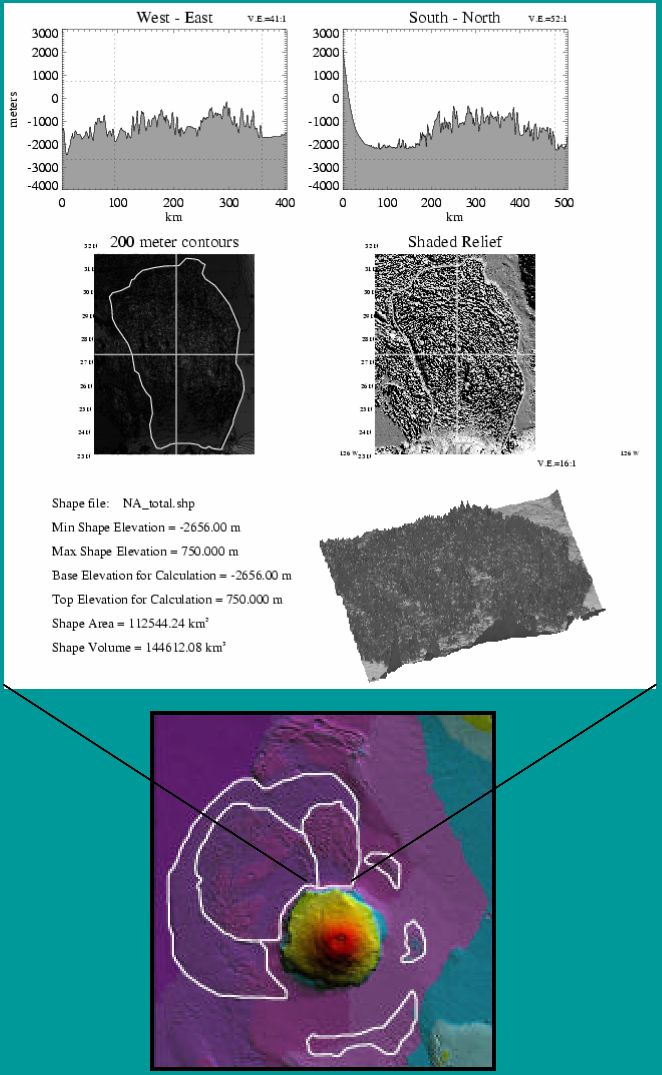

Area and Volume

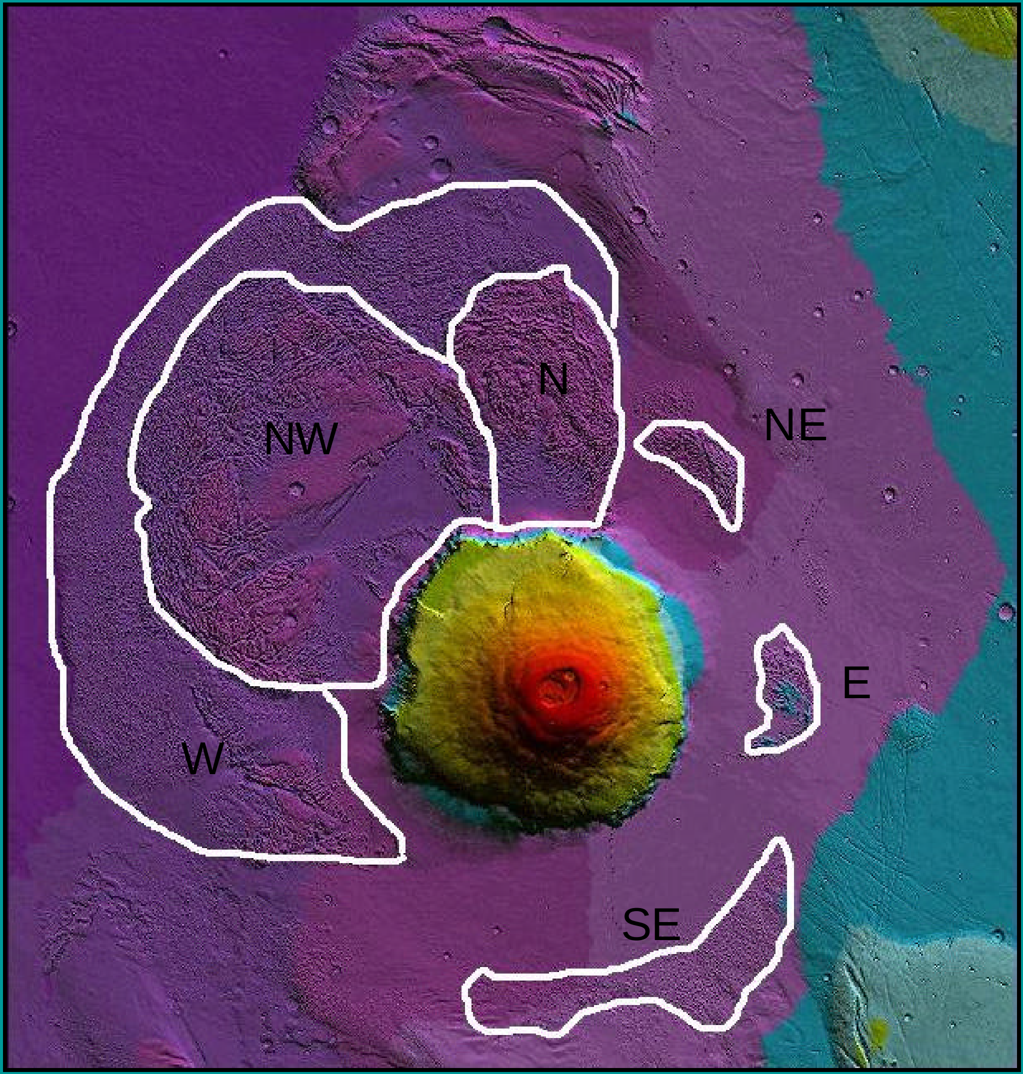

Aureole Unit	Area (x 10^3 km^2)	Volume (x 10^3 km^3)	Lopes (1980) Volume (x 10^3 km^3)	Lopes (1982) Volume (x 10^3 km^3)
North	112.5	144.6		77
Northeast	20.7	25.5	12	33
East	21.5	17.8	10	39
Southeast	74.8	84.8	17	
West	39.3	54.8		75
Northwest	379.8	558.5		197
Southwest			30	
North + Northwest			340	
Total	1002	1379.6	409	421

Olympus Mons edifice volume:
2,701,480.3 km^3

Note: Lopes estimates calculated based only on image data from VO

Area and Volume Relationship

- Do these relationships offer insight into emplacement model?
- Could they *really* be landslides?
- Terrestrial Analogs

Landslide Name	Area (x 10^3 km^2)	Volume (x 10^3 km^3)	Location
North Aureole	112.5	144.6	Mars
Northeast Aureole	20.7	25.5	Mars
East Aureole	21.5	17.8	Mars
Southeast Aureole	74.8	84.8	Mars
West Aureole	39.3	54.8	Mars
Northwest Aureole	379.8	558.5	Mars
Agulhas	20.331	79.488	Submarine SW Africa
Chamais	68.886	17.433	Submarine SW Africa
Cape Town (North and South)	47.952	9.92	Submarine SW Africa
Mauritania	34.3	0.4	Submarine W Africa

Terrestrial landslide data: Dingle (1977), Summerhayes, et al. (1979), and Jacobi (1976)

Conclusions

- Volcanic history is long and dynamic
- MOLA allows for new super-positional relationships to be deduced
- Area and Volume calculations differ from Viking
- Aureole units may be composed of multiple events
- Data support mass movement origin to aureoles but the edifice has changed

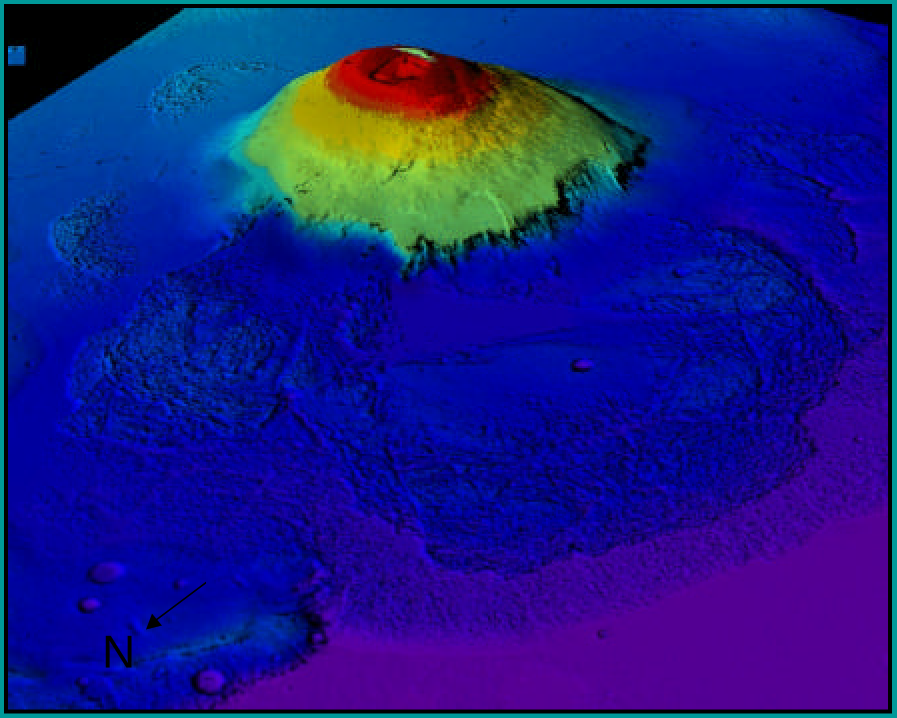

Perspective view (NW/SE) of 128 pixels/degree MOLA image

Acknowledgements and References

Dr. Mark Bulmer
Daniel Beller
Jim Roark, Dr. Scott Mest, Alvin Rentsch
Valerie Casasanto and Dr. Per Gloersen
My fellow Summer Institute Interns
Code 698

- Bulmer, M.H., L.S. Glaze, S. Anderson, and K.M. Shockey (2005), Distinguishing between primary and secondary emplacement events of blocky volcanic deposits using rock size distributions, *J. Geophys. Res., 110.*
- Carr, M.H. (1973), Volcanism on Mars, *J. Geophys. Res.*, 78, 4049-4062.
- Francis, P.W. and G. Wadge (1983), The Olympus Mons aureole: Formation by gravitational spreading, *J. Geophys. Res.*, 88, 8333-8344.
- Lopes, R.M.C., J.E. Guest, and C. J. Wilson (1980), Origin of the Olympus Mons scarp and aureole, *Moon Planets, 22*, 221-234.
- Lopes, R.M.C., J.E. Guest, K. Hiller, and G. Neukum (1982), Further evidence for a mass movement origin for the Olympus Mons aureole, *J. Geophys. Res.*, *87*, 9917-9928.
- McGovern, P.J., J.R. Smith, J.K. Morgan, and M.H. Bulmer (2004), Olympus Mons aureole deposits: New evidence for a flank failure origin, *J. Geophys. Res., 109*,
- Morris, E.C. (1982), Aureole deposits of the Martian volcano Olympus Mons, *J. Geophys. Res., 87*, 1164-1178.
- Morris, E.C., and K.L. Tanaka (1994), Geologic maps of the Olympus Mons region of Mars, *U.S. Geol. Surv. Misc. Invest. Ser. Map, I-2327*.

Northern Aureole
Profile Analysis Observations

- Three elevation 'sets':
  - 1st avg elev = -2000 m
  - 2nd = -1000 m
  - 3rd = -1500 m
- Peaks and troughs associated with different structures and fabric
- Preliminary defining of boundaries

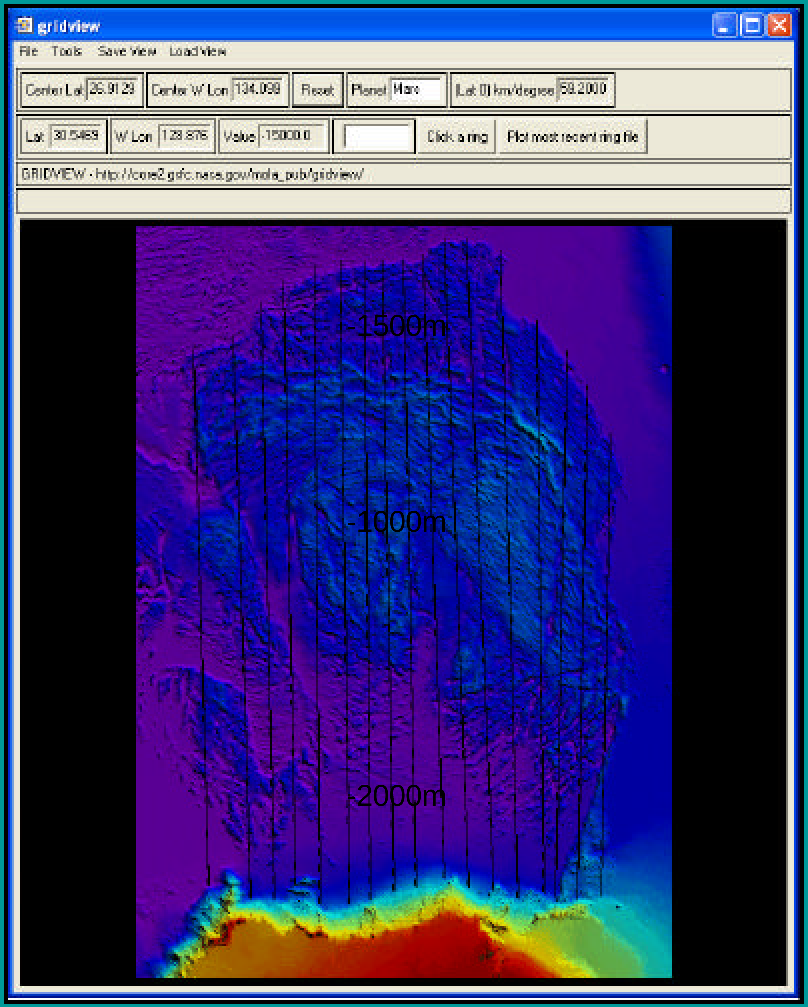

Color enhanced MOLA Image [128pixels/degree] North/South Profiles

Northeastern Aureole
Profile Analysis Observations

- Increase in height moving northeast
- Sharp decrease as end of deposit is reached
- Across aureole (N/S) each profile has a change in elevation of about 1000 m from beginning of profile to highest elevation
- Similar fabric throughout aureole

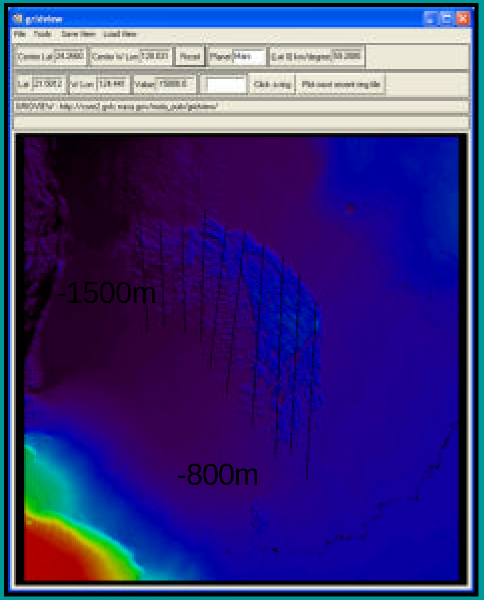

North/South Profiles

Color enhanced MOLA Image [128pixels/degree]

East/West Profiles

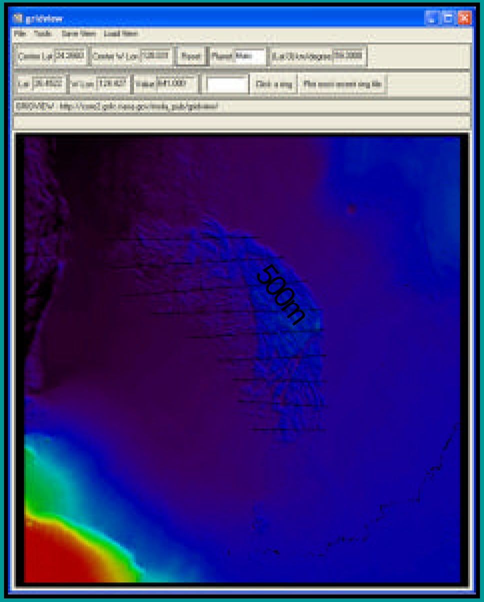

Eastern Aureole

Profile Analysis Observations

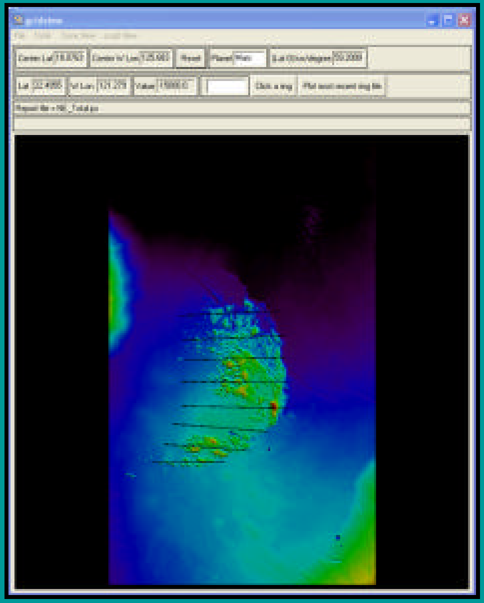

East/West Profiles

Color enhanced
MOLA Image
[128pixels/degree]

North/South Profiles

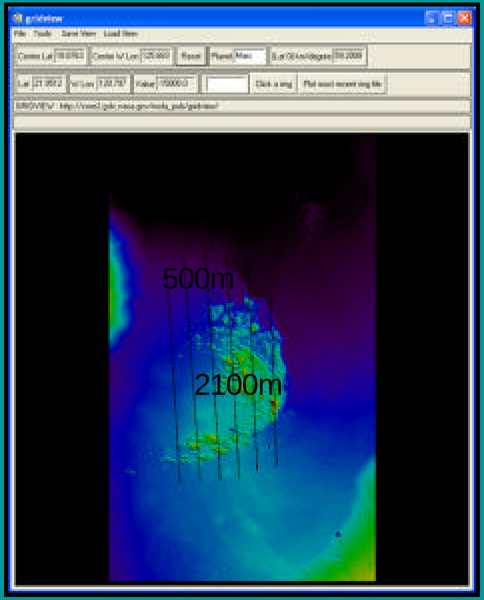

- Blocky in northern part of aureole
- Difficult to relate back to edifice
- Surrounded by smooth surface
- Elevation increasing from ~ 500m to ~ 2000m
- No notable ‘fabric’ to the deposit

Southeastern Aureole

Profile Analysis Observations

- Rougher terrain in western part (peak frequency)
- Surrounded by smooth lava flow that decreases in elevation moving west
- Eastern part of deposit surrounded by lower elevation

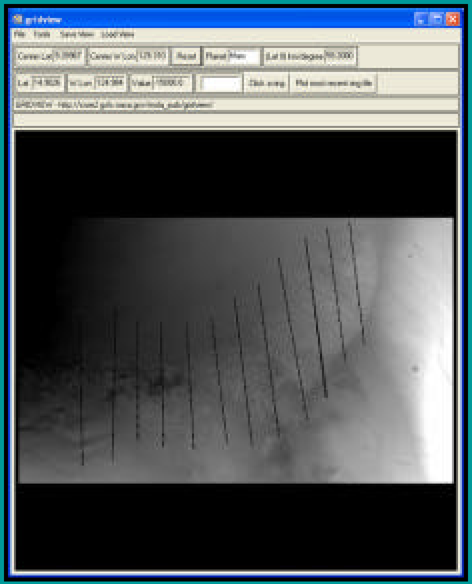

North/South Profiles

East/West Profiles

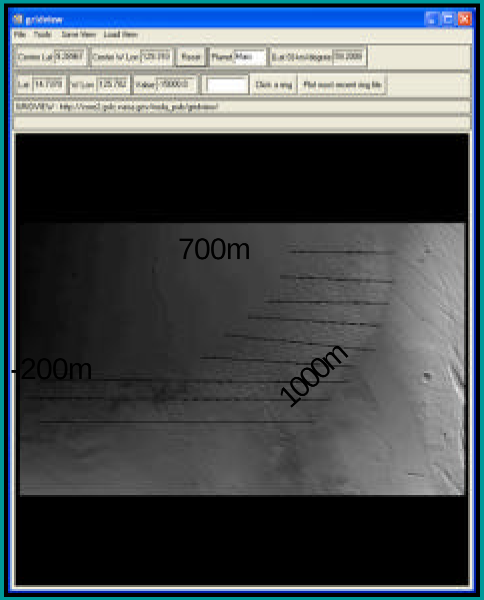

Color enhanced MOLA Image [128pixels/degree]

Northwestern Aureole

Profile Analysis Observations

- Different elevation ‘sets’ possibly corresponding to different depositional units
- Abrupt change from dark blue to lighter blue in eastern part
- Elevation decreases toward edge of aureole (~-2500m)

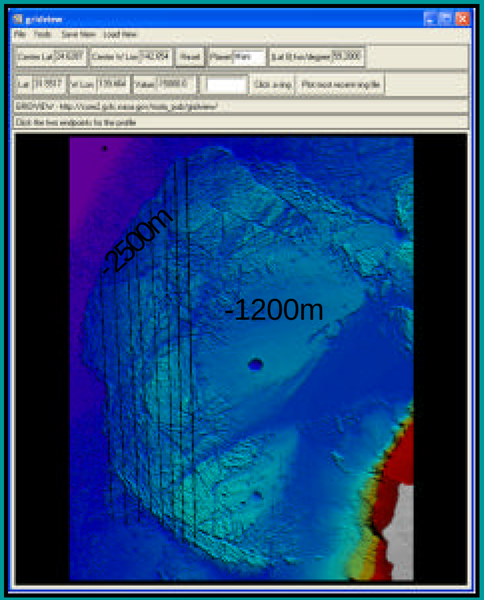

North/South Profiles

East/West Profiles

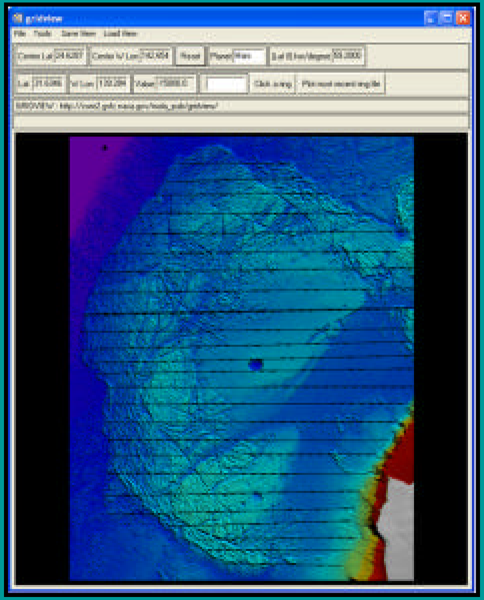

Color enhanced MOLA Image [128pixels/degree]

Western Aureole

Profile Analysis Observations

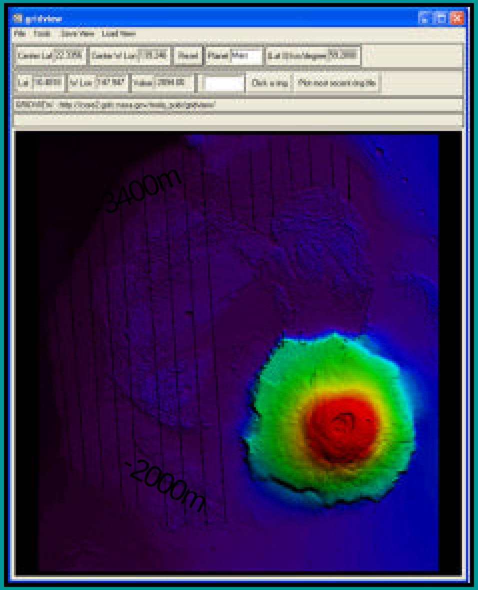

North/South Profiles

East/West Profiles

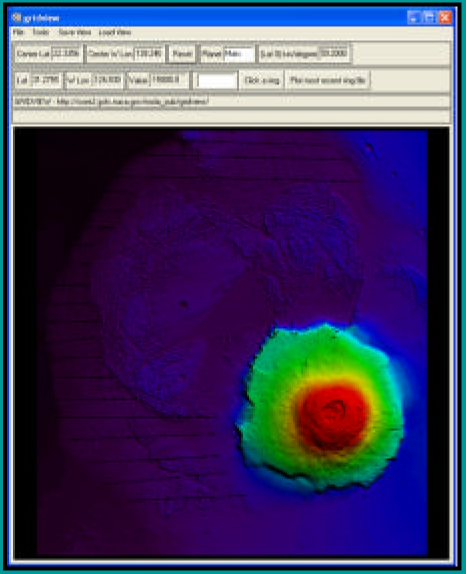

Color enhanced MOLA Image [128pixels/degree]

- Increase in elevation moving south
- Northwestern-most material -3400m
- Southwestern-most material ~-2000m
- Elevation increases toward NW Aureole

MOLA MEGDR Analysis

- Use Fly Through tool in Gridview for aerial images

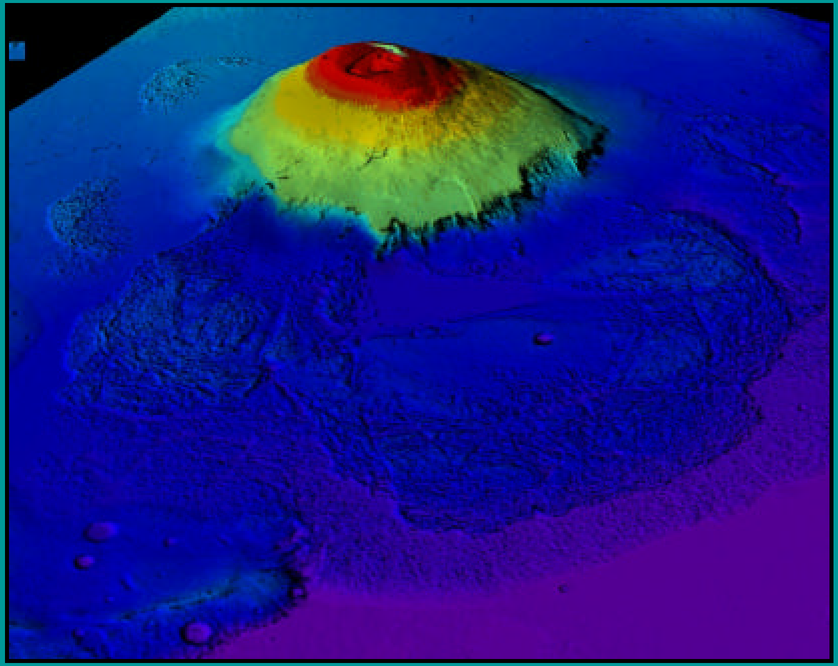

128 pixels/degree MOLA image

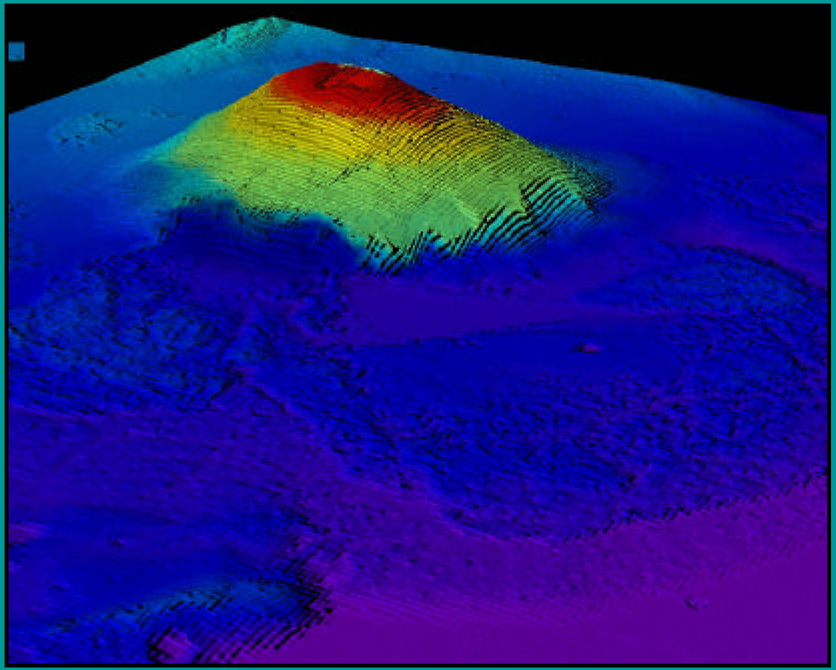

8 pixels/degree MOLA image

Are There Questions to Address?

- Number of aureole units and boundaries
- Dimensional characterization [length, width, slope, area, and volume]
- Topographic variability
- Geomorphology of Area

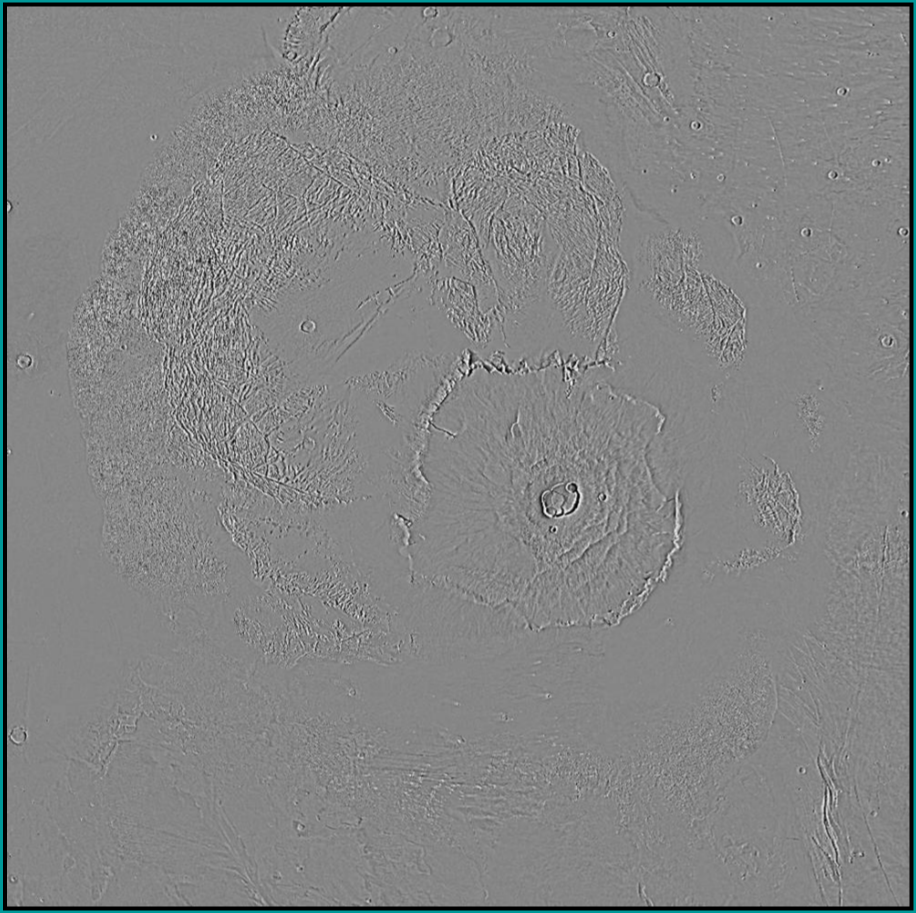

Viking MDIM 32ppd; 1.851 km/pixel

Creating the Map Base

- Combines:
  - THEMIS day IR image mosaic
  - Color coded MOLA 128 pixels/degree data
  - Shaded relief made with MOLA 128 pixel/degree data
- Begin examination of geomorphology

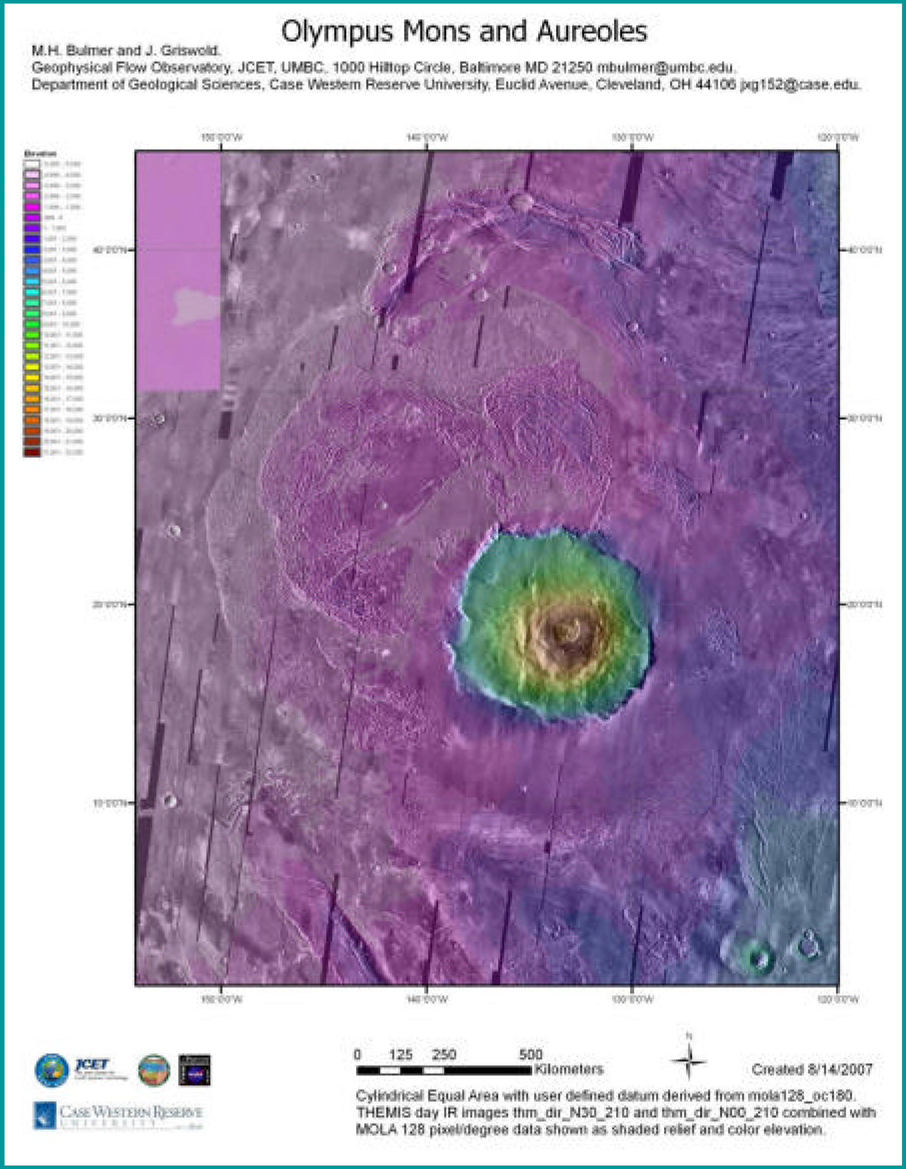

Retrieval of global Aerosol properties

Validation and climatology from MODIS

2007 GSFC Summer Institute

Natalia A. Rodríguez González

Introduction

- Since 2000, MODIS has been deriving aerosol properties over land and ocean by observing spectral radiances in 36 channels (from 0.412 to 14.2µm).

- But MODIS sometimes may over or under predict aerosol properties as the aerosol optical depth (t) and the fine weighting(?).

- With this in mind validation processes are being done to evaluate and learn how to fix the algorithm. Using the AERONET data from more than a hundred of sites around the world we will compare AERONET products with MODIS´s for a better understanding of MODIS working progress .

Aerosols

- What are aerosols?

Aerosols are suspended liquids or solids in the atmosphere, ranging in size from a few molecules to tens of micrometers. Those having radii of about 0.1 and 20µm denotes the approximate separation between “fine” and “coarse” aerosol.

Where do they come from?

Some aerosols occur naturally, originating from volcanoes, dust storms, forest and grassland fires, living vegetation, and sea spray. Human activities, such as the burning of fossil fuels and the alteration of natural surface cover, also generate aerosols.

Why do we care?

Aerosol play an important role in precipitation processes, reduced visibility and because most aerosols reflect sunlight back into space, they have a "direct" cooling effect by reducing the amount of solar radiation that reaches the surface.

Methods

- With an average co-locating of 50 X 50 km MODIS with 1 hour of AERONET, we intend to identify, given a ¨giant¨ spreadsheet of thousands of MODIS/AERONET co-locations around the world from the entire MODIS mission, the regions where MODIS compares well or not so well with AERONET.

- We will separate the data in five main regions: North America, East and West, Central America and The Caribbean, South America and Africa. For each region we will plot the t against the DOY (Day of the year), FW, Angstrom exponent and the water vapor, as well AERONET products vs. MODIS´s

North America-East

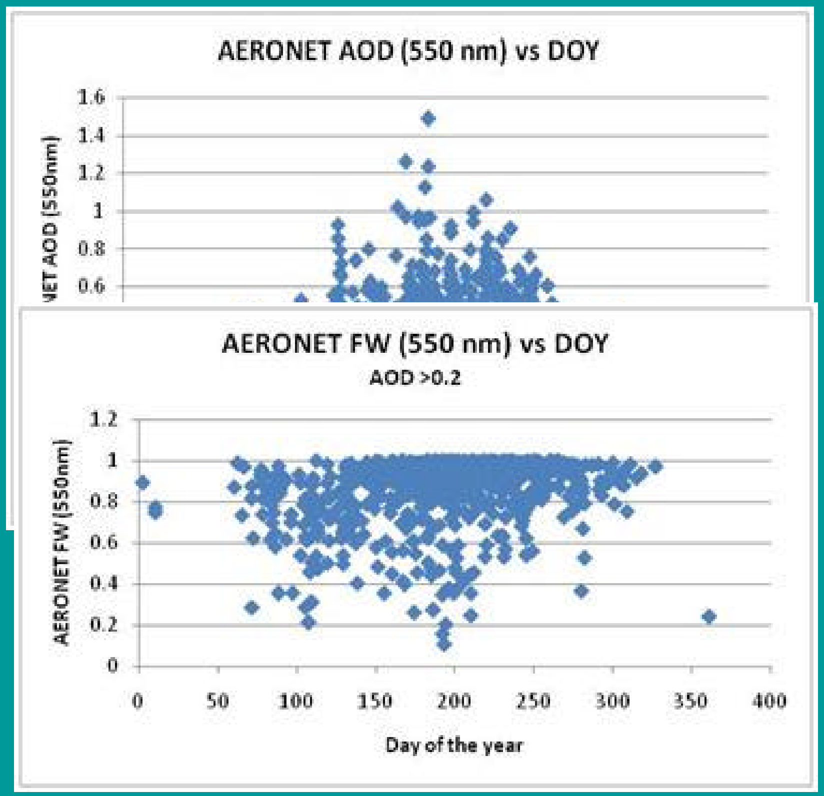

In this side of the continent AERONET data shows that most of the year it has an AOD under 0.2 , but during the summer the AOD values go up during most of the days, with the highest point reaching an AOD = 1.4 in COVE

Mostly during summer there´s a FW=1 in the East the aerosol the type of aerosol that can be found is basically fine mode aerosol with a FW rating between 0.8 and 1. In the other hand we also find data with a FW lower than 0.2, as in Bondville site on DOY 192 were is registered a FW= 0.1559, almost coarse aerosol.

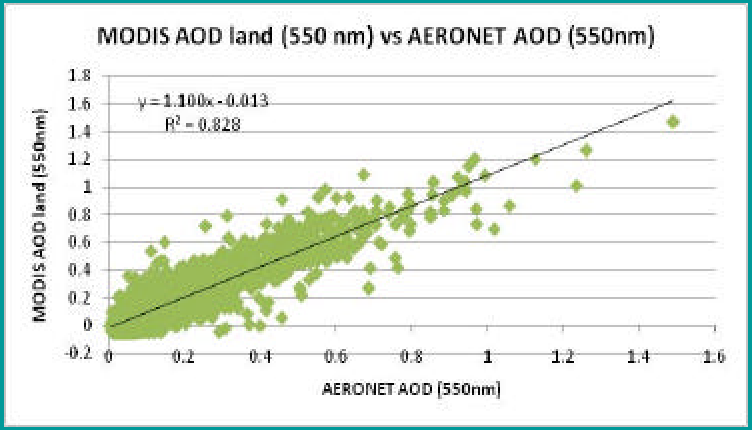
MODIS AOD land (550 nm) vs AERONET AOD (550nm)
y = 1.100x - 0.013
R² = 0.828
MODIS AOD land (550nm)
AERONET AOD (550nm)

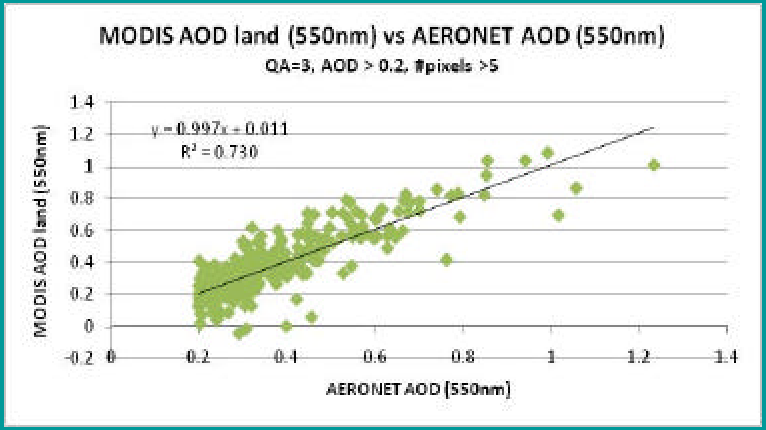
MODIS AOD land (550nm) vs AERONET AOD (550nm)
QA=3, AOD > 0.2, #pixels >5
y = 0.997x + 0.011
R² = 0.730
MODIS AOD land (550nm)
AERONET AOD (550nm)

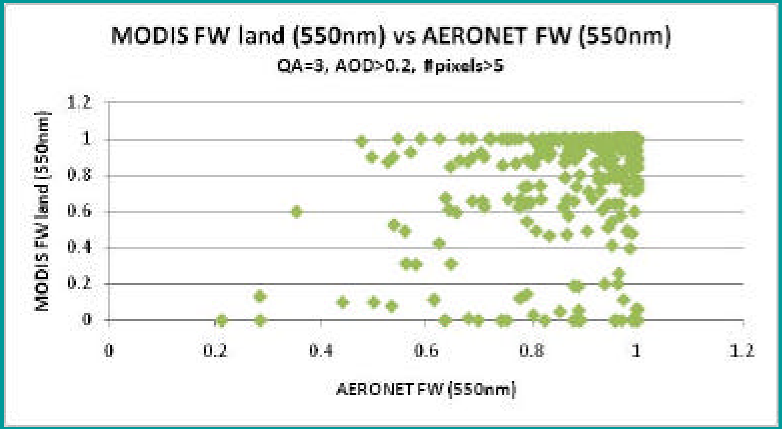
MODIS FW land (550nm) vs AERONET FW (550nm)
QA=3, AOD>0.2, #pixels>5
MODIS FW land (550nm)
AERONET FW (550nm)

North America-West

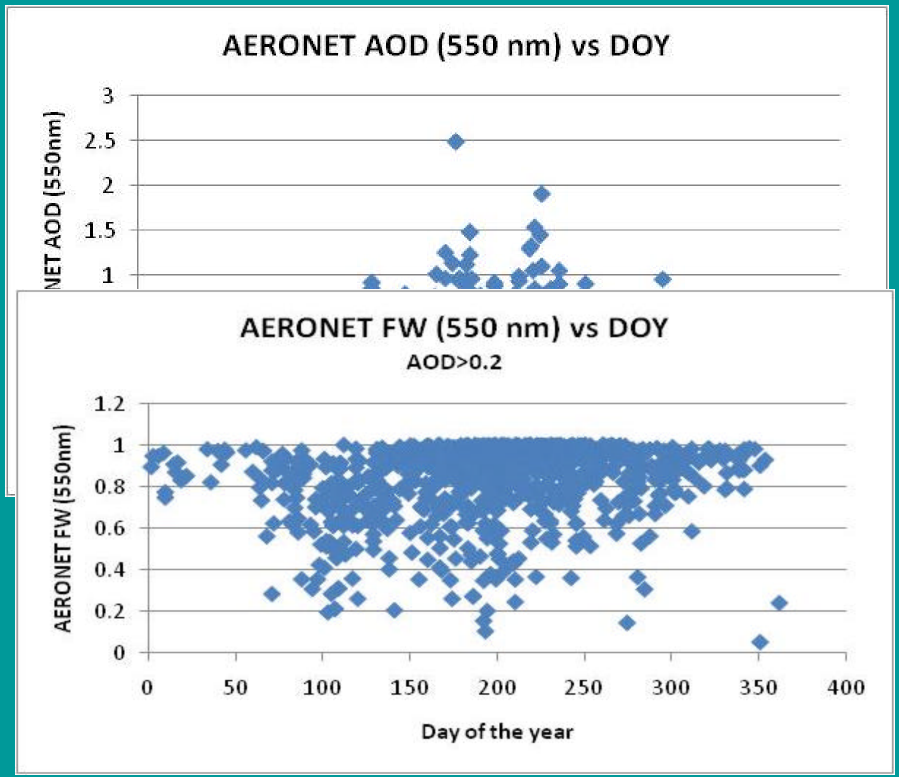

In the west of North America the values of AOD remain most of the year under 0.5, but with the summer season these values arise considerably, not in the number of the days but in the intensity of the values, what may be due to the constant forests fires. Most of the year the aerosol we find in this region is fine mode aerosol with higher concentrations during the summer time with an FW = 1. But we also have cases that show low FW values during the summer as on day 350 La Jolla site show a FW = 0.0541.

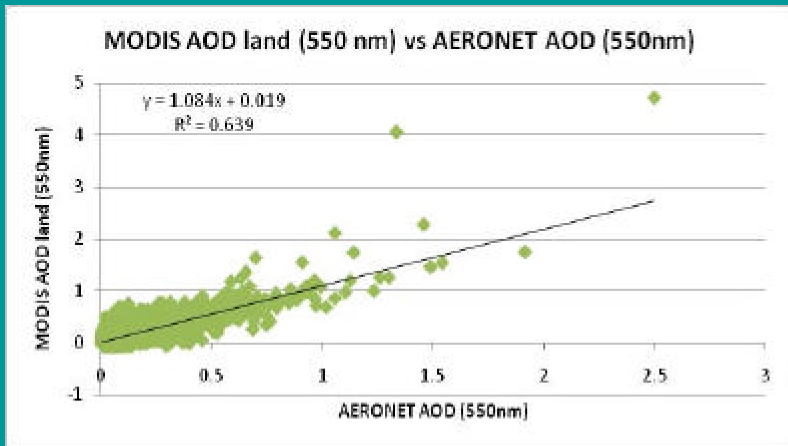
MODIS AOD land (550 nm) vs AERONET AOD (550nm)
y = 1.084x + 0.019
R^2 = 0.639
MODIS AOD land (550nm)
AERONET AOD (550nm)

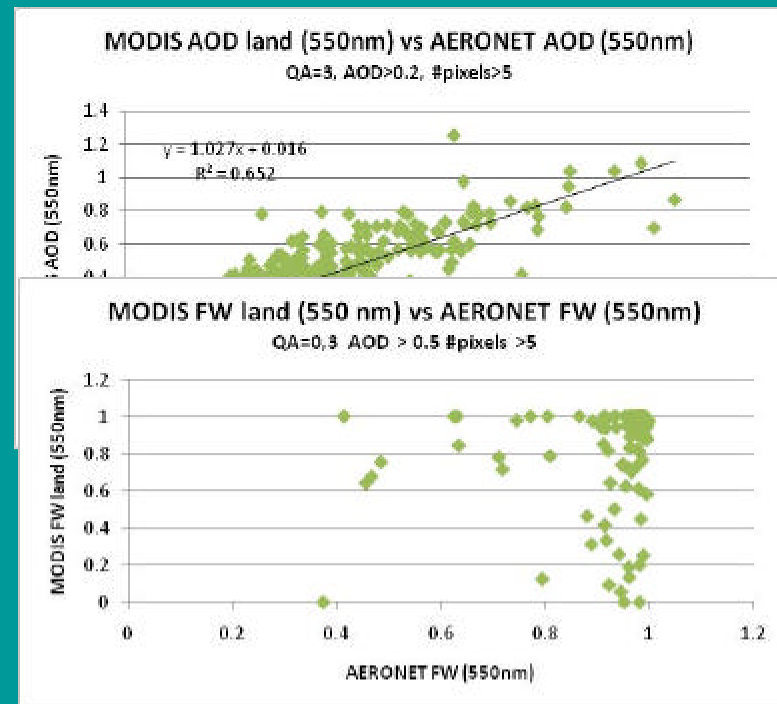
MODIS AOD land (550nm) vs AERONET AOD (550nm)
QA=3, AOD>0.2, #pixels>5
y = 1.027x + 0.016
R^2 = 0.652
MODIS FW land (550 nm) vs AERONET FW (550nm)
QA=0,3 AOD > 0.5 #pixels >5
MODIS FW land (550nm)
AERONET FW (550nm)

Central America and The Caribbean

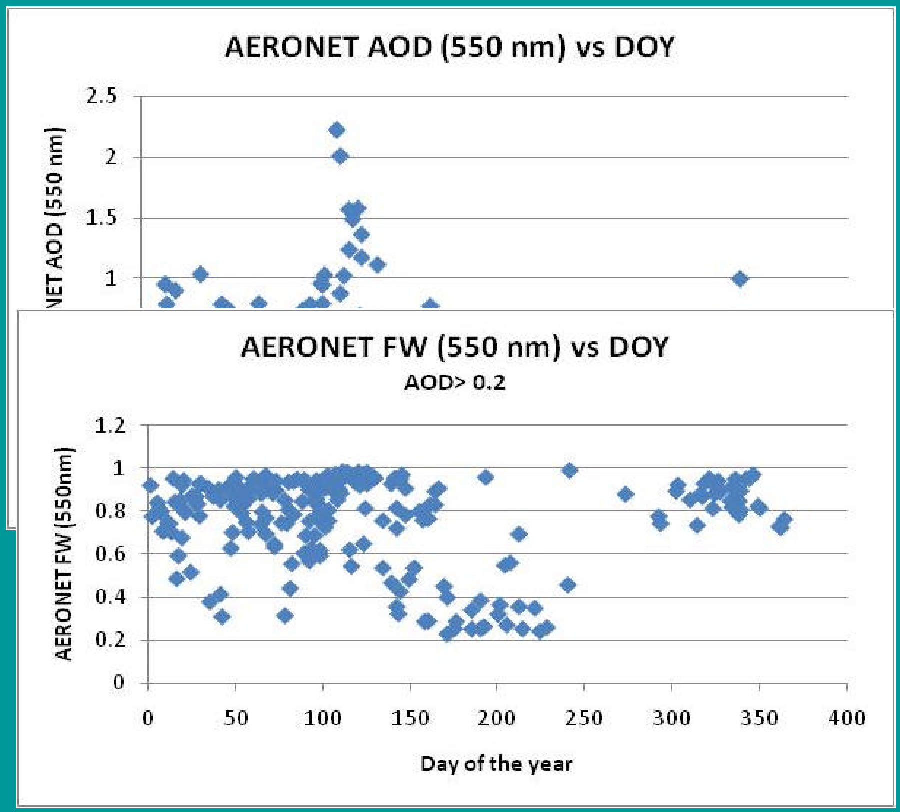

In Central America and the Caribbean, the high AOD values are given at the beginning and the end of the year, where we encounter a maximum AOD of 2.2 on DOY 111, with a FW values between 0.6 and 1 (AOD>0.2) .

But during the summer, AOD values are quite low, with an AOD under 0.5 and a FW between 0.2 – 0.6.

We found that during the summer the data received is mostly from the Caribbean Sea, (La Parguera, Puerto Rico) .

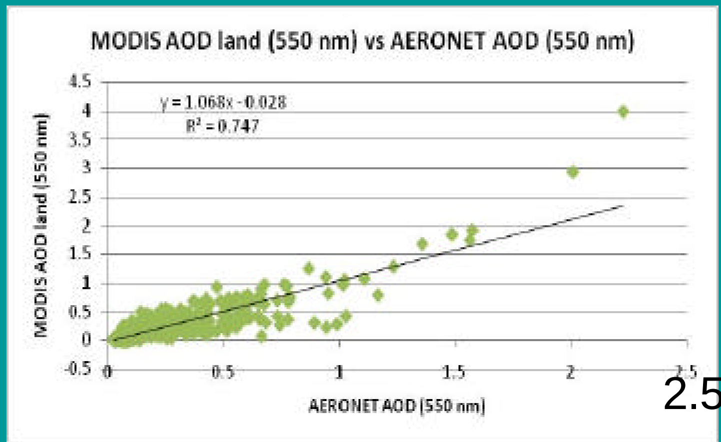
MODIS AOD land (550 nm) vs AERONET AOD (550 nm)
y = 1.068x - 0.028
R² = 0.747
MODIS AOD land (550 nm)
AERONET AOD (550 nm)
2.5

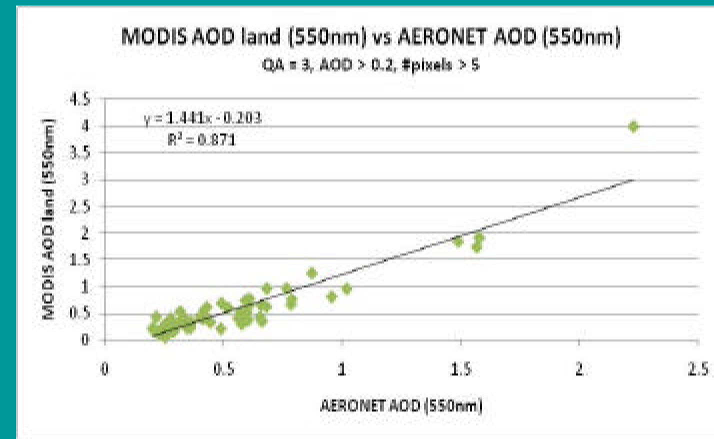
MODIS AOD land (550nm) vs AERONET AOD (550nm)
QA = 3, AOD > 0.2, #pixels > 5
y = 1.441x - 0.203
R² = 0.871
MODIS AOD land (550nm)
AERONET AOD (550nm)

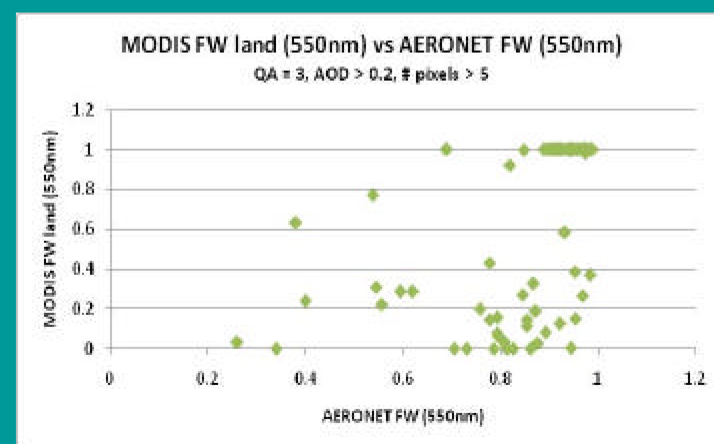
MODIS FW land (550nm) vs AERONET FW (550nm)
QA = 3, AOD > 0.2, # pixels > 5
MODIS FW land (550nm)
AERONET FW (550nm)

South America

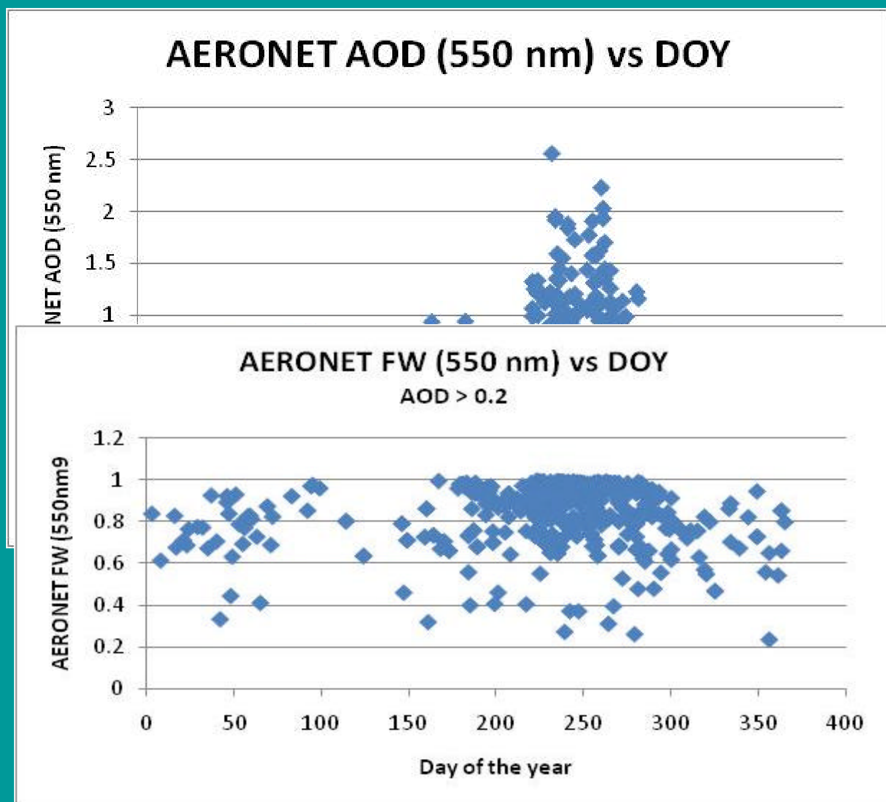

During most of the year in South America the values of AOD remain under 0.5, but during the summer this values arise up to 2.5, with a FW mostly reaching 1 during this period that coincides with the slash and burning season that starts in the summer with the end of rains.

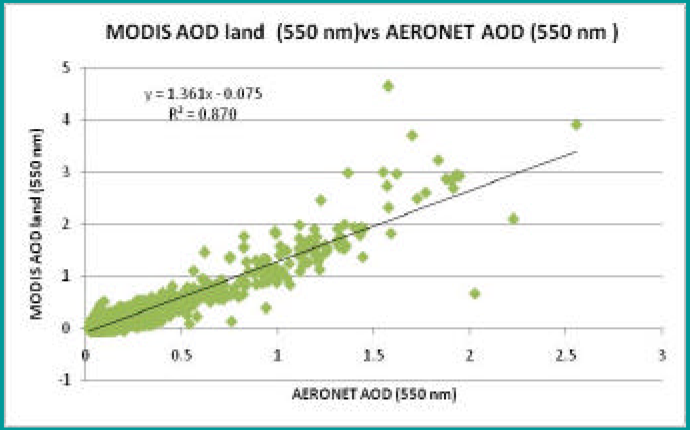
MODIS AOD land (550 nm)vs AERONET AOD (550 nm)
y = 1.361x - 0.075
R^2 = 0.870
MODIS AOD land (550 nm)
AERONET AOD (550 nm)

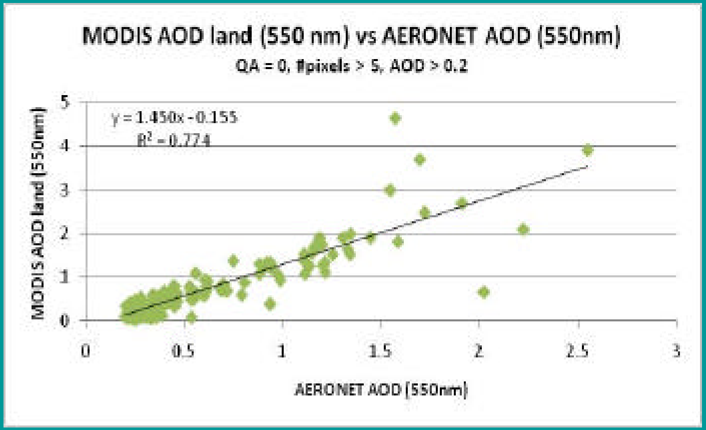
MODIS AOD land (550 nm) vs AERONET AOD (550nm)
QA = 0, #pixels > 5, AOD > 0.2
y = 1.450x - 0.155
R^2 = 0.774
MODIS AOD land (550nm)
AERONET AOD (550nm)

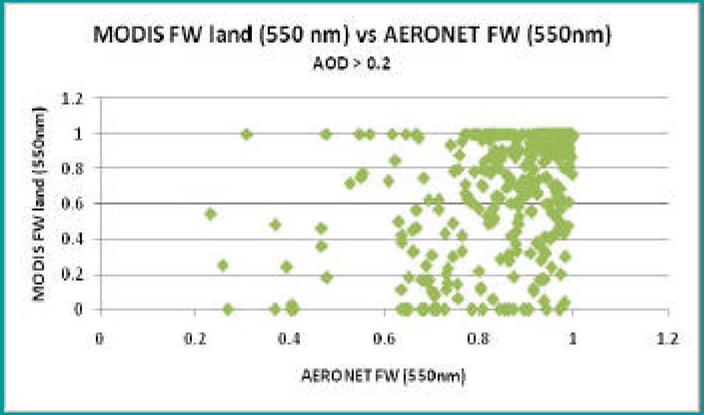
MODIS FW land (550 nm) vs AERONET FW (550nm)
AOD > 0.2
MODIS FW land (550nm)
AERONET FW (550nm)

Africa

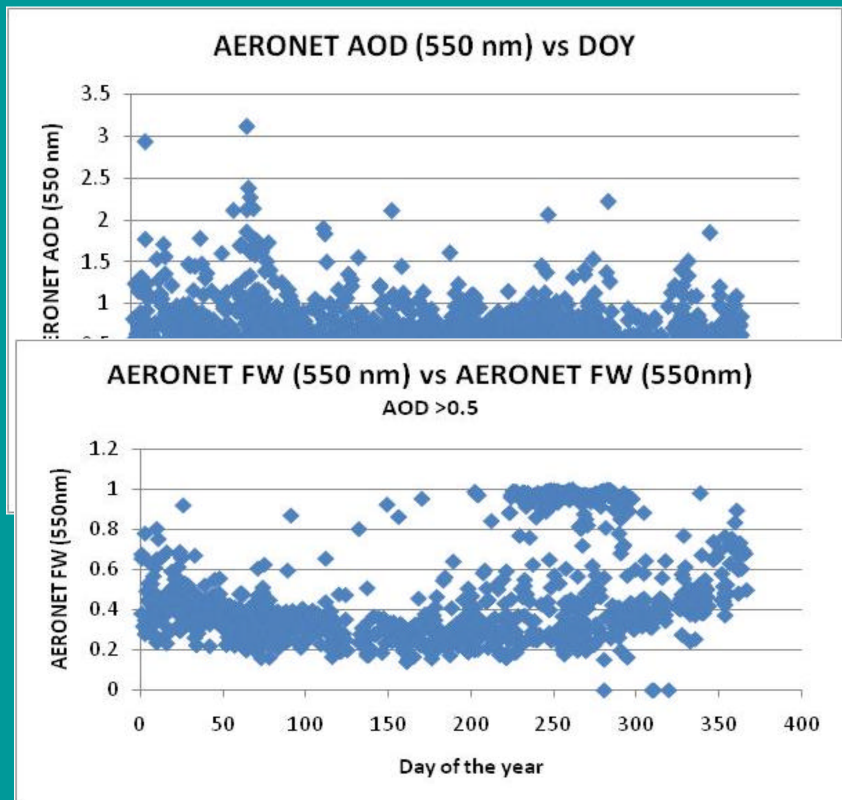

With more than a hundred stations over the entire continent, AERONET products show that most of the year AOD values remain generally under 1, but it also show some scatter data over 1 but nothing distinctive, no patron of elevation or a drop in values. With an AOD >0.5, we found that the prevailing type of aerosol is the fine mode aerosol with a FW between 0.2 and 0.4 during the middle of the year and high and low at the beginning and end of the year. But we also find a separation of points during the period from day 200 to 300, with a group of points with a clear FW value of one, all of this points come from AERONET site in south Africa.

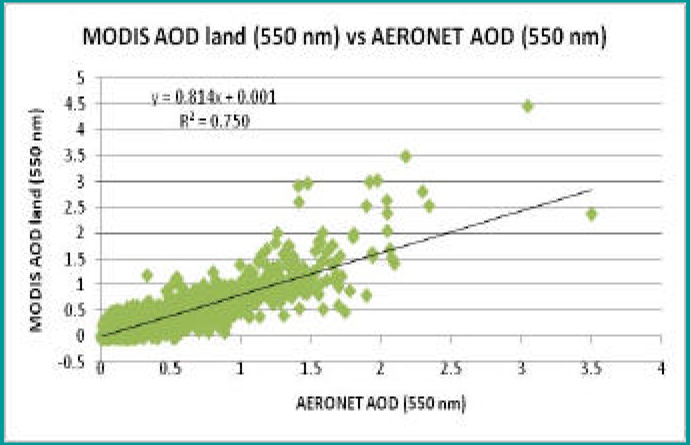
MODIS AOD land (550 nm) vs AERONET AOD (550 nm)
y = 0.814x + 0.001
R² = 0.750
MODIS AOD land (550 nm)
AERONET AOD (550 nm)

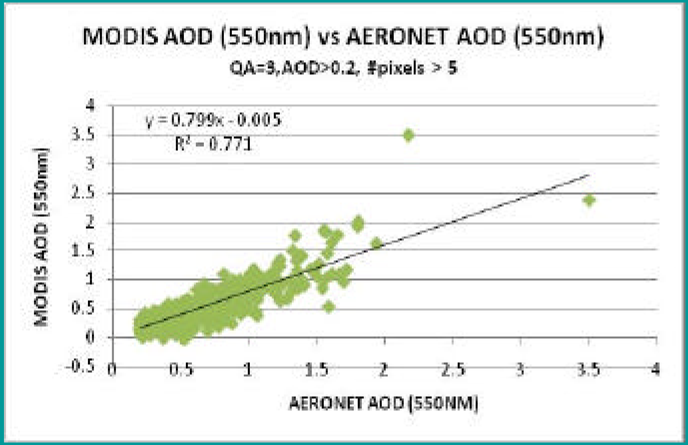
MODIS AOD (550nm) vs AERONET AOD (550nm)
QA=3,AOD>0.2, #pixels > 5
y = 0.799x - 0.005
R² = 0.771
MODIS AOD (550nm)
AERONET AOD (550NM)

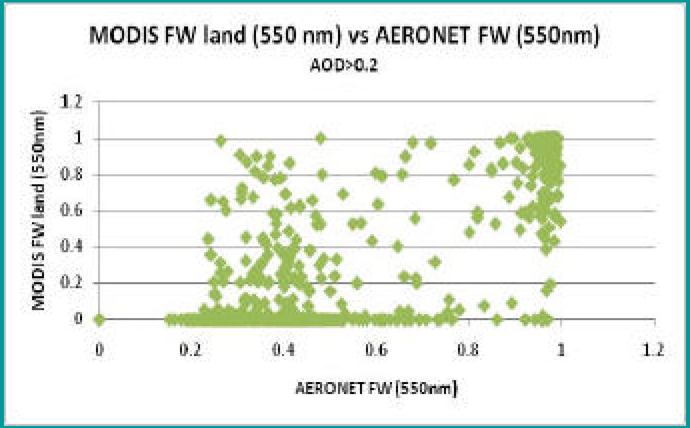
MODIS FW land (550 nm) vs AERONET FW (550nm)
AOD>0.2
MODIS FW land (550nm)
AERONET FW (550nm)

Conclusion

- During are validation of MODIS products we found that over the five regions that were studied, MODIS retrievals of aerosol properties as the aerosol optical depth are fairly well in comparison with AERONET´s and its variability has a seasonal dependence, with higher values during the summer in most regions.

- MODIS algorithm still shows room for improvement since there´s no correlation between products when it comes to the aerosol fine weighting, where only a slight portion of our data has a good retrieval from both, MODIS and AERONET, showing the places where the algorithm works.

Compiling a climatology of smoke plume injection heights from satellite measurements

By: Shawn Gindhart (Millersville University)
Mentor: Charles Ichoku (UMD/ESSIC, NASA/GSFC, Code 613.2)

MillersvilleMeteorology

Presented at the GSFC 2007 Summer Institute Program

Image: Terra MODIS, May 11, 2007, 16:30 UTC, Courtesy of MODIS Rapid Response Team

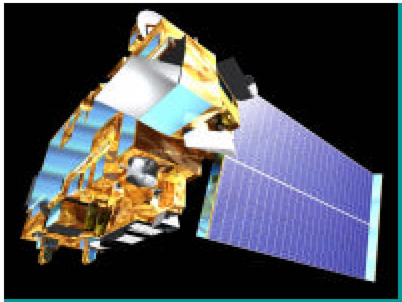

Terra Spacecraft

Overview…

- Find Fires
- Database
- Satellite Remote Sensing
- Smoke plume injection heights
- Showing all heights on a global picture, using IDL

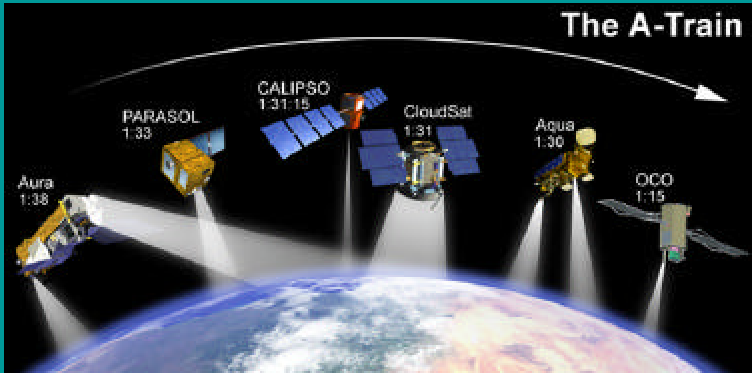

The Main Websites Used to Find Fires

http://rapidfire.sci.gsfc.nasa.gov/

http://earthobservatory.nasa.gov/

http://eosweb.larc.nasa.gov/HPDOCS/misr/misr_html/misr_gallery_index.html

Smoke Plume Statistics

- Date
- Time (UTC)- Time was given in the MODIS Rapid Response System Images only
- Latitude/Longitude – Used Google Earth
- Fire Source – Aqua or Terra MODIS
- Name of location
- Mean Plume Heights (km) = MISR plume height minus topographic heights
- Minimum plume heights
- Maximum plume heights
- Data Source (MISR, CALIPSO, ICESat GLAS)
- Topographic heights (km)
- Website

Moderate resolution Imaging Spectroradiometer (MODIS)

- On board Terra…

  Launched December 1999

- On board Aqua…

  Launched May 2002

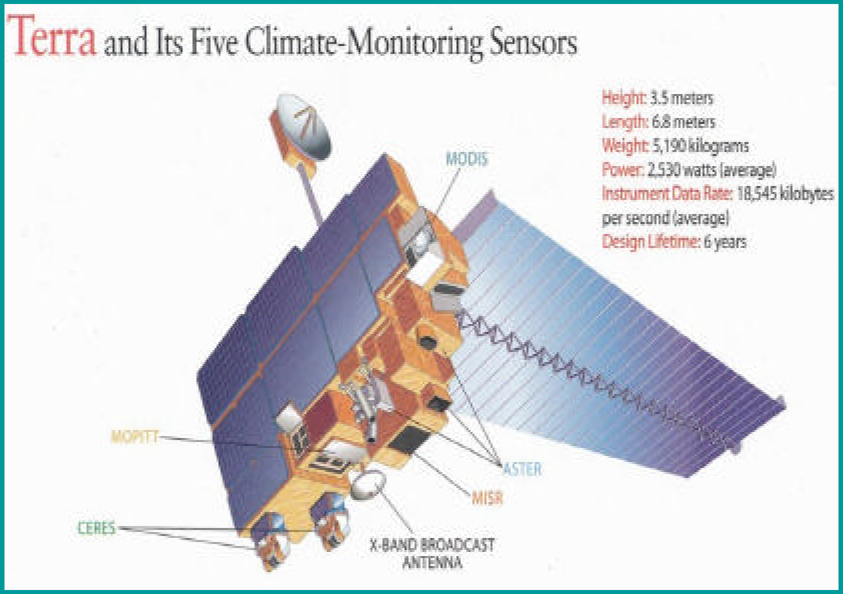

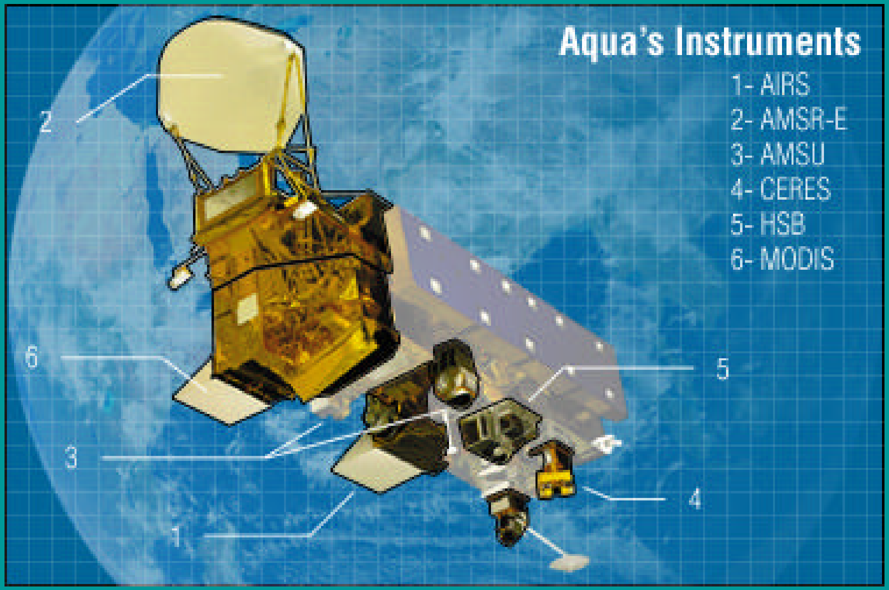

MODIS cont.

- MODIS has 36 spectral bands distributed across the 400-14,000 nm wavelength range, going from the visible through the thermal infrared.
- MODIS has a spatial resolution of 1 km, although 7 of its 36 bands also have a resolution of 500 m, while two of those have a resolution of 250 m.
- Terra and Aqua MODIS each view the entire Earth's surface every 1 to 2 days.
- How MODIS detects fires
  - For fire detection, the mid-infrared (3,960 nm) and thermal infrared (11,017 nm) spectral bands are used.
  - For visualization purposes, red dots are often used to indicate fire locations in the true color imagery, which are generated by assigning the visible bands 1, 4, and 3 to red, green, and blue, respectively, in the computer visualization system.

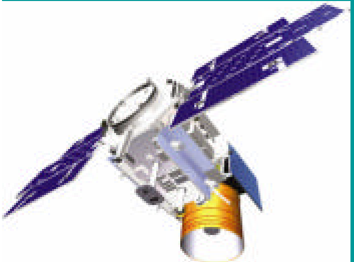

Geoscience Laser Altimeter System (GLAS) on board ICESat

Launched on January 13, 2003

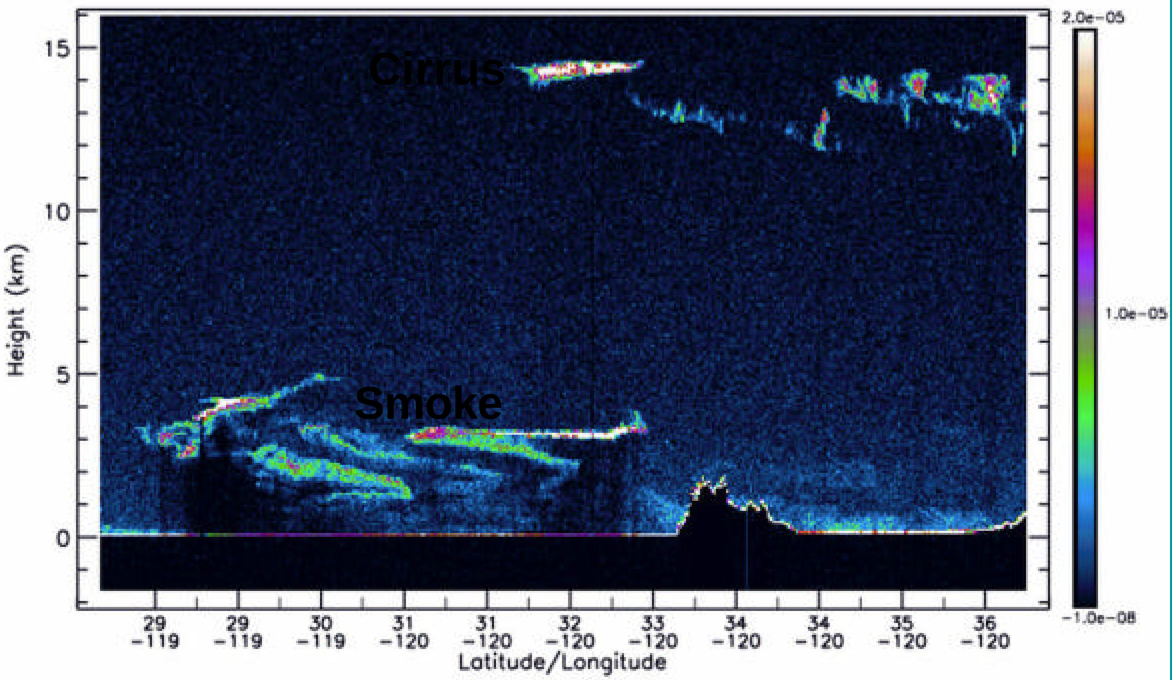

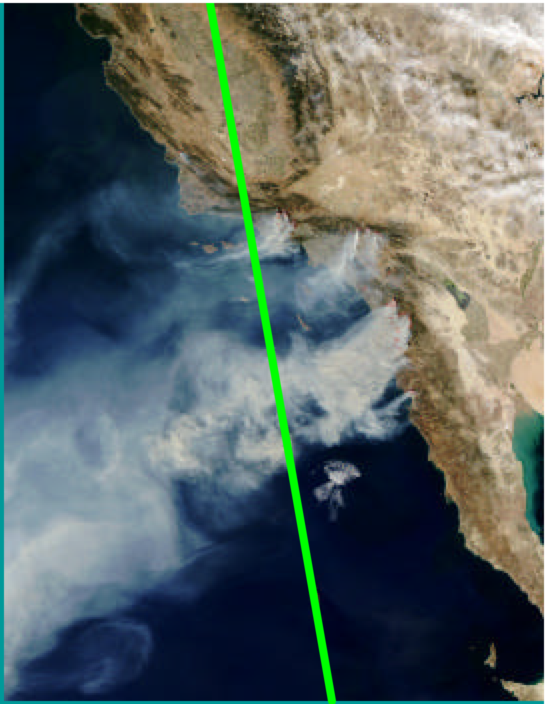

Image: Off the coast of Southern California, Aqua MODIS, October 28, 2003, 7 hours earlier, Courtesy of NASA Earth Observatory

- Transmits a green beam of laser downward (short pulses 4 nanoseconds) of infrared light (1064 nanometers wavelength) and visible green light (532 nanometers)
- Measuring the amount of light that is backscattered back up into space
- GLAS can determine the vertical structure of clouds and my need of smoke plume heights.

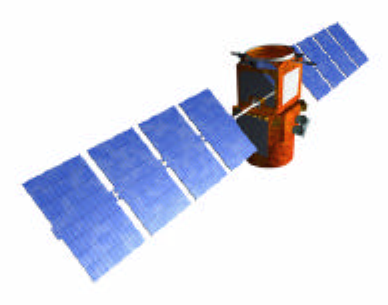

Launched April 2006

Cloud-Aerosol Lidar and Infrared Pathfinder Satellite Observation (CALIPSO)

- Purpose: Learn the effects of clouds and aerosols (airborne particles) on changes in the Earth's climate
- Replaces the missing piece->the altitude of aerosol layers in the atmosphere.
  - Vertical distributions of cloud and aerosol layers
  - Bulk cloud microphysical properties (ice/water content of clouds)
  - Aerosol types and associated optical properties
- A 2-wavelength (532 nm and 1064 nm) polarization sensitive lidar
- 30 meter vertical resolution, 335 meter horizontal resolution
- 3 channel LIDAR (**Light Detection and Ranging)**

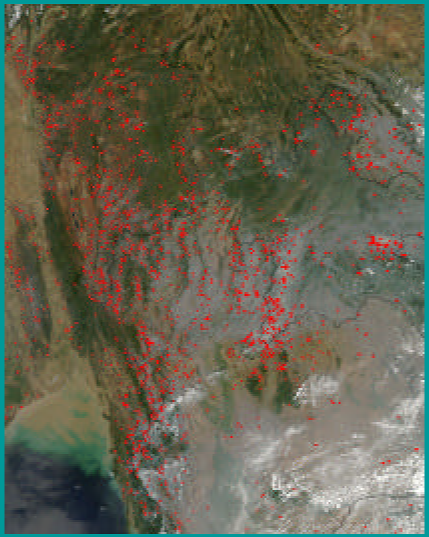

Image: Aqua MODIS, March 4, 2007, 06:55 UTC, Southeast Asia

532 nm backscattered signal from CALIOP, the CALIPSO lidar

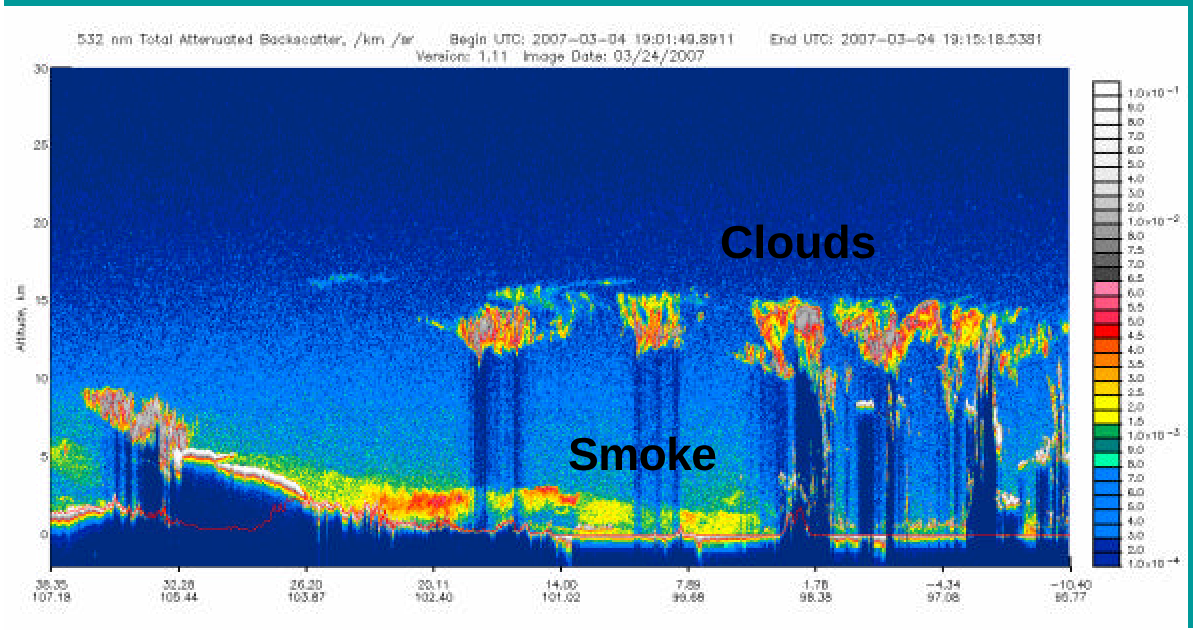

cloud

aerosol

molecular

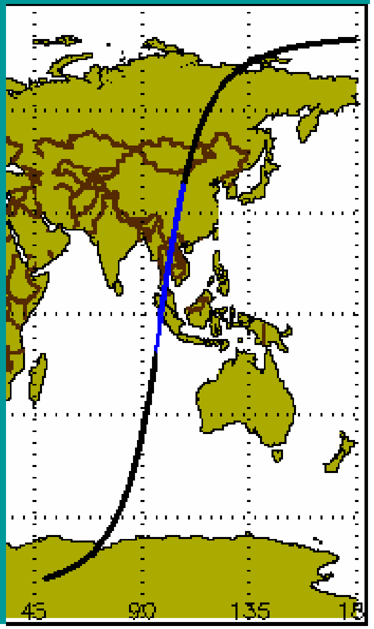

Example of Calipso's Track Day/Night

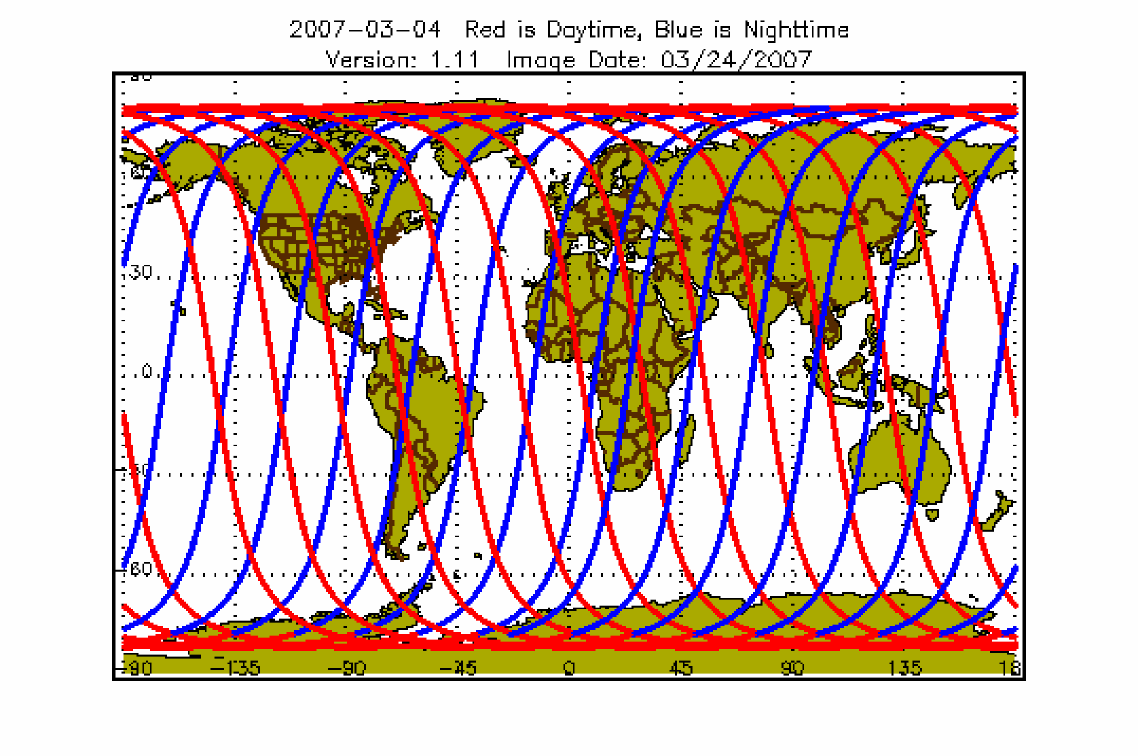

Multi-angle Imaging SpectroRadiometer (MISR)

- On board Terra

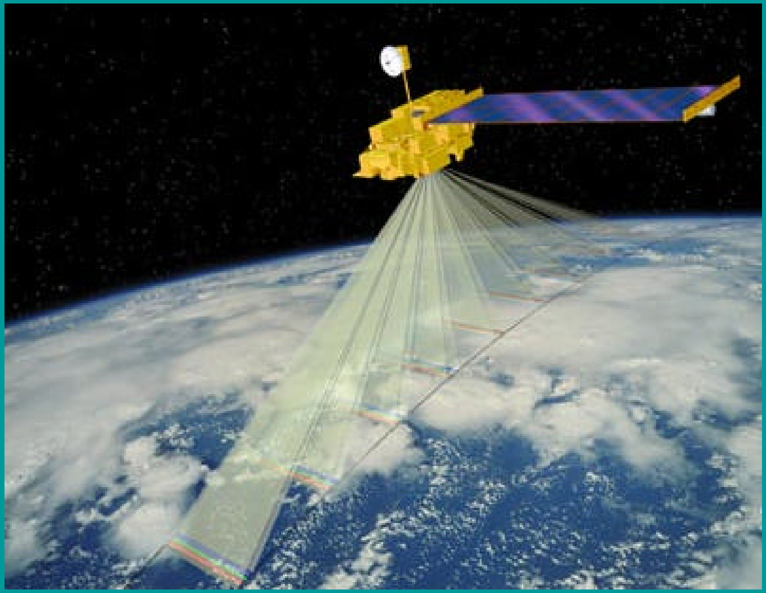

- 9 cameras pointed at fixed angles
- Nadir direction (vertically downward)
- 4 each viewing the forward and aftward directions
- 26.1, 45.6, 60.0, and 70.5 degrees
- Its nominal resolution is 275 m (250 m for nadir) and its swath width is 380 km.
- The Swath captures the entire Earth's surface in a period of 9 days
- Views the entire globe between 82 degrees north and 82 degrees south latitude.

Ordering MISR Data

- http://delenn.gsfc.nasa.gov/~imswww/pub/imswelcome/index.html

Earth Observing System Data Gateway

Search for and order earth science data products from NASA and affiliated centers

MISR LEVEL 2 TOA/CLOUD STEREO PARAMETERS V002

Thank you NASA Langley Atmospheric Sciences Data Center!

Reading data from a .hdf file

Download browse images from the data pool:

Fires in Southern Portugal 8/13/03

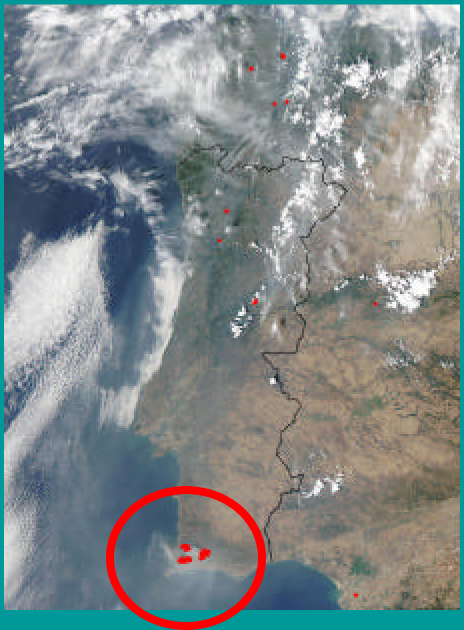

I used the MISR Paths/Blocks Intersecting a Lat/Lon Box tool to pin-point the block (which is shown on the right) and path number.

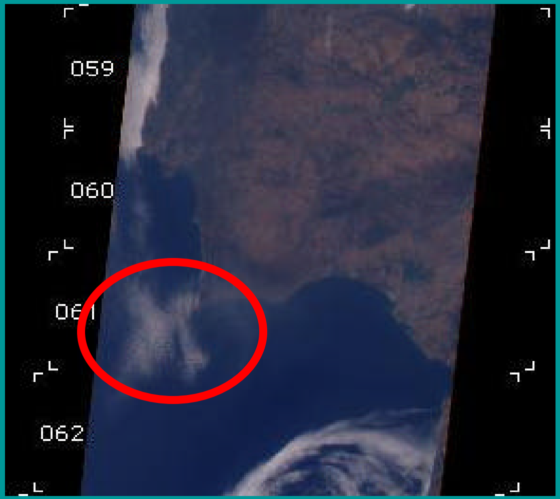

Path 203, block 61

HDFLook
Multifunctional Data Processing and Visualization tool for Land,Ocean and Atmosphere MODIS data

Stereo Heights without wind correction

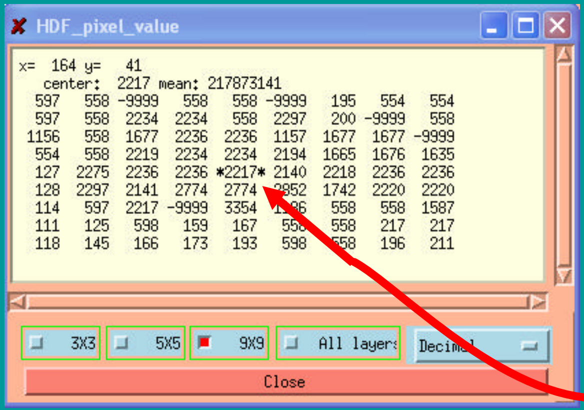

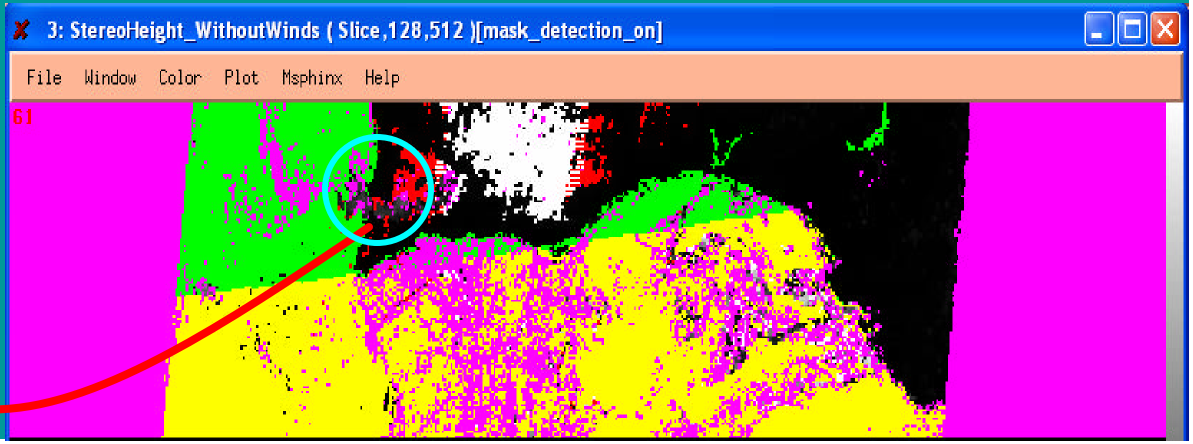

MISR

Smoke Plumes from the B&B Complex Fires, Oregon

More enhanced!

Features exhibiting sufficient spatial contrast for their elevations

Clouds

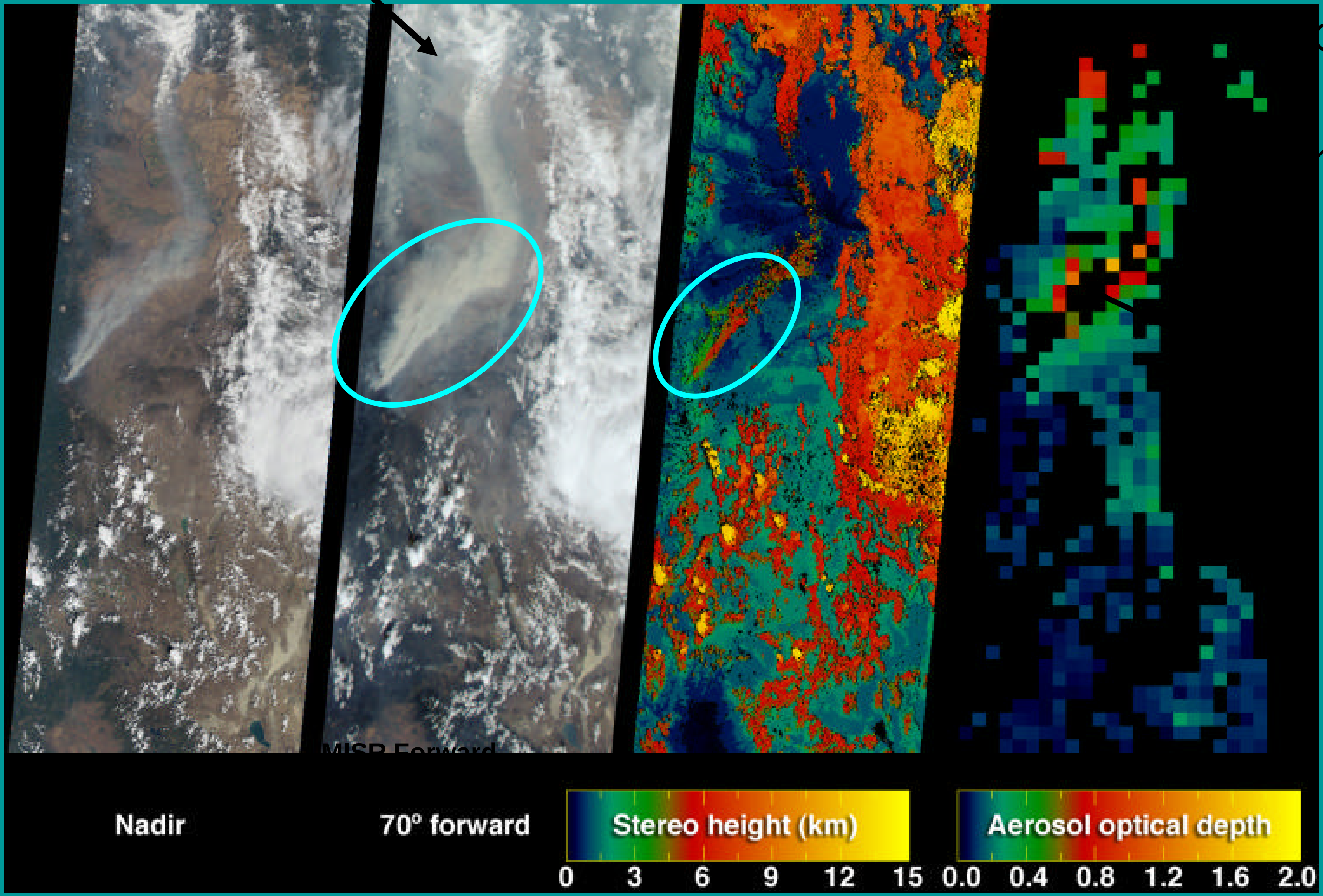

Thick!

~amount of aerosol particles present within the atmospheric column

Image: MISR Nadir, September 4, 2003, Courtesy of NASA Earth Observatory

Smoke from Colorado Wildfires

Haze

MISR Forward Viewing Camera

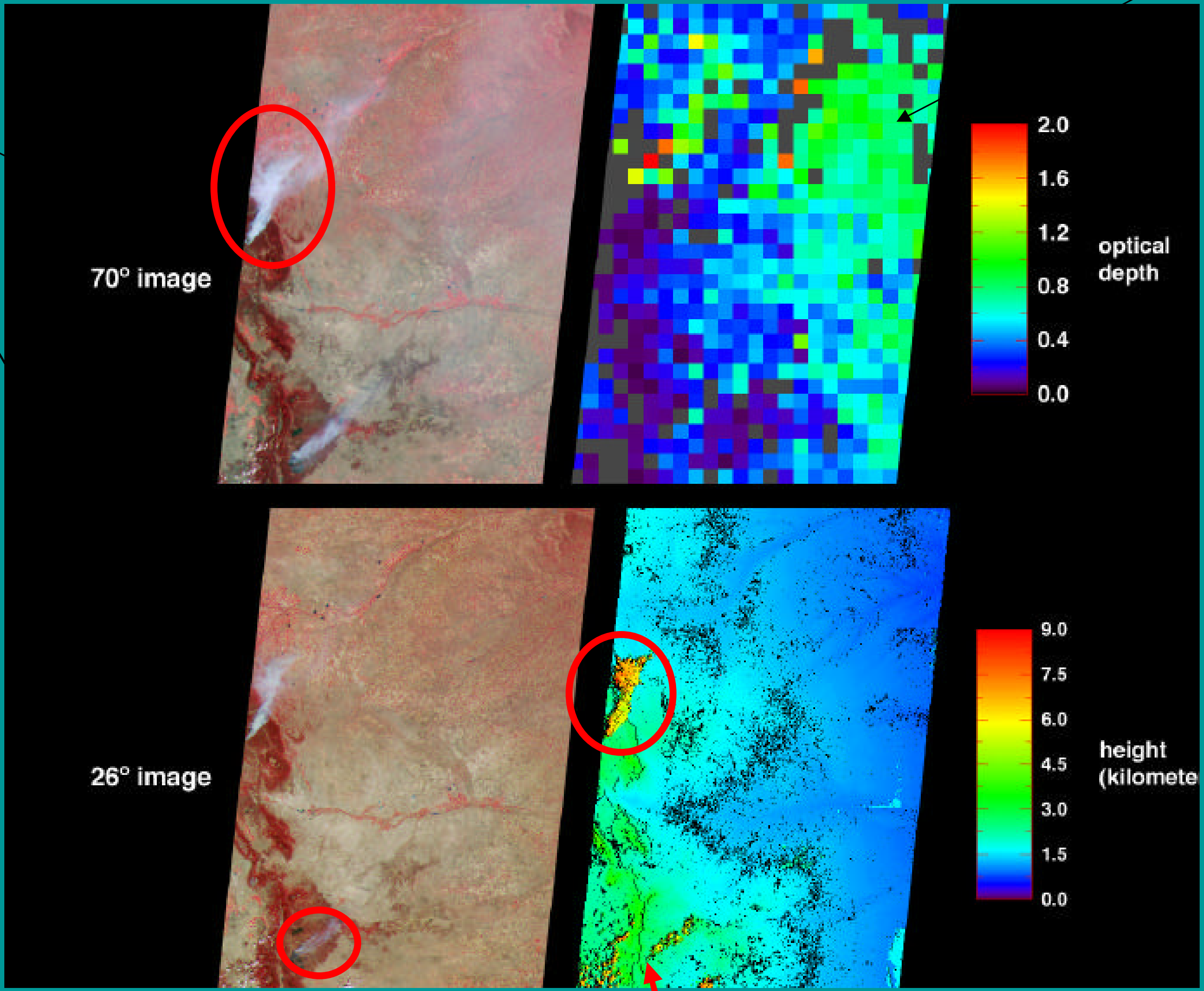

Image: June 9, 2002, Courtesy of NASA Earth Observatory

Plotting in IDL

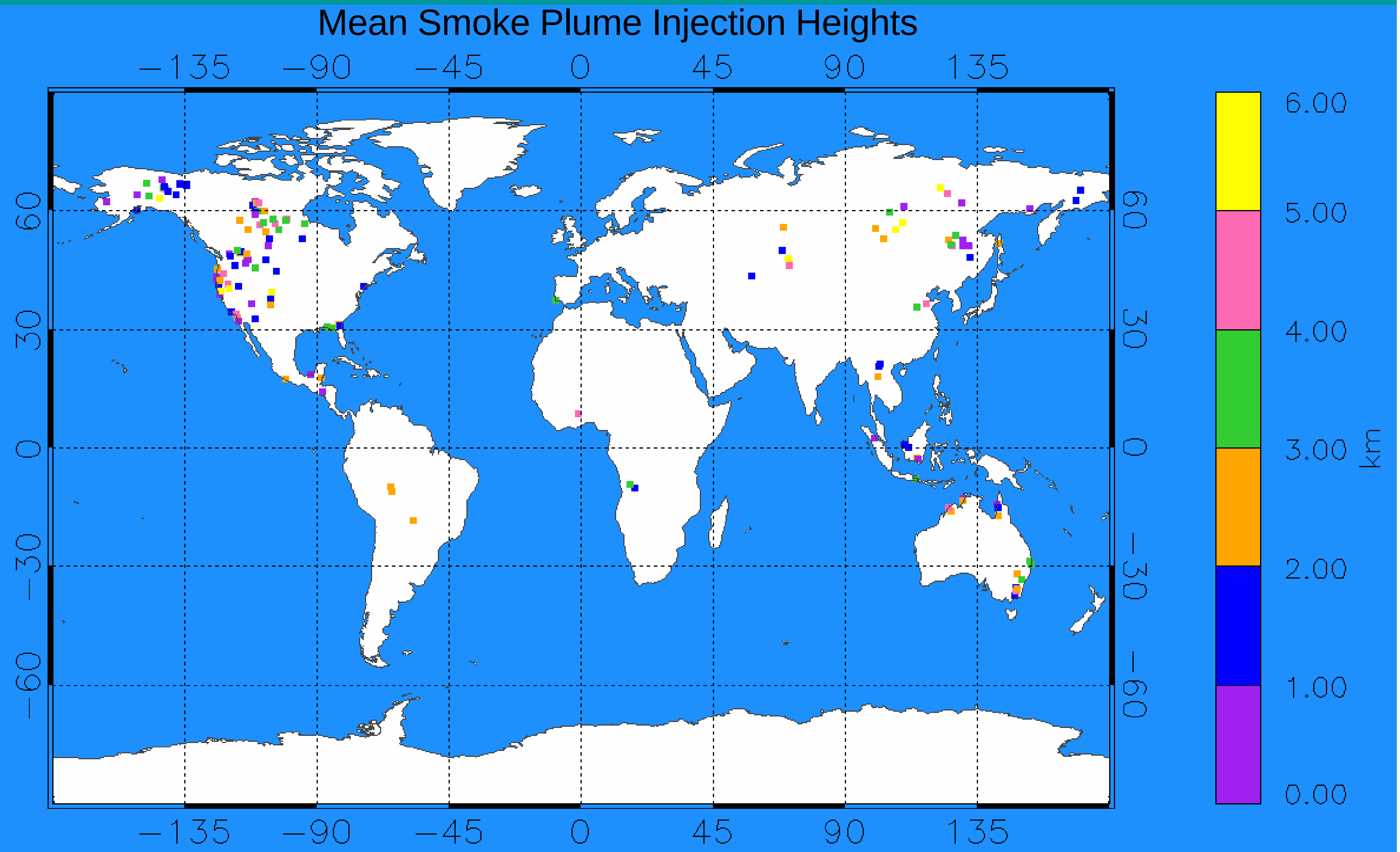

Conclusions

- Smoke plume heights can be estimated using the following:
  - Two Spaceborne Lidar (GLAS and Calipso)
  - Multi-Angle Imager (MISR)
- From the smoke plume heights I collected I can conclude that:
  - World average 2.33 km (Range .41 – 5.04 km)
  - North America roughly average around 3 km

References

- Sites used:
  - NASA Earth Observatory
  - MODIS Rapid Response System
  - NASA Langley ASDC
  -
  - http://icesat.gsfc.nasa.gov/
  -
  - http://www-misr.jpl.nasa.gov/mission/introduction/welcome.html -
  -
  -

Thanks to my mentor, Valerie, Per, and of course…all the cool kids here!!! ☺ Had a great time!

Up to the Minute Weather report prepared as a courtesy by the Serpent River First Nation, Northern, Ontario, Canada.

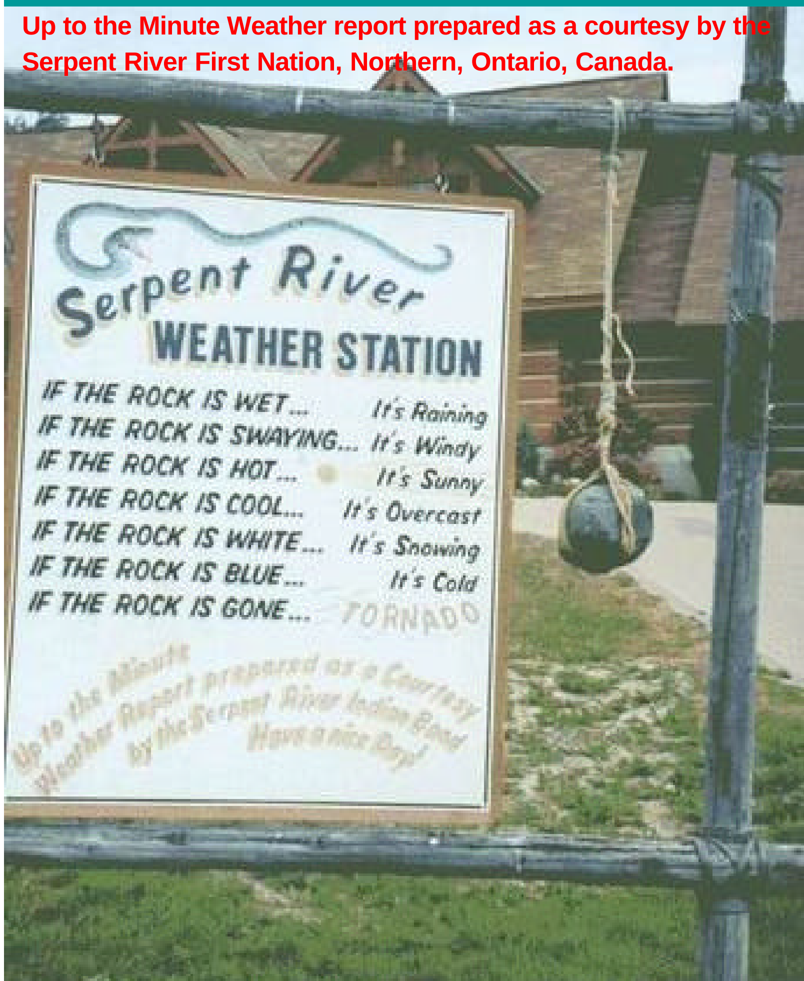

Questions???

A Tale of Two Cities

A study of aerosol effects on radiative transfer in Beijing and New York City


Yiheyuan
(Summer Palace)
Forbidden City
Temple of Heaven
Beijing

Images of the AERONET site in Beijing.

Notice the color of the sky….

New York

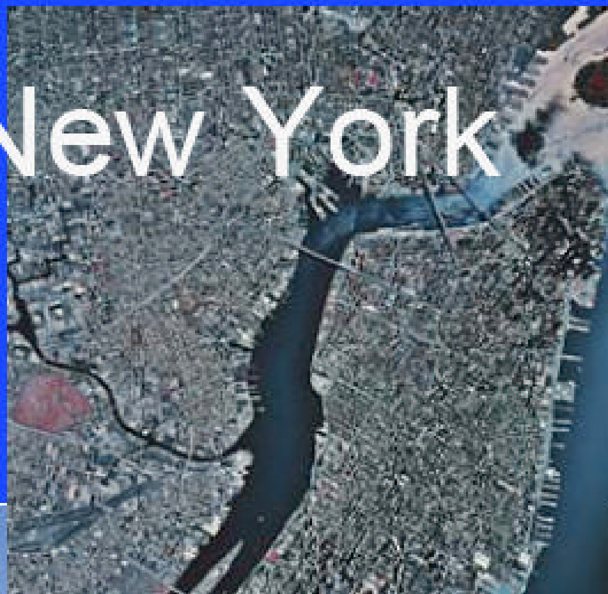

Images of the AERONET site…

…at CCNY in Manhattan.

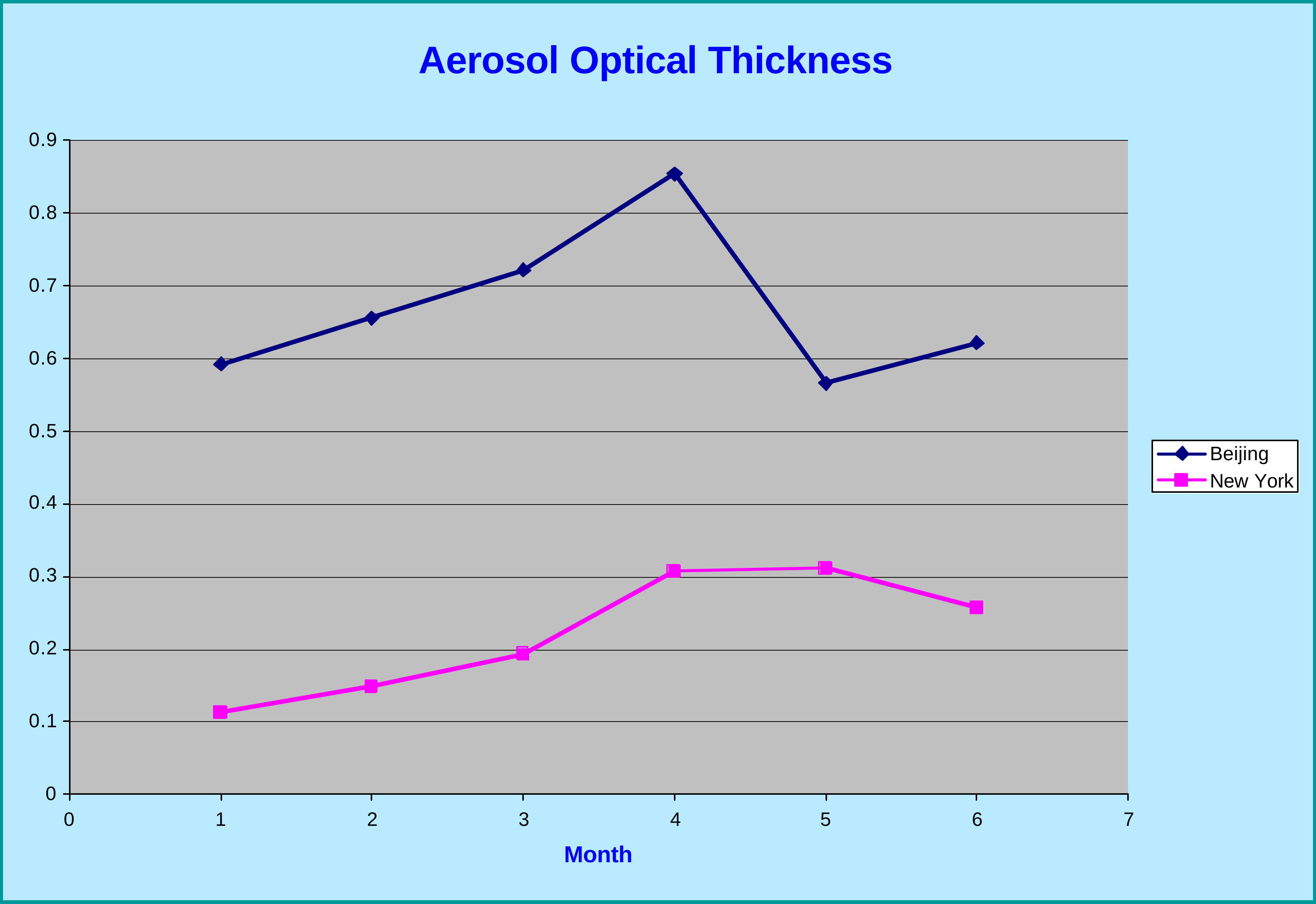
Aerosol Optical Thickness
0.9
0.8
0.7
0.6
0.5
0.4
0.3
0.2
0.1
0
0
1
2
3
4
5
6
7
Month
Beijing
New York

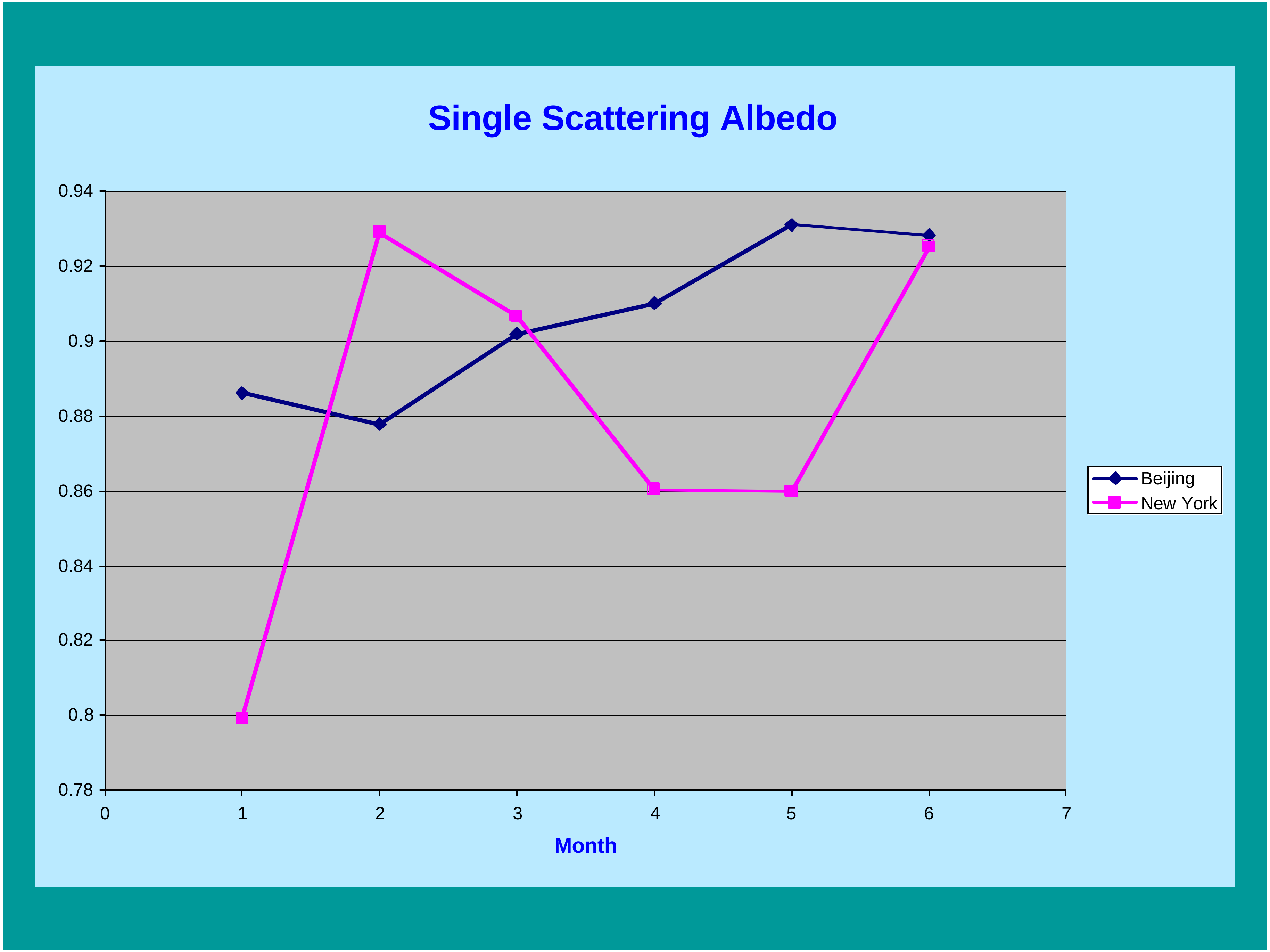
Single Scattering Albedo
0.94
0.92
0.9
0.88
0.86
0.84
0.82
0.8
0.78
0
1
2
3
4
5
6
7
Month
Beijing
New York

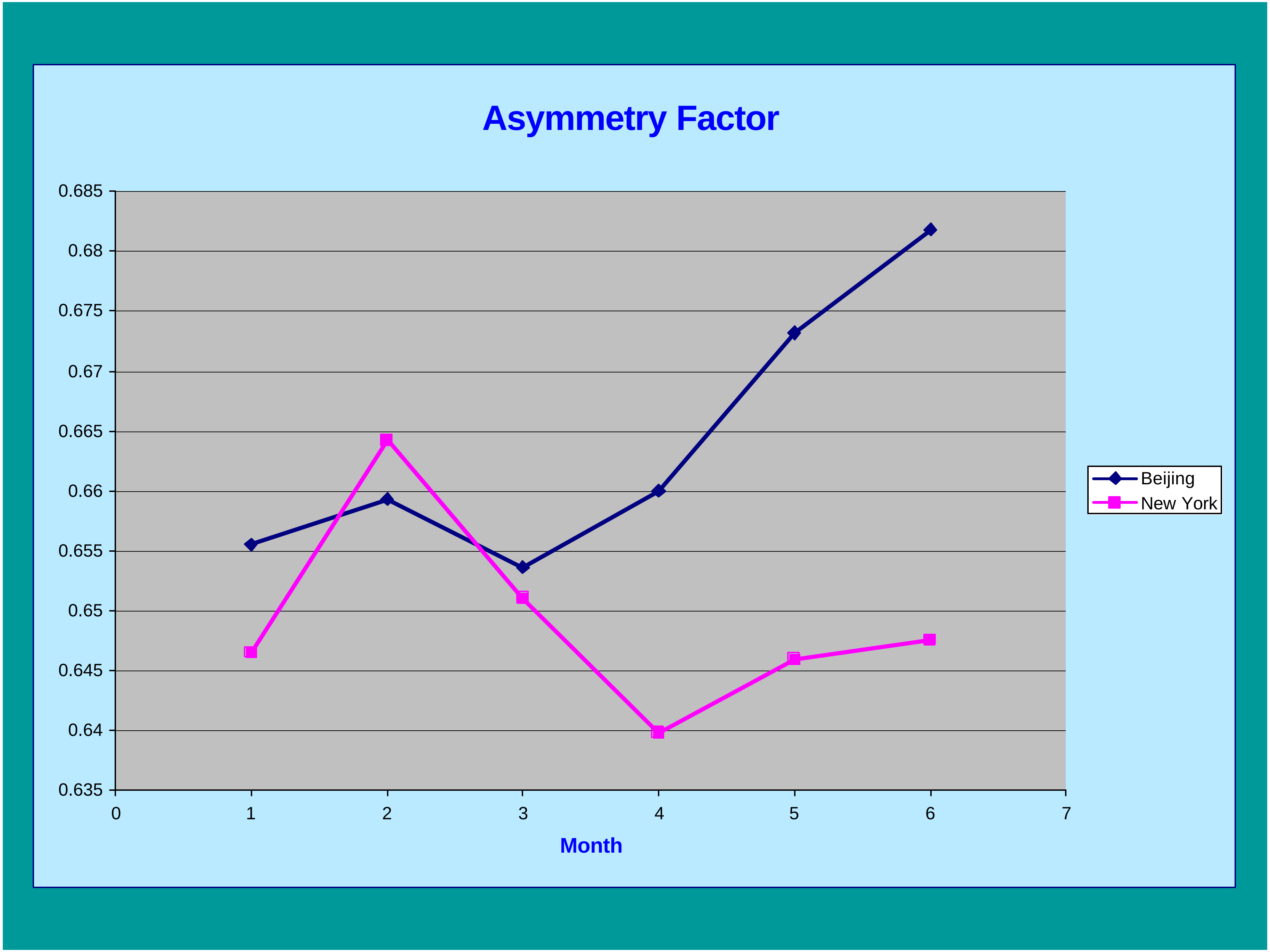

Asymmetry Factor
0.685
0.68
0.675
0.67
0.665
0.66
0.655
0.65
0.645
0.64
0.635
0
1
2
3
4
5
6
7
Month
Beijing
New York

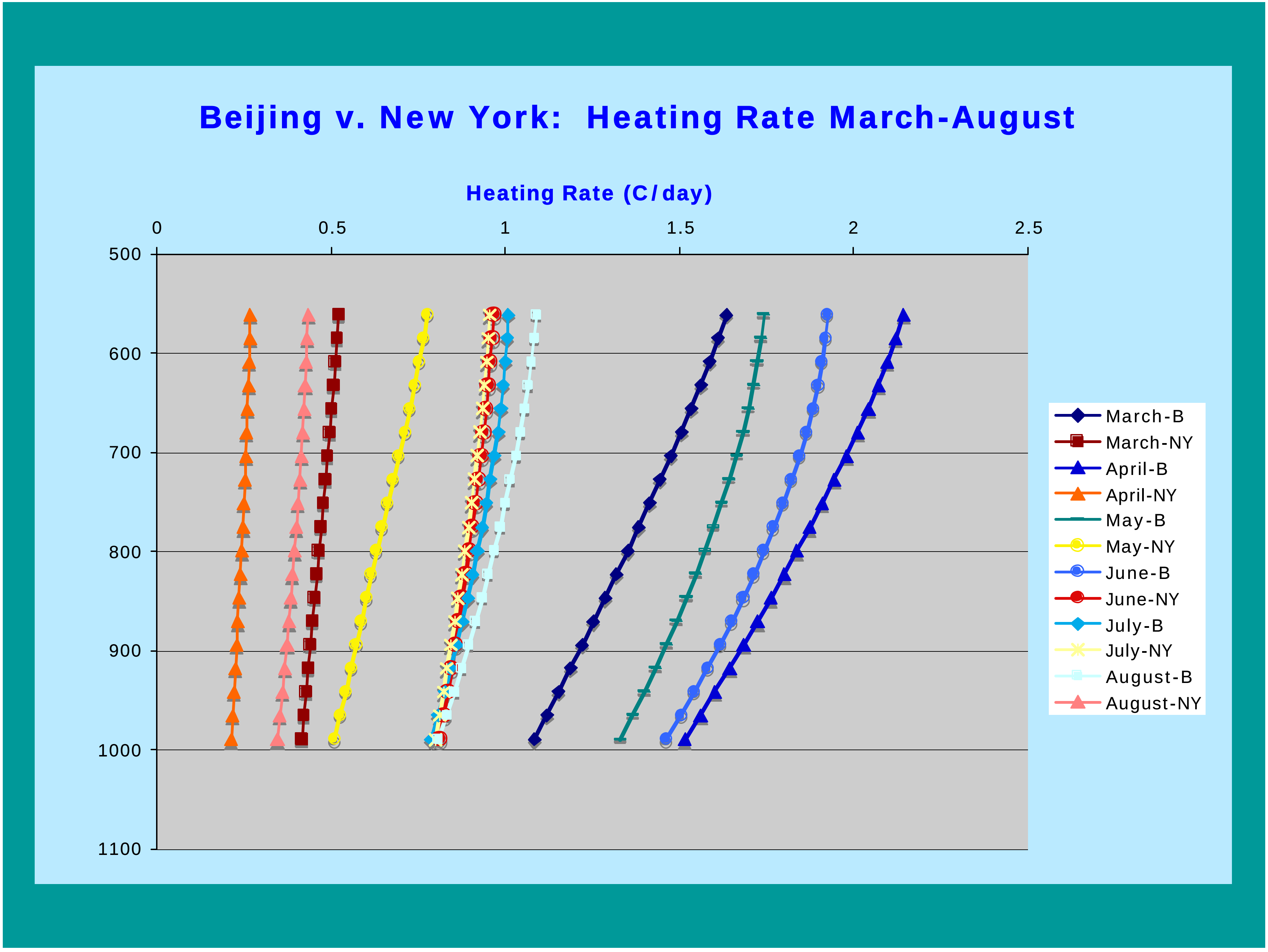
Beijing v. New York: Heating Rate March-August
Heating Rate (C/day)
0
0.5
1
1.5
2
2.5
500
600
700
800
900
1000
1100
March-B
March-NY
April-B
April-NY
May-B
May-NY
June-B
June-NY
July-B
July-NY
August-B
August-NY

Beijing v. New York: April Heating Rate

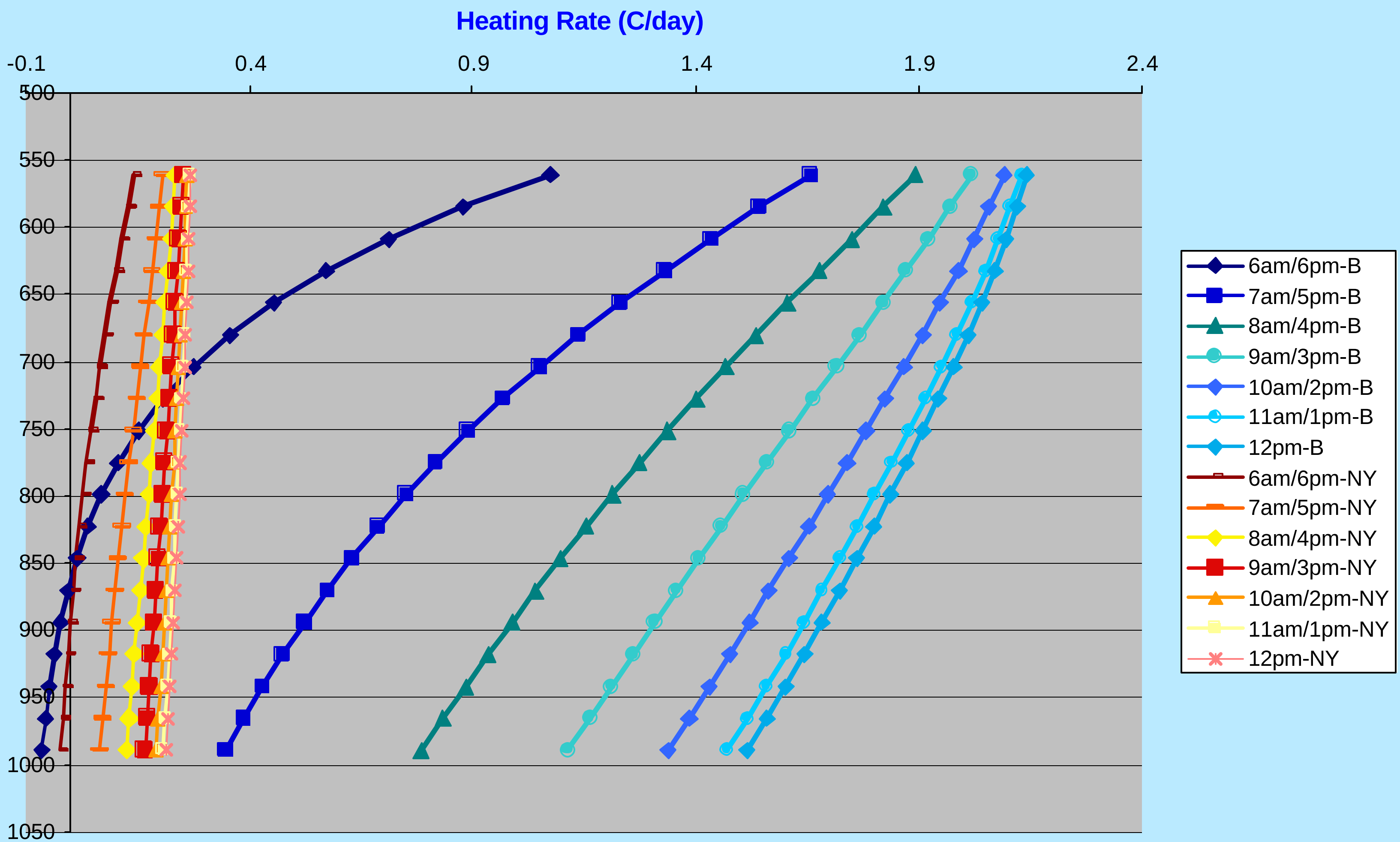

Beijing v. New York: June Heating Rate

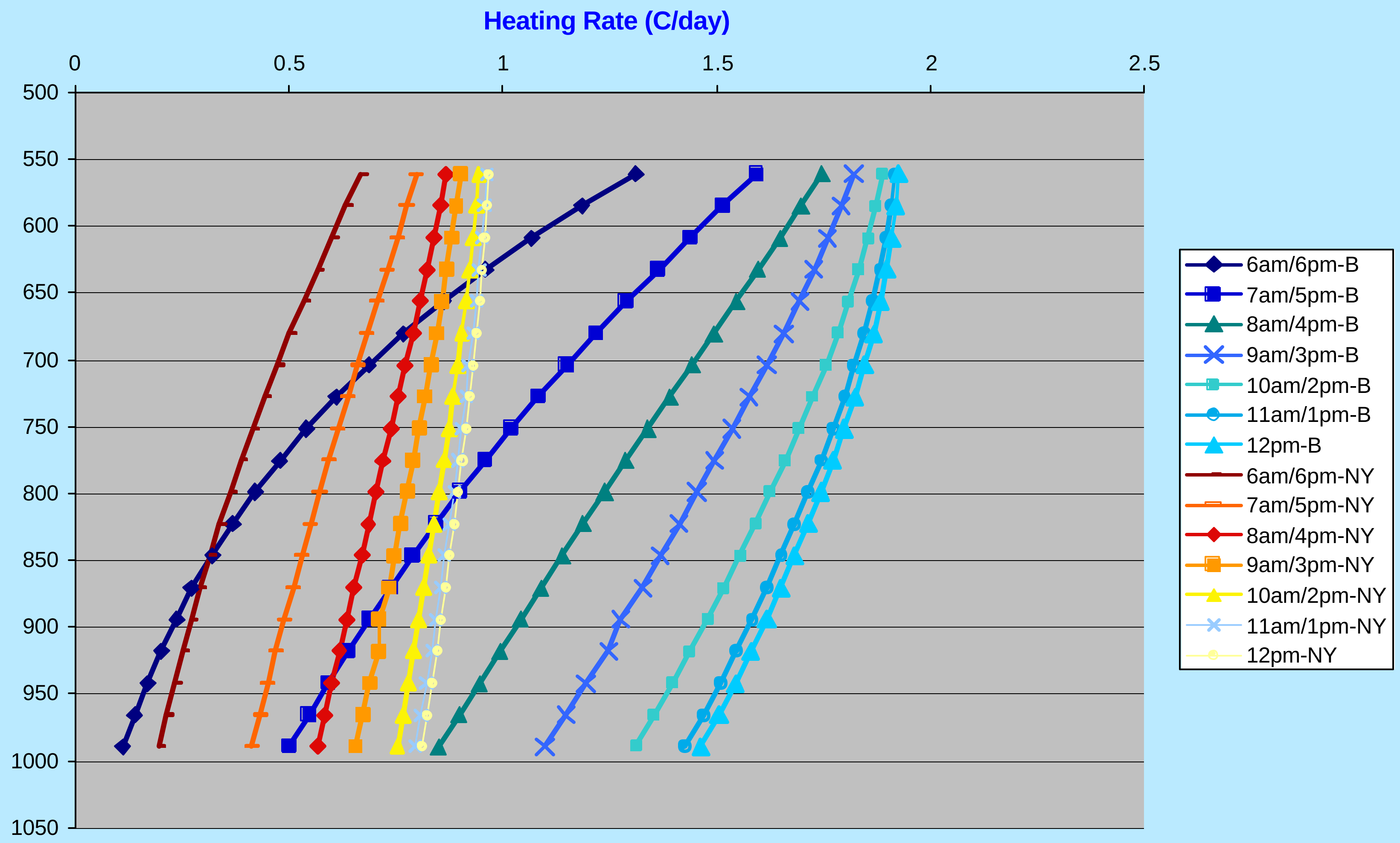

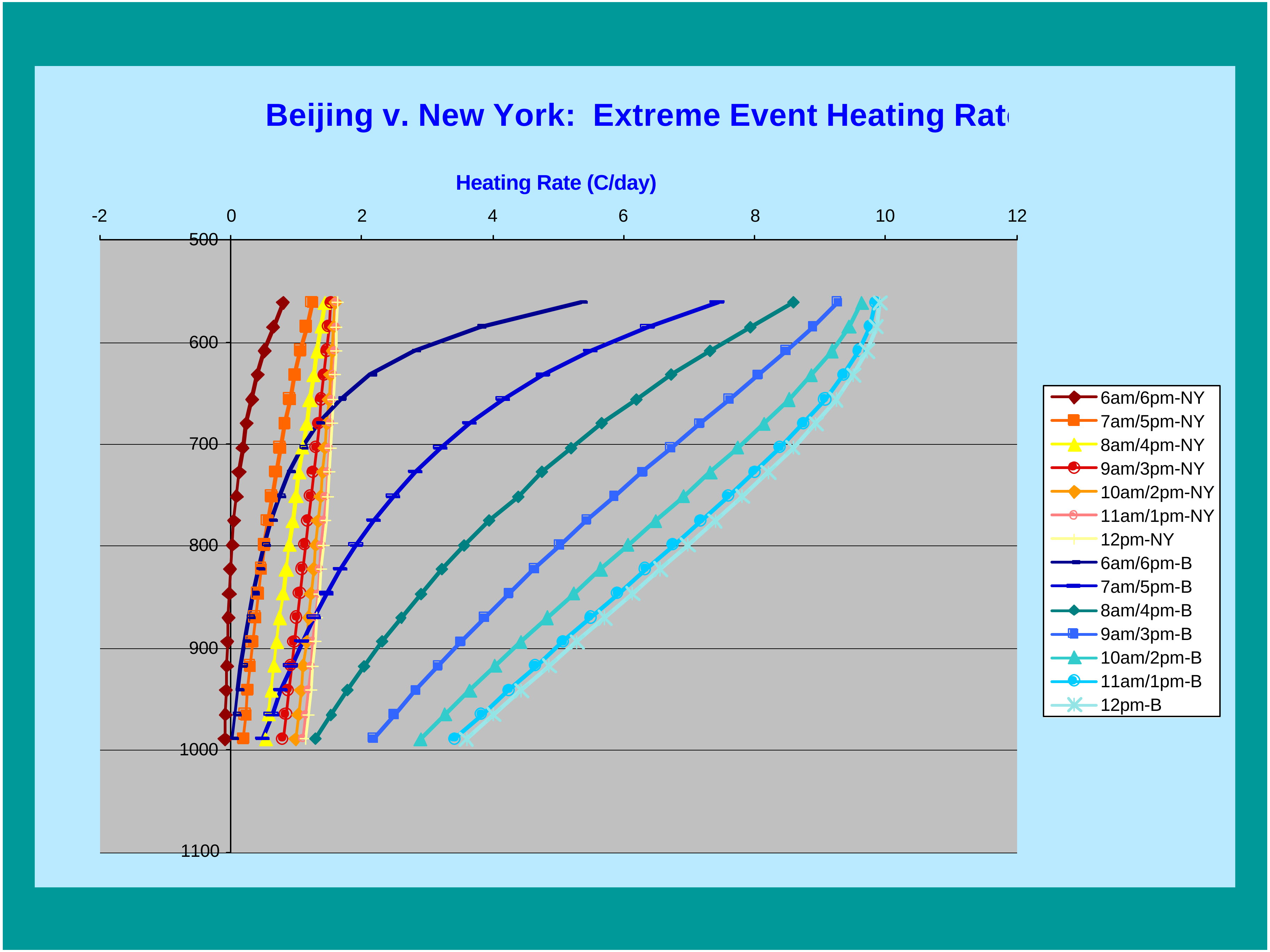

Beijing v. New York: Extreme Event Heating Rat
Heating Rate (C/day)
-2
0
2
4
6
8
10
12
500
600
700
800
900
1000
1100
6am/6pm-NY
7am/5pm-NY
8am/4pm-NY
9am/3pm-NY
10am/2pm-NY
11am/1pm-NY
12pm-NY
6am/6pm-B
7am/5pm-B
8am/4pm-B
9am/3pm-B
10am/2pm-B
11am/1pm-B
12pm-B

Beijing v. New York: 24 hr avg. of Radiative Forcing

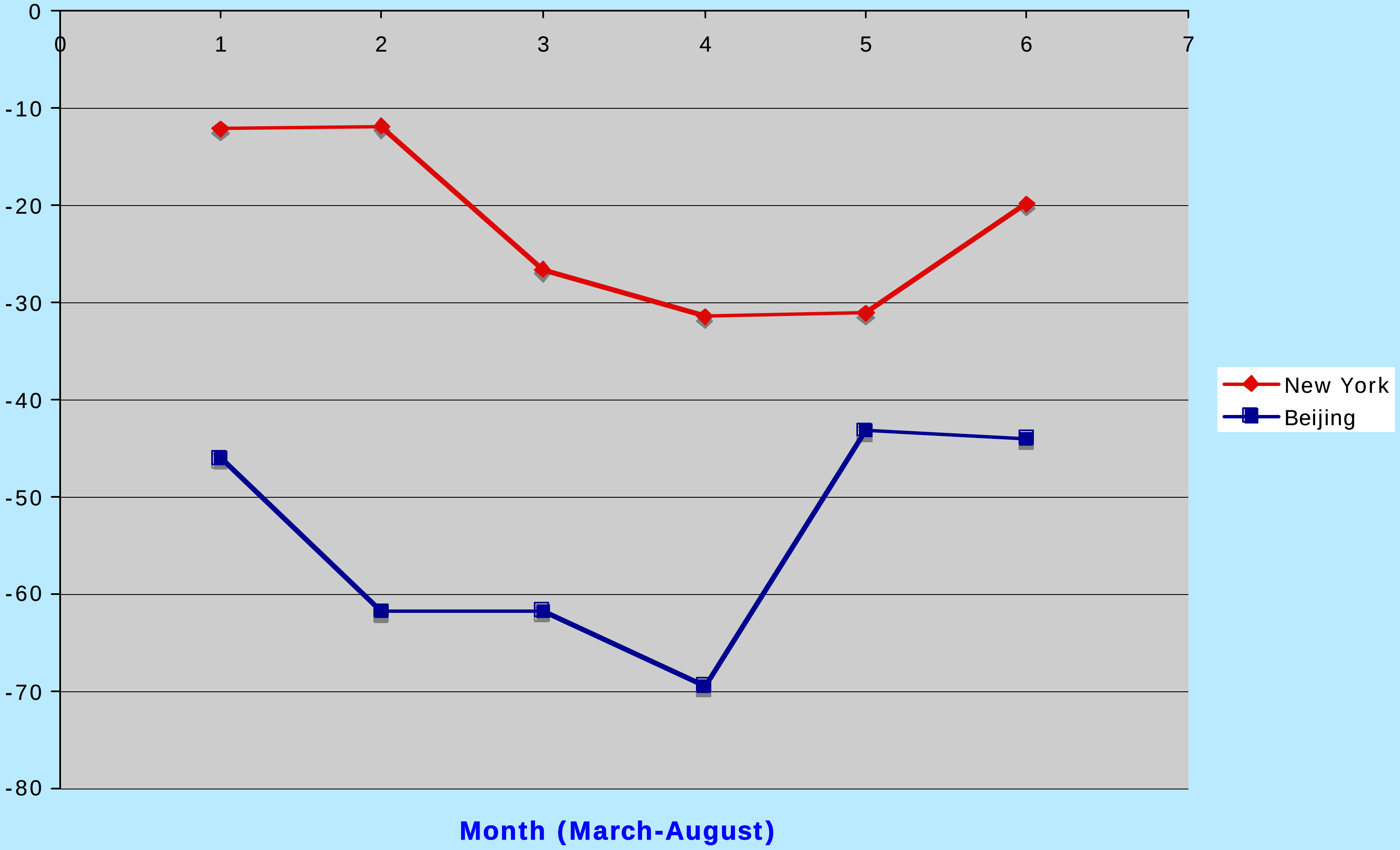

24 hr avg. Radiative Forcing Values

New York monthly: ~ -35 to ~ -10 W/m^2.

New York extreme event: -62.1167 W/m^2.

Beijing monthly: ~ -70 to ~ -40 W/m^2.

Beijing extreme event: -219.675 W/m^2.

East Coast US summer: -9 W/m^2.

Greenhouse gas forcing: +2.5 W/m^2.

Suspected total global aerosol forcing: -1 W/m^2.

So where do we go from here?

What I could do:

-Look at other cities (ie. Sao Paulo)

-Examine other layers of the atmosphere

What is planned:

-Take the heating rates calculated and use them to figure out aerosol effects on circulations in the atmosphere

Snow and ICESat: Techniques for Satellite-Based Snow Depth Measurements

Rachel Mauk[1], Michael Jasinski[2], Jordan Borak[3], Jeremy Stoll[4]

1. Ohio State University, Columbus OH; 2. NASA GSFC Code 614.3, Greenbelt MD;
3. RSIS, Lanham MD; 4. SSAI, Lanham MD

Why Use Satellites for Snow?

- Snow depth important for:
  - Climate and hydrologic modeling
  - Water management

- In-situ problems
  - Expensive
  - Localized

Map from Perry-Castañeda Library Map Collection, Univ. of Texas Libraries <http://www.lib.utexas.edu/maps/>

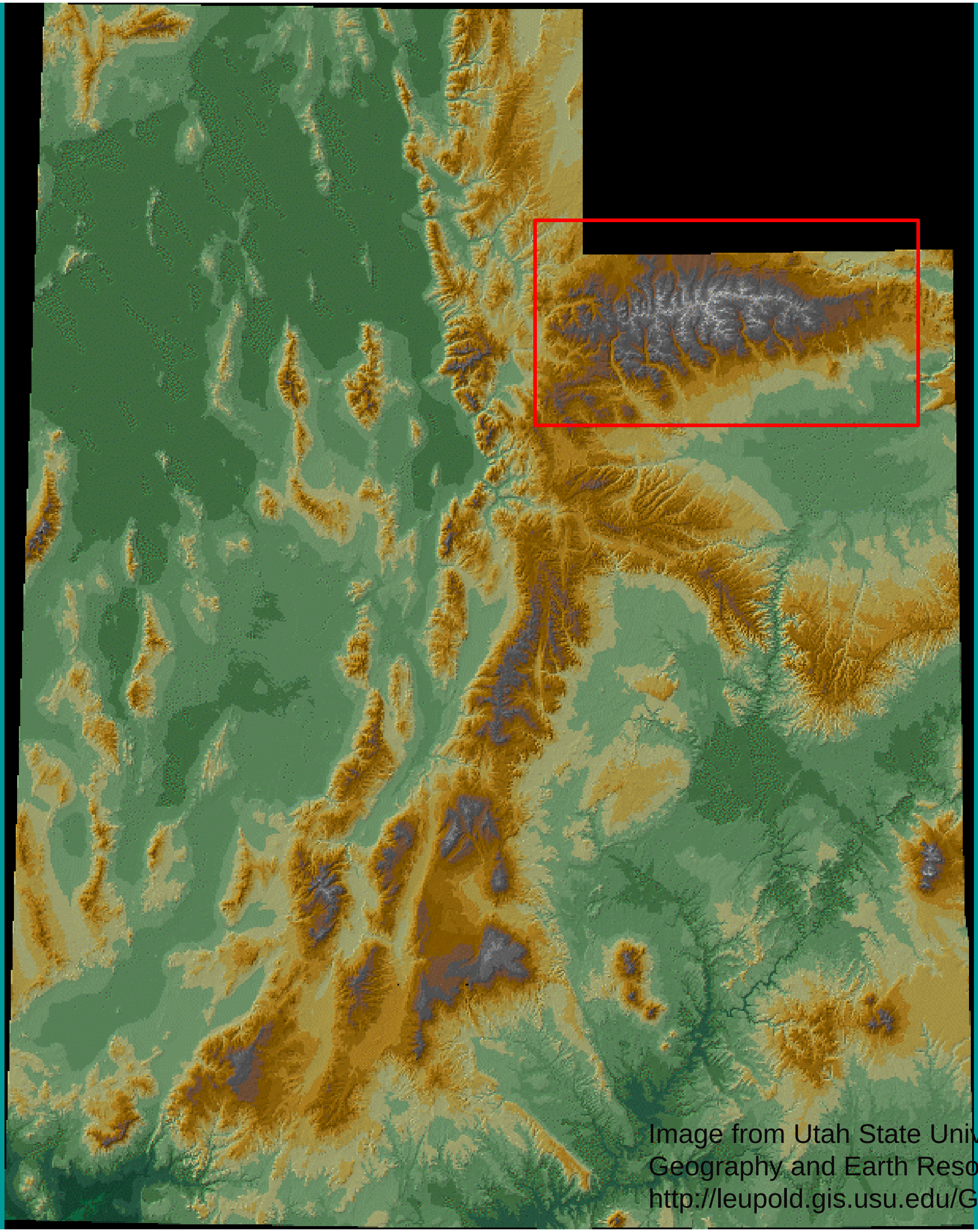

Image from Utah State University Dept of
Geography and Earth Resources
http://leupold.gis.usu.edu/Geography-Department/


Image courtesy H. K. Wright


Image courtesy utahpictures.com

Uinta Mountains

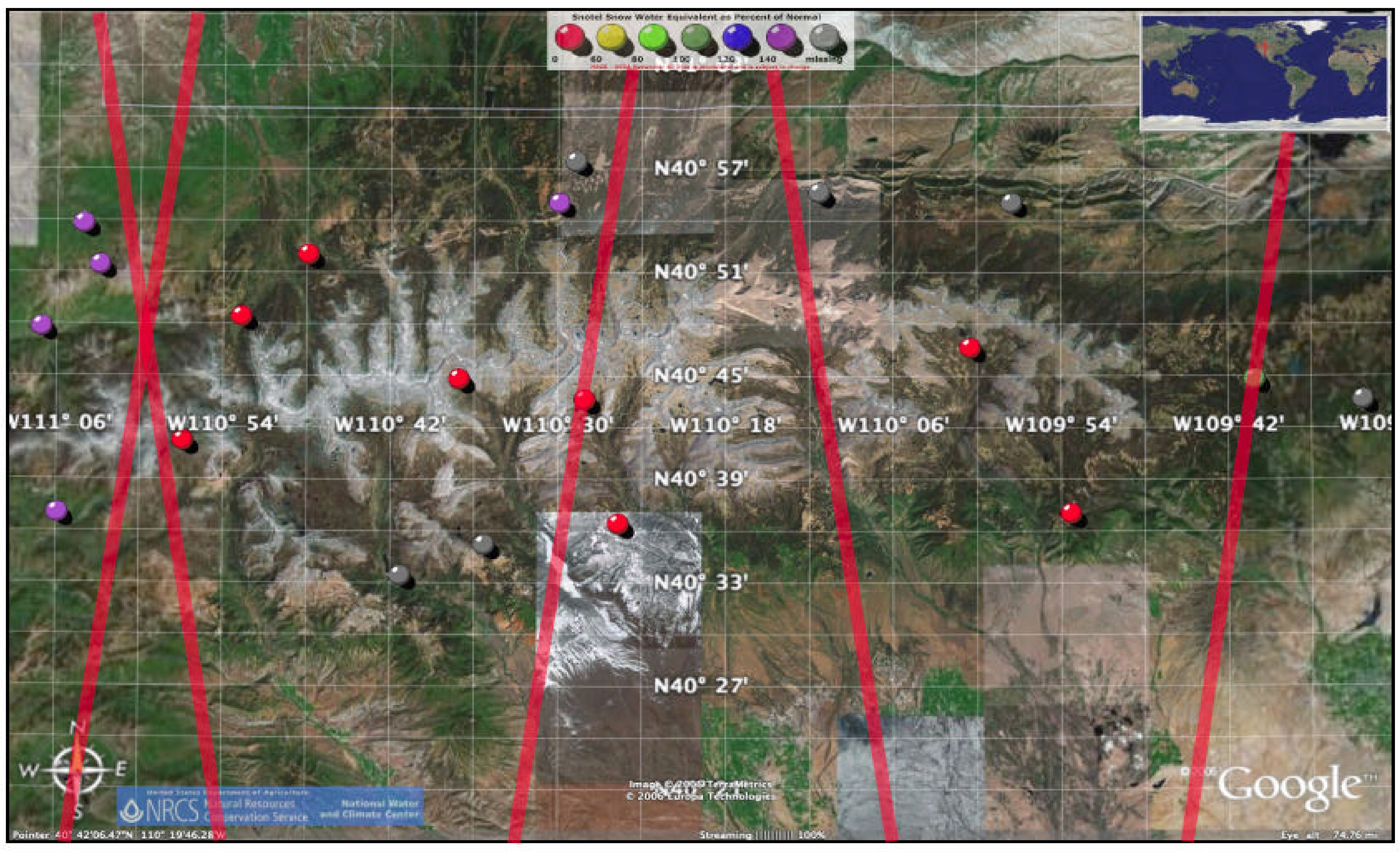

2_0351

1_1331

± 1 km width
centered on ICESat
91-day reference track

A Brief Introduction to ICESat

- Jan 2003 launch
- GLAS: Geoscience Laser Altimeter System
  - Ice sheet thickness, land cover and elevation
  - Cloud thickness, aerosols
  - 70m footprint every 175m

ICESat logo from ICESat homepage at http://icesat.gsfc.nasa.gov/

Challenges of ICESat

- Elevation is peak of 70m footprint
  - Slopes
  - Vegetation
- Clouds
  - Low clouds can interfere with returns
- Frequency of passes
  - Feb/Mar, May/Jun, Oct/Nov
- Separation of passes

ICESat Pass Comparison

- Methodology:
  - Identify two close tracks (NS/NS and S/NS cases) and subtract
- Ideal results:
  - 0 m difference for NS/NS case
  - ~2 m average snow depth for S/NS case

1_1331 Passes

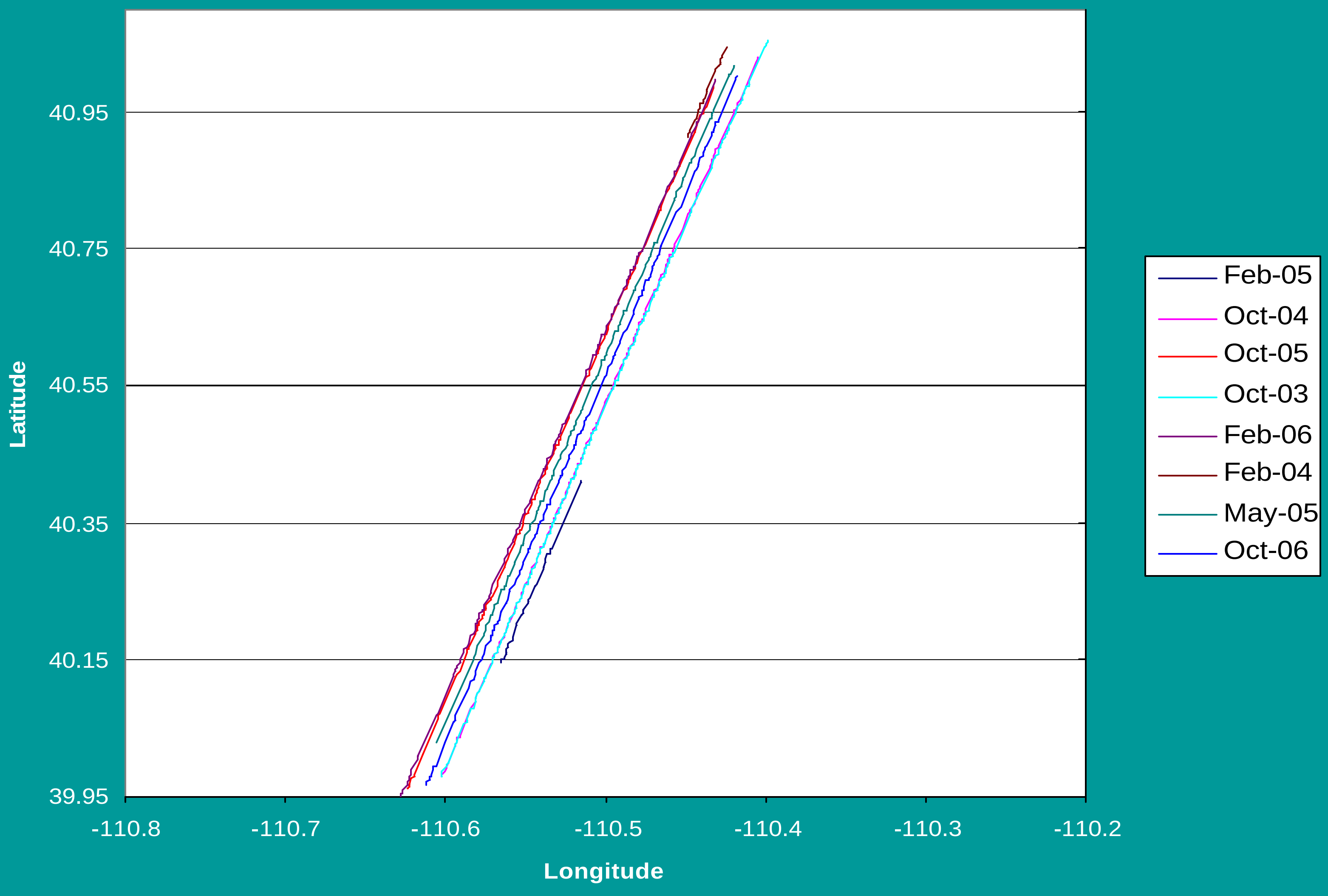

Track 1_1331 No Snow: Oct 2003 and Oct 2004

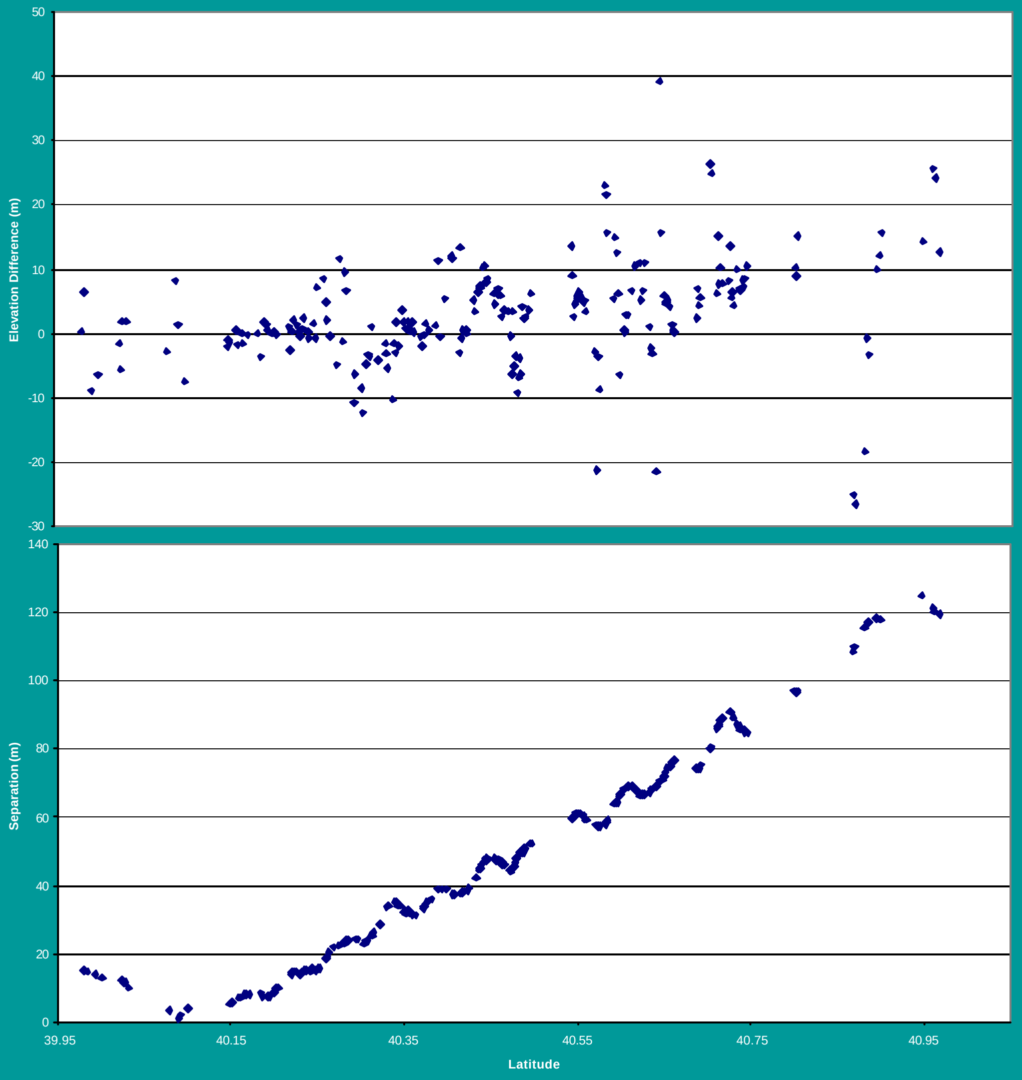

- Elevation diff vs. latitude
- Average difference 3m
- Separation distance vs. latitude

2_0351 Passes

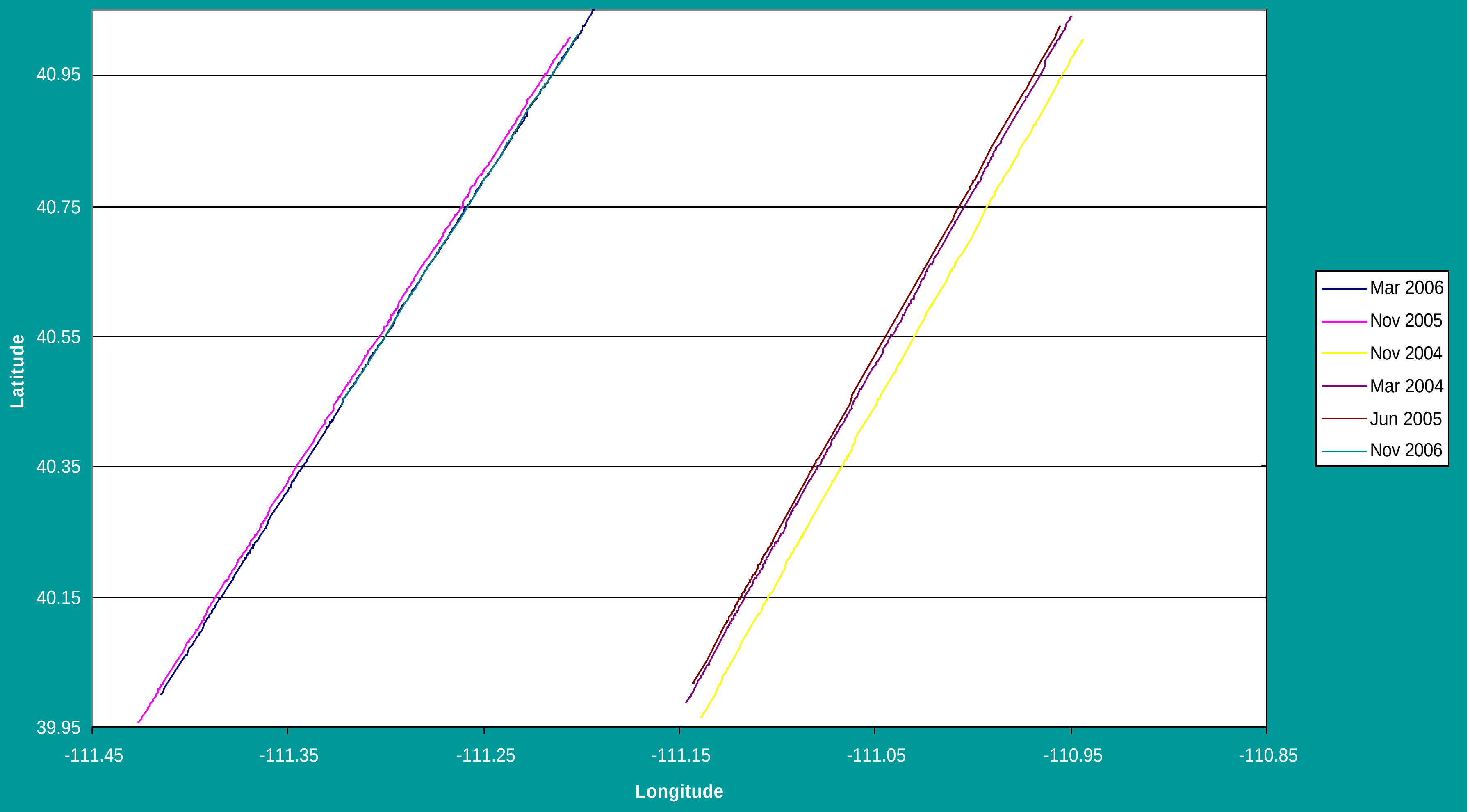

Track 2_0351 Snow: Mar 2006 and Nov 2006

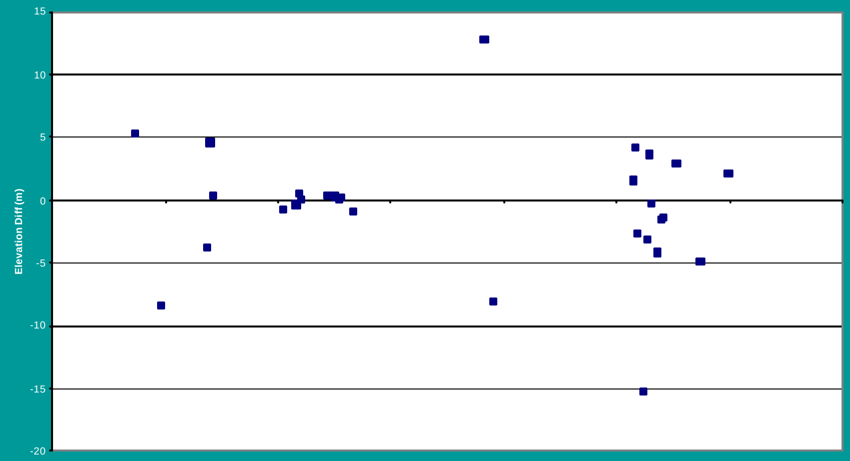

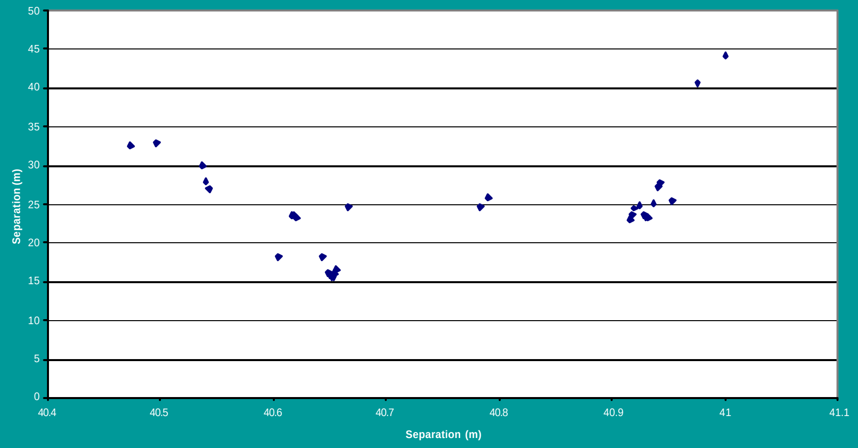

- Elevation diff vs. latitude
- Average difference -0.5m

- Separation distance vs. latitude

Applying an Elevation Baseline

- NED: National Elevation Dataset, USGS
- Retrieved corresponding NED values for ICESat points
- Corrected for projection
- Subtracted NED from ICESat

Track 1_1331 Oct 2004 (No Snow)

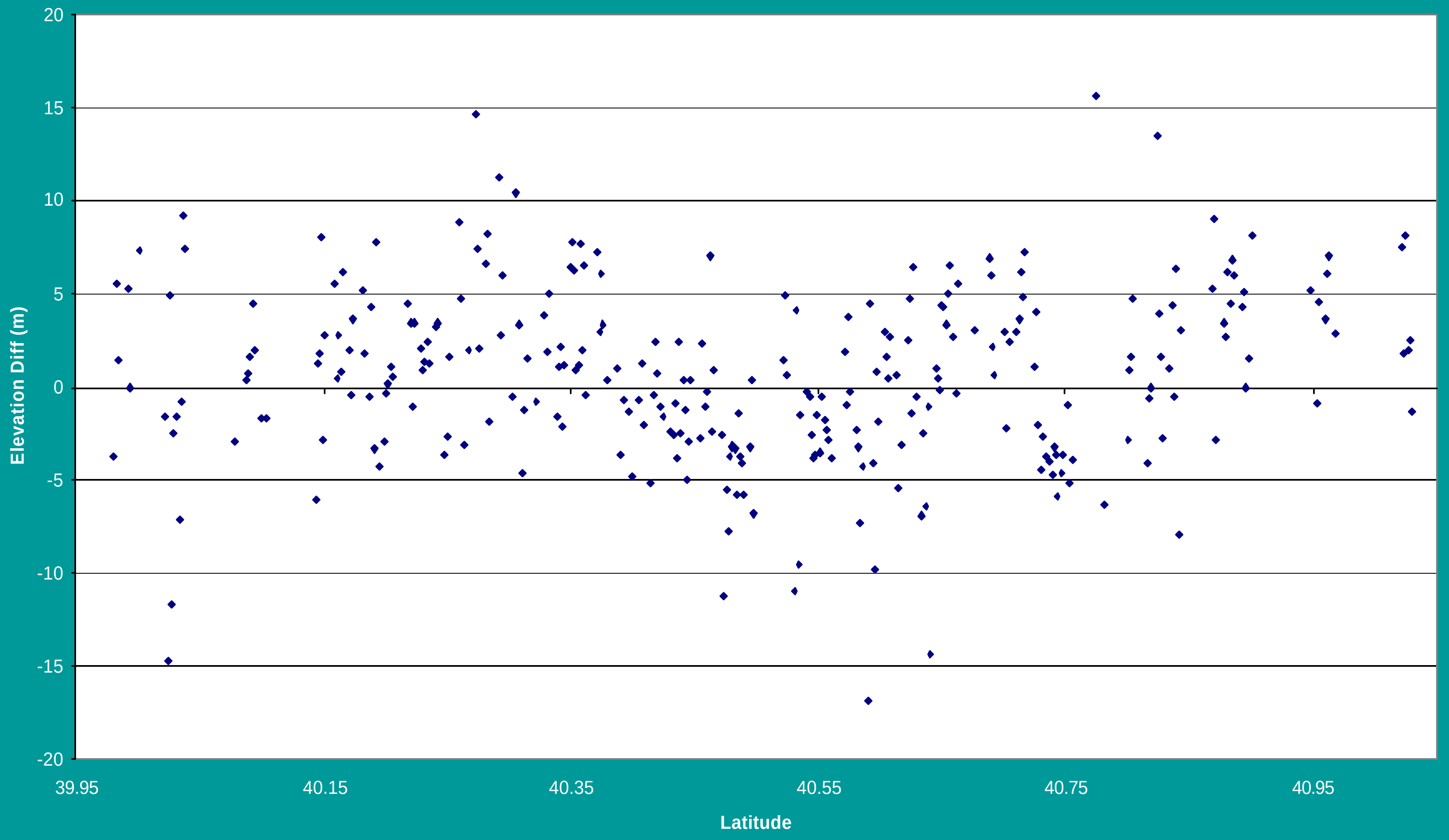

Track 1_1331 Feb 2006 (Snow)

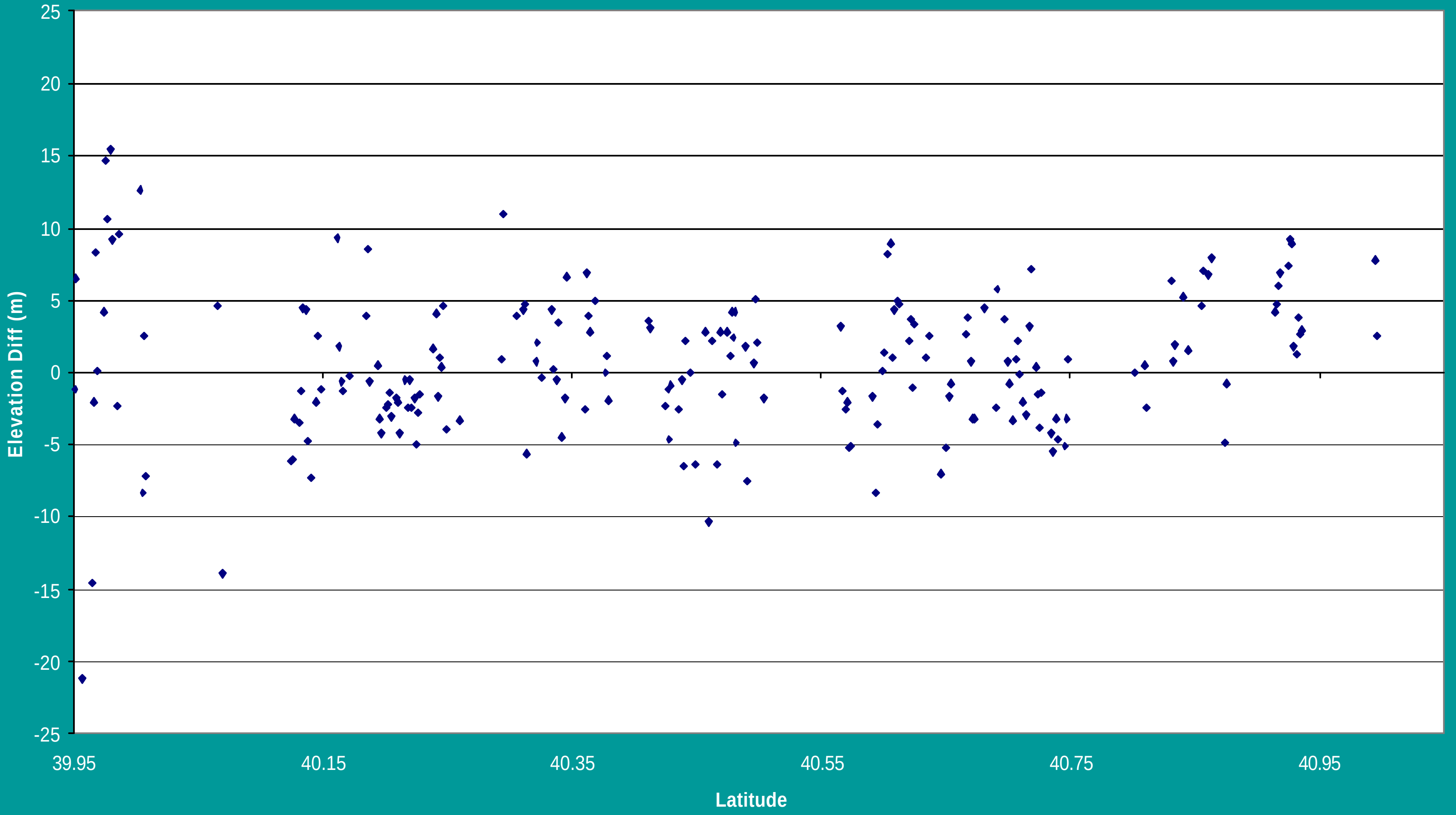

Next Steps

- Create a baseline
  - Use slopes from snow-free tracks to extrapolate elevations along snow tracks
- Future satellites
  - importance of accurate pointing

Acknowledgments

- Deepest thanks are extended to:
  - Summer Institute Program
  - Dr. Per Gloersen
  - Valerie Casasanto
  - Mike Jasinski
  - Jordan Borak
  - Jeremy Stoll
  - Fellow SI students

Using NASA Products to help Improve Water Forecasting: A study of a riparian case along the Middle Rio Grande (MRG)

Alvin Rentsch University of Louisville

David Toll, Kristi Arsenault,
Jiarui Dong, Mutlu Ozdogan
Mentors 614.3

arrentsch@hotmail.com

17 August.2007

Outline

- Describe the Project
- Introduce Objectives
- Describe my contributions
- Future work for the study

Importance of study

- **Agricultural Water Resources Decision Support (AWARDS):**
  - The Bureau of Reclamation operates AWARDS ET Toolbox primarily to assess the amount of water available for agriculture.
  - These assessments are used to portion out limited water resources for various agricultural interests while retaining a portion for other uses (ecosystems, recreation, commerce, etc.).

Reclamation's AWARDS ET Toolbox

- Describe Reclamation Metrics
  - USBR is the nation's largest wholesale water supplier

AWARDS ET Toolbox ~

? Validation:

➔ Eddy Covariance Flux Towers

? Establish metrics based on validation at select sites

Land Information System (LIS)

- The software is developed to parameterize and force multiple land surface models (LSMs) with data from ground and space-based observing systems.

- Mosaic LSM – NASA GSFC

- The Community Land Model, version 2 (CLM2)

➔ **<u>NOAA's Noah Land Surface Model, version 2.7.1</u>**

- <u>Temperature, Humidity, Wind, etc.:</u> NOAA's Eta Model

- <u>Precipitation</u>: *Stage II Doppler Radar and CPC Rain gage products*

- <u>Shortwave Radiation</u>: GOES Radiation Products (Pinker et al)

Other Model Parameters

- Used Local station information
- Statsgo Soil Parameters
- Downscaled NLDAS Forcing Fields

Local Observation Towers

- UNM eddy covariance flux tower network
  - J. Cleverly et al (2006)
  - Sites: Cottonwood, salt cedar, alfalfa, etc.
- Use local meteorological forcing data
- Validation data: energy and moisture fluxes

The Big Question?

- Can We obtain more accurate components and fluxes of the water and energy budgets, respectively, to help with water resources management and decision-making processes?
- We want to demonstrate that by using NASA satellite and modeled data we may be able to provide more spatial information in place of some of the current point/station measurements used by USBR.

Why conduct this study?

- The USBR currently accounts for only rainfall and evapotranspiration in the AWARDS ET Toolbox; whereas, with land surface models (LSM) in LIS, we model also runoff and ground/soil storage (aimed to close the water budget at a point in the model).
- Local meteorological forcing data are used to test and validate the NASA products, like LIS.
- Focusing on:
  - Estimating and validating components of the water and energy budgets.
  - Modeling and predicting water fluxes spatially – evapotranspiration, precipitation, river runoff.

My contribution to the Application of NASA Land Information System Products for ET Toolbox

Testing NASA LIS Land Cover Products

- The task of developing a model runs to assess riparian case at the Middle Rio Grande.
- Key fields of interest:
  - Riparian case
  - Need to quantify and validate water consumption at a riparian site.
  - To asses models capacity to perform using spatial data (albedo, greenness fraction, and spatial forcing)

Local forcing applied

- Local forcing data used to validate LIS model runs with the hope of improving our results.
- Problems that we face include:
  - Errors in the *in situ* observations.
  - Errors in the model parameters (default model parameters used).
  - Errors in the models physics.(model has deficiencies in areas like semi-arid environments like this one e.g groundwater physics)

Studies Conducted

- A study of riparian areas has been completed.
- A study of an irrigated site will be accomplish in the future.
- Key findings:
  - Riparian areas have access to ground water by deep root extraction. (trees gain water needed by reaching the water table)
  - Current default model is not designed to consider this.
  - To asses models capacity to account for this local forcing is applied.

Site Parameters

Soil type	**Loamy sand**	
	Porosity	**0.421**
	SMCREF	**0.248458**
	SMCWLT	**0.0285**
	PSISAT	**0.04**
	DKSAT	**$1.41*10^{-5}$**
	BEXP	**4.26**
	QUARTZ	**0.82**
Vegetation type	**Salt Cedar**	
	NROOT	**4**
	LAI	**5.0**
	Greenness fraction	**Seasonal**
	RSMIN	**150**
	Roughness length	**1.089**

LIS Runs Completed

MODEL: LISv4.3 == NOAH v2.7.1

1. LIS NLDAS: Using NLDAS forcing

2. LIS OBS: Using *In Situ* **forcing**

Initialized at 01/01/2004 (00Z)

Forcing Comparison

Selected experiment site at Sevilleta, NM

LAT: 34.265^{o}N

LON: 106.858^{o}W

Observation time interval: 30 min

Results: Heat Flux

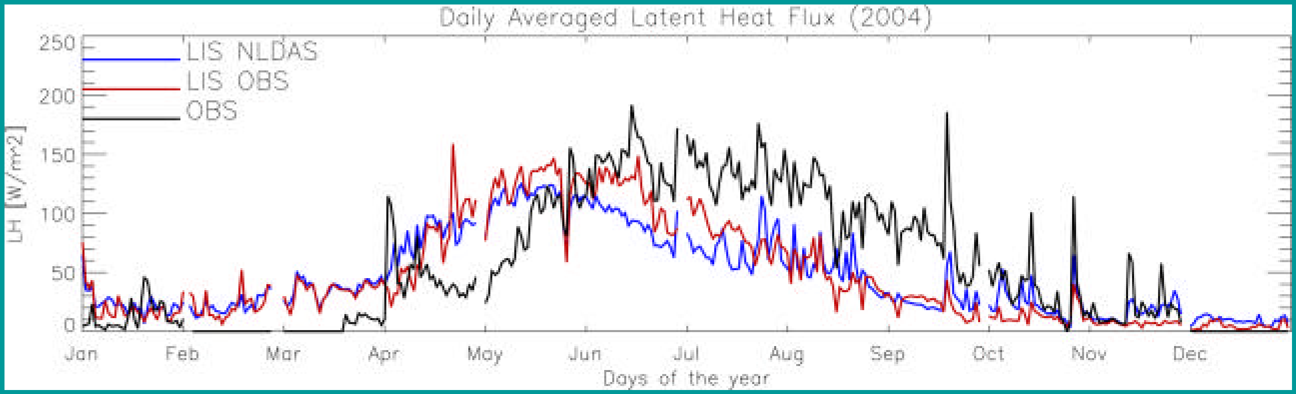

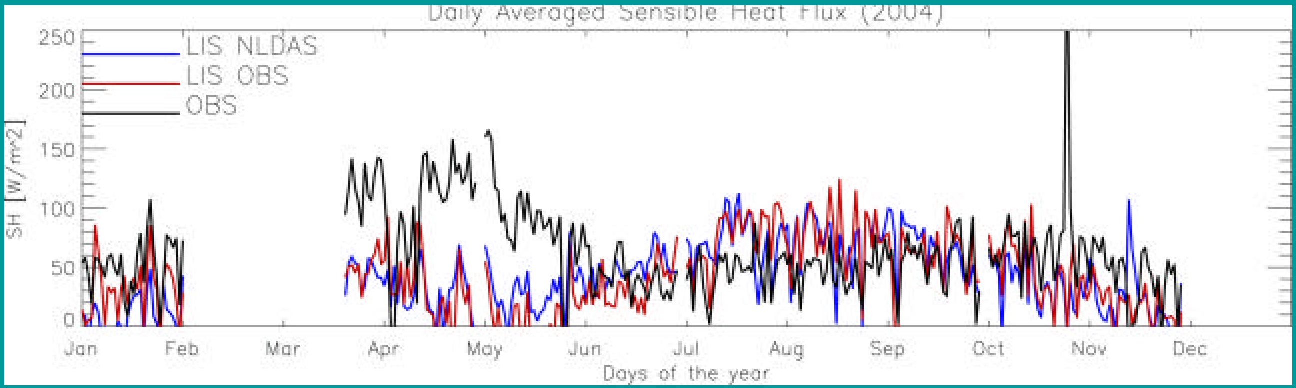

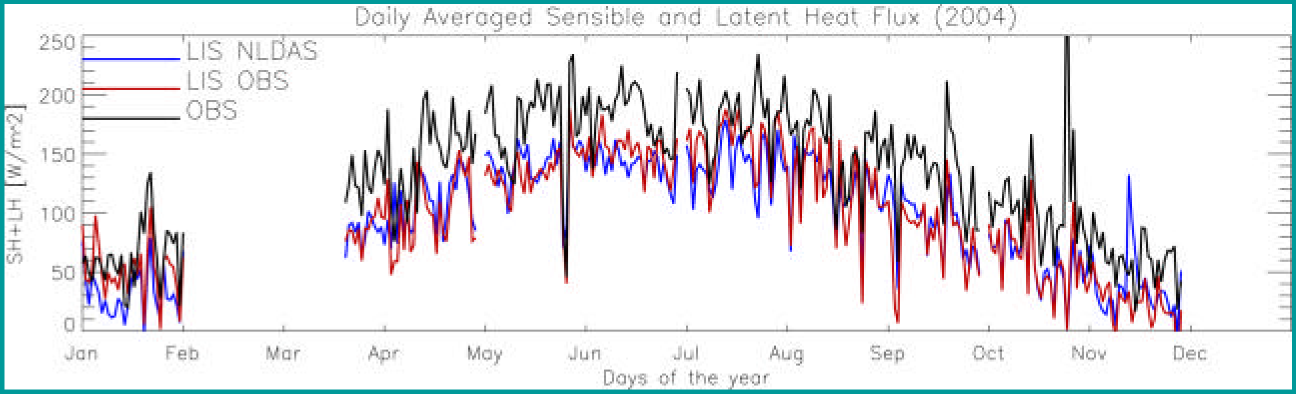

Results: Soil Moisture

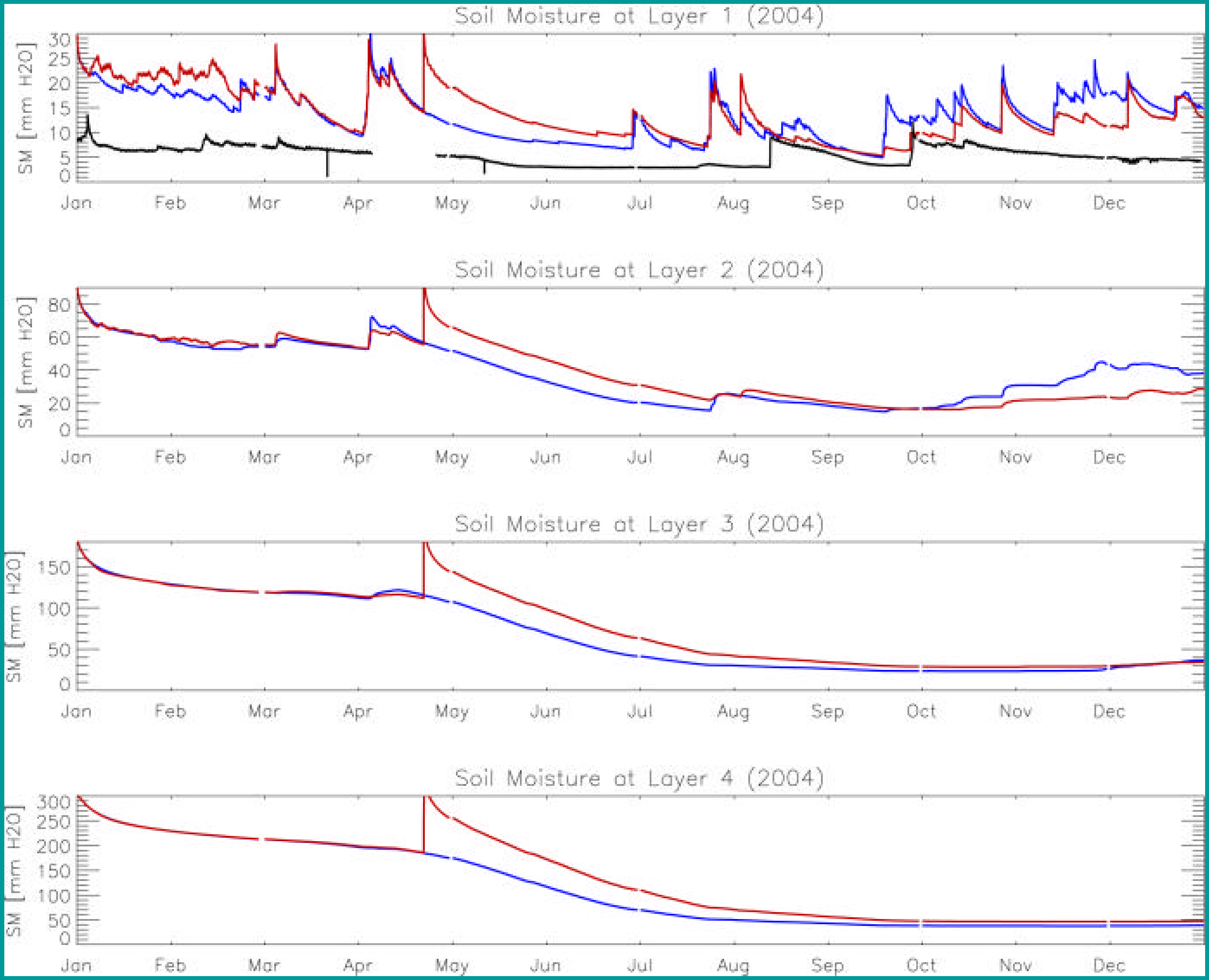

Results: Precipitation vs. ET

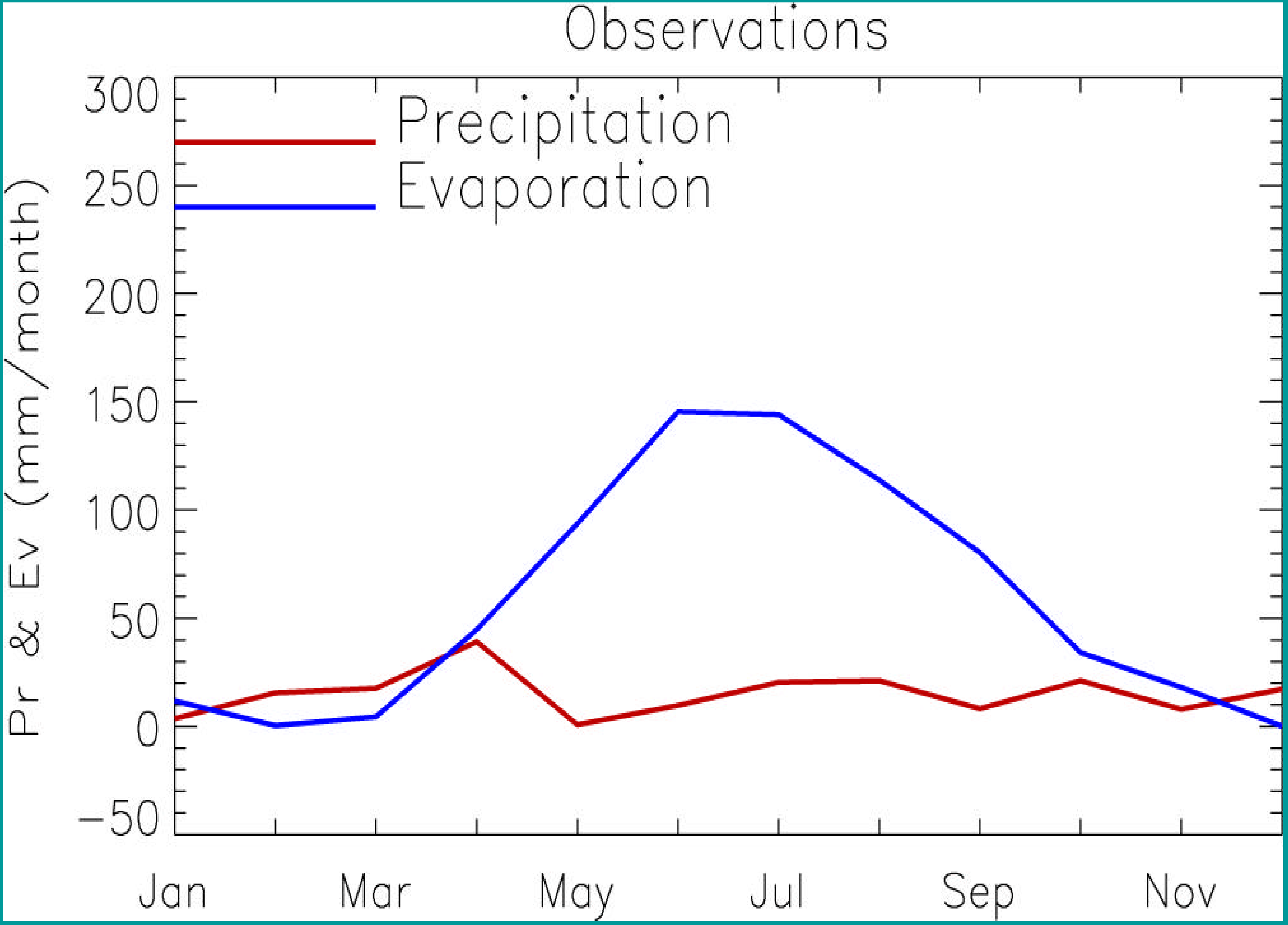

Future Studies

- Continue with specialized land cover cases
  - Irrigation
  - Riparian
  - Bare soil
- Parameter Sensitivity studies

Acknowledgements:

- Kristi Arsenault –UMBC Code 614.3 Code Goddess
- Jairui Dong- UMBC Code 614.3
- David Toll - GSFC Code 614.3
- Erik Jensen – Pacific University
- James Cleverly – University of New Mexico
- Per Gloersen – Summer Institute Program Director
- Valerie Casasanto - Summer Institute Program Manager

Questions?

GRACE Validation and Analysis

Erik Jensen

Mentor: Matthew Rodell

Overview

- About GRACE (Gravity Recovery and Climate Experiment)
- Comparing GRACE with ground based observations in Arizona
- Using data from NOAH model
- Finding the Chari River Watershed
- Looking at GRACE data for the upper regions

About GRACE

- Water is an important resource
- Can be hard to measure *In Situ*
- GRACE measures remotely by analyzing changes in Earth's magnetic field

- Detected through the changing distance between two satellites

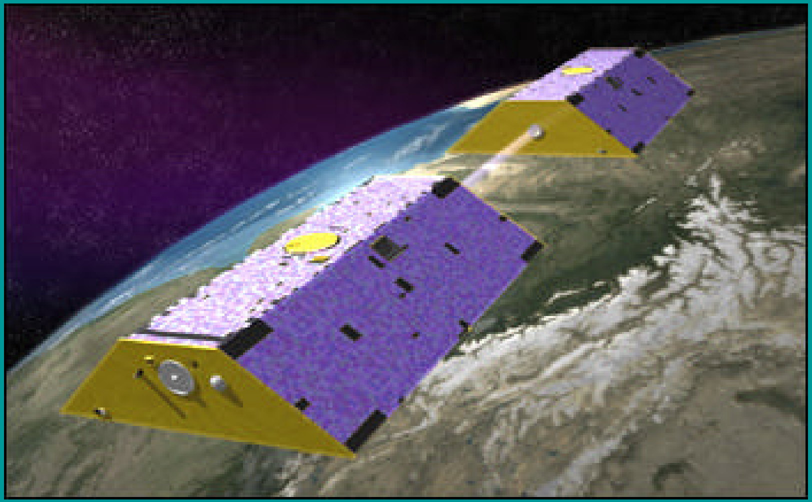

Extracting GRACE Data

- Locate *In Situ* stations
- Generate one degree resolution mask
- Use GrADS to average values over the area

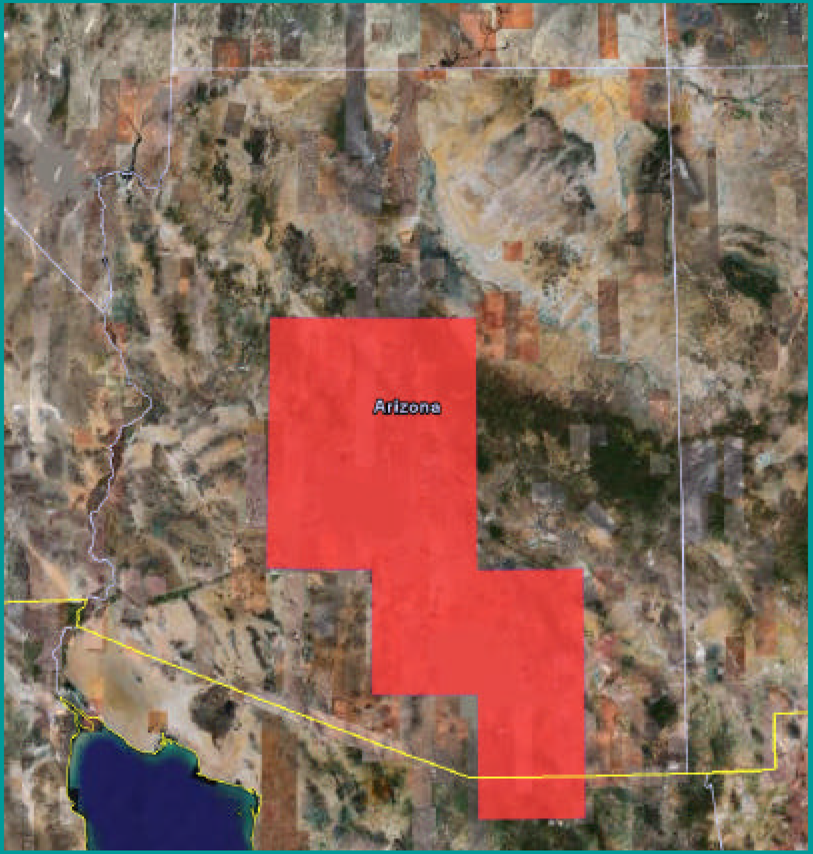

Result

- Limited agreement
- Sparse In Situ data

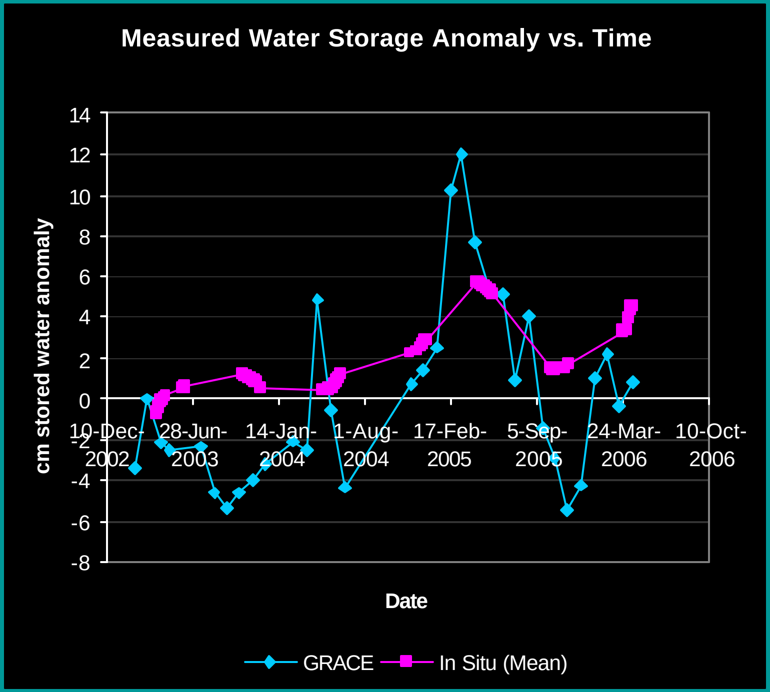

NOAH Model

- Looked at total soil moisture from model
- Shows fairly good correlation

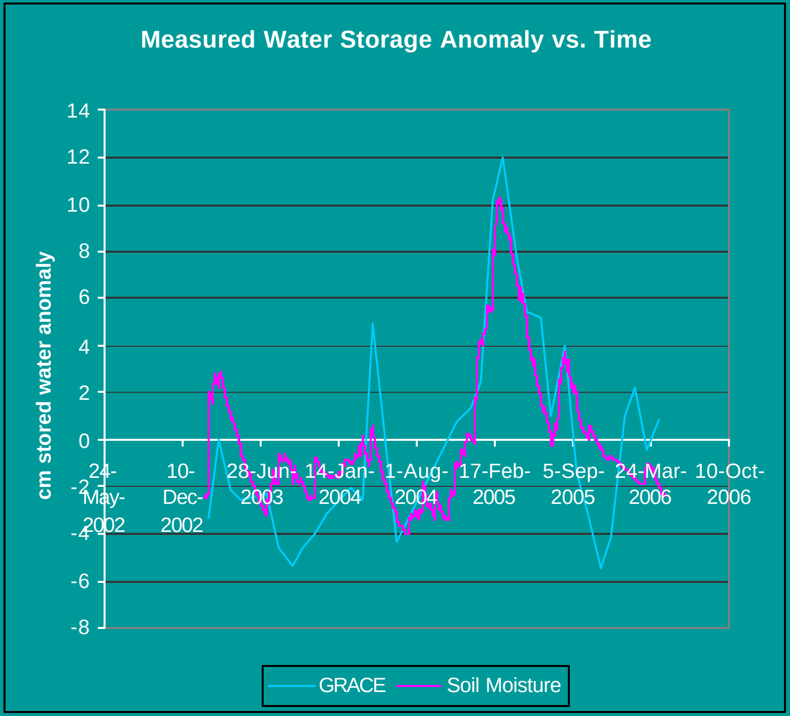

Chari River Watershed

- Used HYDRO1k flow direction data
- Used flow directions to determine the area of the watershed
- Reduced resolution to one degree mask
- Focused on upper regions

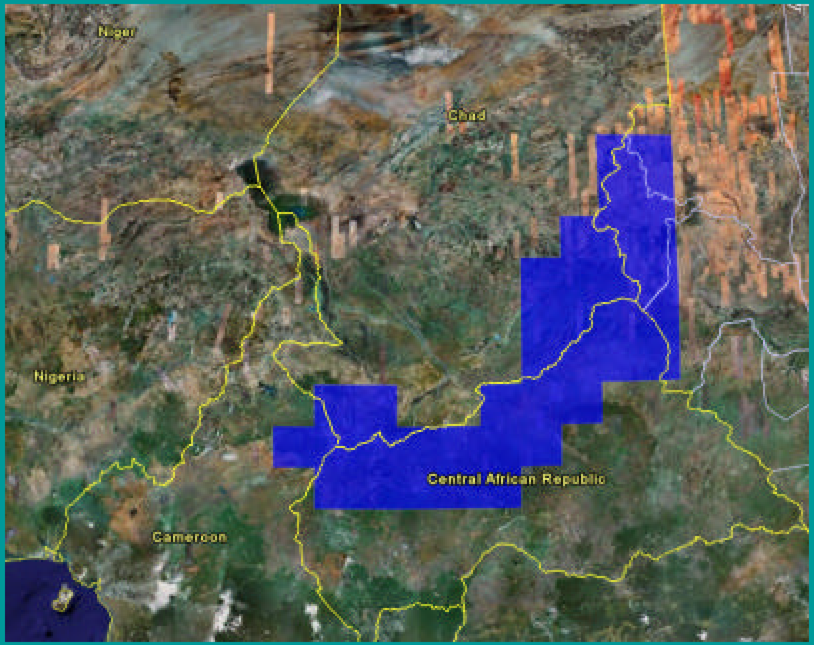

Comparing with NOAH Model

- Extracted Soil Moisture and GRACE data using the mask
- Again showed good correlation
- Second peak missed due to missing data

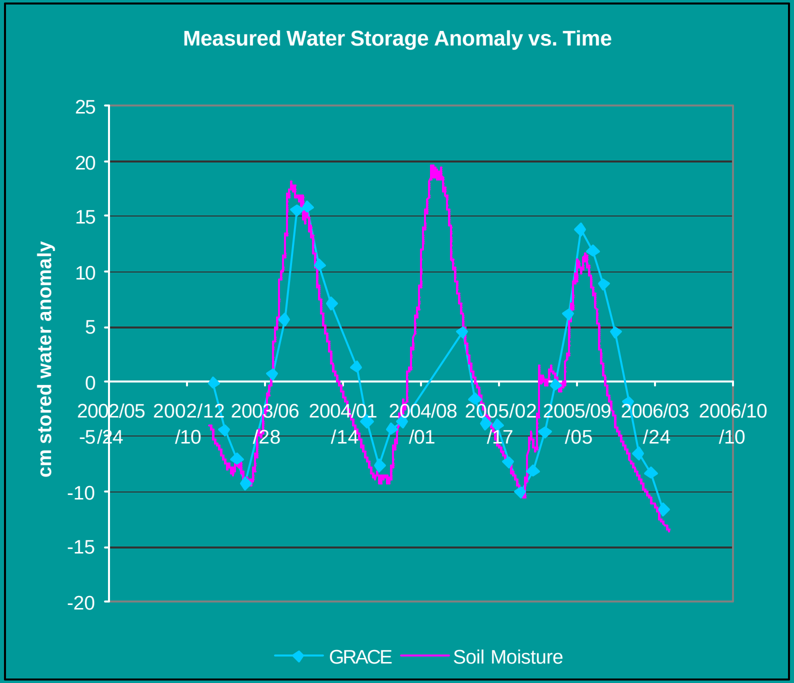

Future Work

- Continue looking at correlations for various measurements in Arizona, including soil moisture and well levels, and taking possible lag into consideration
- Analyze correlations between the water present in the upper Chari River watershed and the amount of water available in Lake Chad, determining the lag time between the two measurements

Acknowledgements

- Matt Rodell – Mentor
- Charon Birkett – Information about Lake Chad Region
- Hiroko Kato – NOAH Model
- Don Pool – In Situ Gravity Data for Arizona
- ODIN – A less than adequate computer

Hurricane Intensity and Ocean Vertical Structure

Lisha M. Roubert Rodriguez
University of Puerto Rico
NASA GSFC Summer Institute 2007

Mentor: Dr. Paolo de Matthaeis
Code 614.6 - Instrumentation Sciences Branch
NASA Goddard Space Flight Center

Outline

- Introduction
- Instrumentation and Data
- Data Analysis
- Results
- Conclusions

Introduction

- Hurricanes strengthen or weaken depending on the ocean upper layer temperature and thickness

  ? knowledge of ocean vertical structure is crucial.
- In-situ and satellite measurements were taken in order to calculate the upper ocean heat content.
- The data were taken in the Gulf of Mexico during the months of August and October of 1999 and 2000.
- Our objective is to determine the reliability of the results obtained from the satellite data by comparing them to the results obtained with the measured data.

Instrumentation and data:
In-Situ measurements

- Expendable conductivity temperature and depth profiler (XCTD)
  - ? temperature and salinity at different depths
- Expendable Bathythermograph (XBT) and Expendable Current Profiler (XCP)
  - ? XBTs only temperature
  - ? XCPs temperatures and currents

(All Data collected in the Gulf of Mexico. Source: Dr. S. Daniel Jacob, Code 614.6)

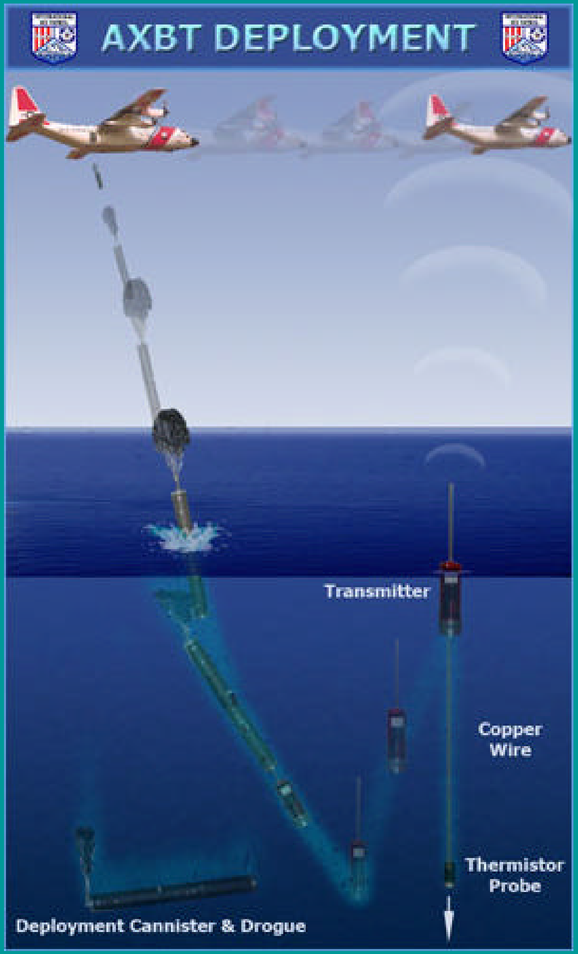

Instrumentation and data: Satellite data

- TOPEX/POSEIDON? Radar Altimeter

  Sea Surface Height (Accuracy ~ 5cm)

- Advanced Very High ? Resolution Radiometer (AVHRR)

  Sea Surface Temperature (1-km spatial resolution)

Vertical ocean structure model

- 2-layer model

? allows estimate of Q from satellite data (Reference: Shay et al. 2000)

- N-layer model

? temperature profiles can be used to refine the estimation of Q from satellite data

2-layer model

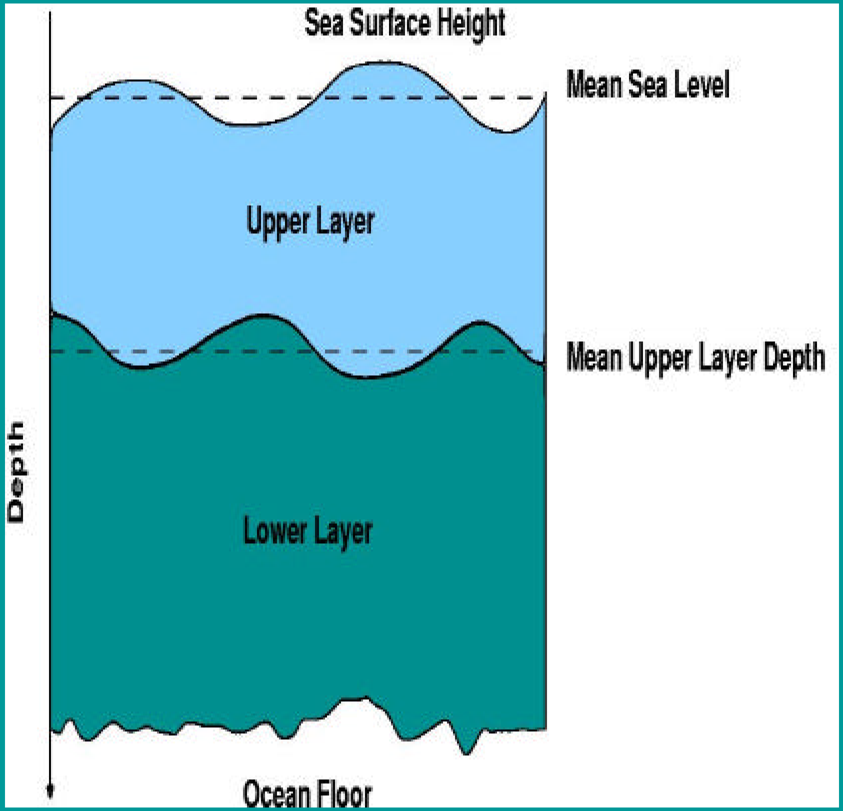

DATA ANALYSIS

1) XCTD temperature and salinity profiles are used to find salinity-temperature relationship.

Temperature and Salinity profiles

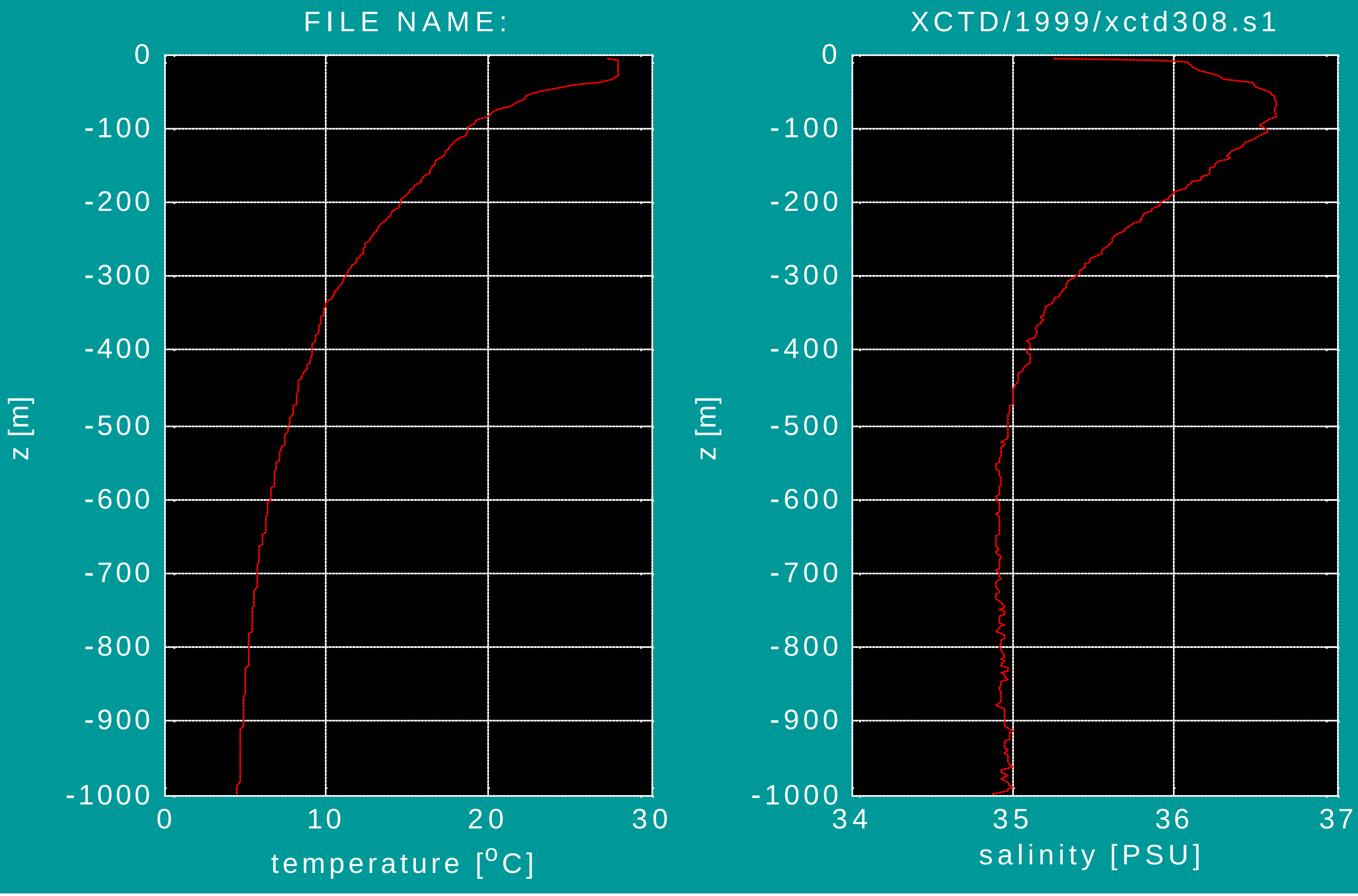

Ocean Upper Layer

- Salinity vs. temperature plots were used to study the ocean mixed layer and discriminate between areas of shallow upper layers (SUL) and deep upper layers (DUL).

- Above 20°C the SUL tends to maintain a relatively constant salinity value, as opposed to the DUL where the salinity value increases and then drops when the water temperature reaches approximately 23°C.

26°C isotherm and ocean upper layer

- Temperature profiles were used to determine depth of the 26°C isotherm d_{26}
- d_{26} was used to discriminate between SUL and DUL:

$d_{26} \geq 100$m ? DUL

$d_{26} < 100$m ? SUL

Temperature-Salinity Relationship

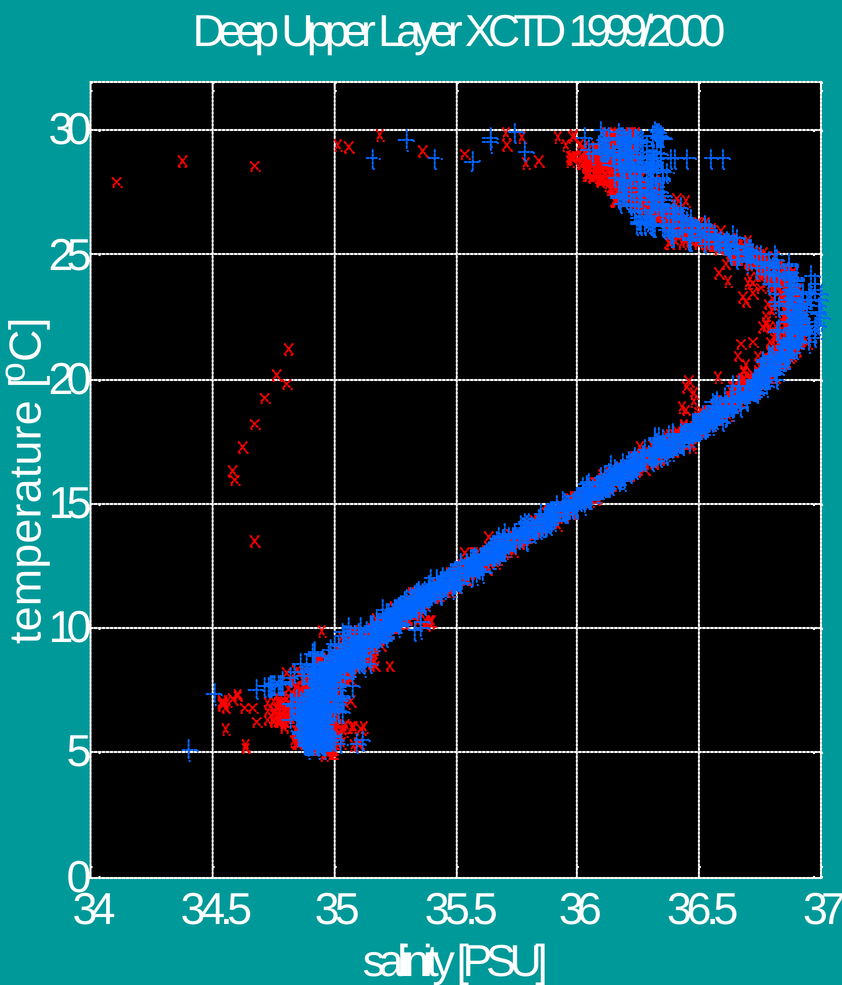

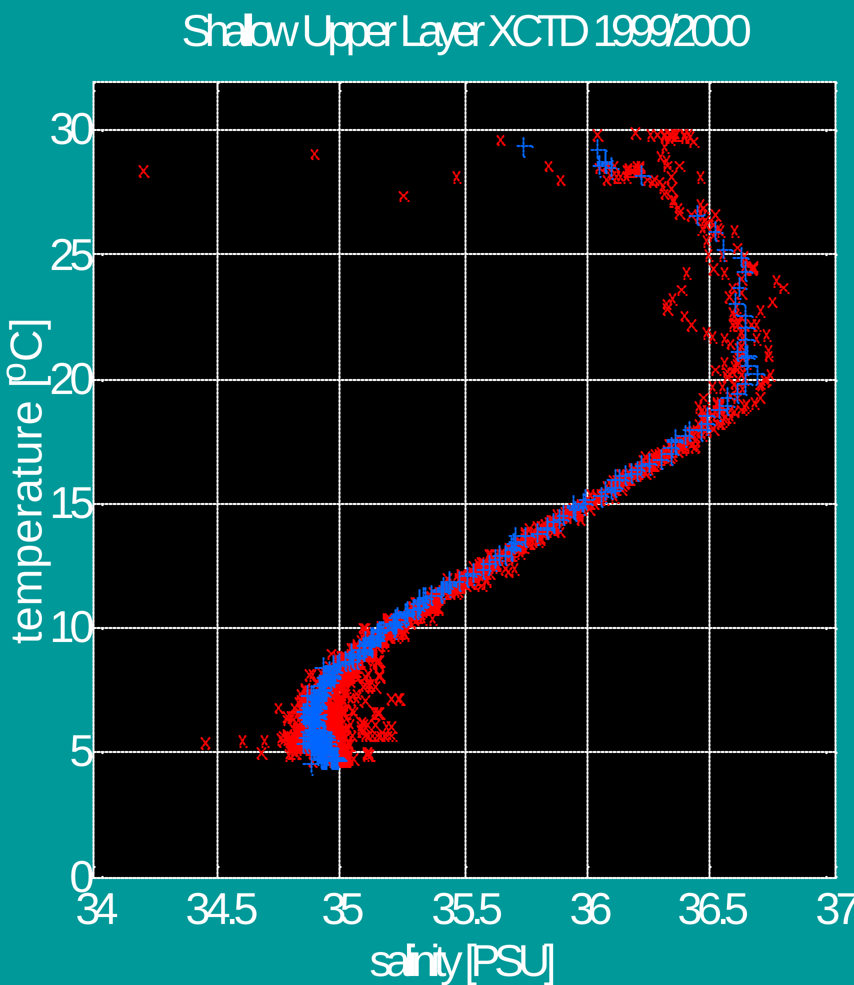

DATA ANALYSIS

1. XCTD temperature and salinity profiles are used to find salinity-temperature relationship
2. salinity-temperature relationship is used to derive salinity for XBT and XCP data

Salinity Estimate

- Unlike XCTD probes , XBT and XCP probes do not provide salinity values.

- A fitting technique was applied to XCTD probes data to determine salinity for XBT and XCP probes in the two distinct SUL and DUL cases, using a 9th order polynomial regression:

$$S = S_n\ p_n\,[(T-T_m)/s_T]^n$$

where

S = estimated salinity

p_n = coefficients determined for SUL or DUL

T = temperature

T_m = mean temperature

s_T = temperature standard deviation

- In order to verify reliability of results, salinity vs. temperature plots of the XCTD profiles were compared to corresponding XBT and XCP plots taken in close proximity.

Salinity Estimate: Fitting Technique

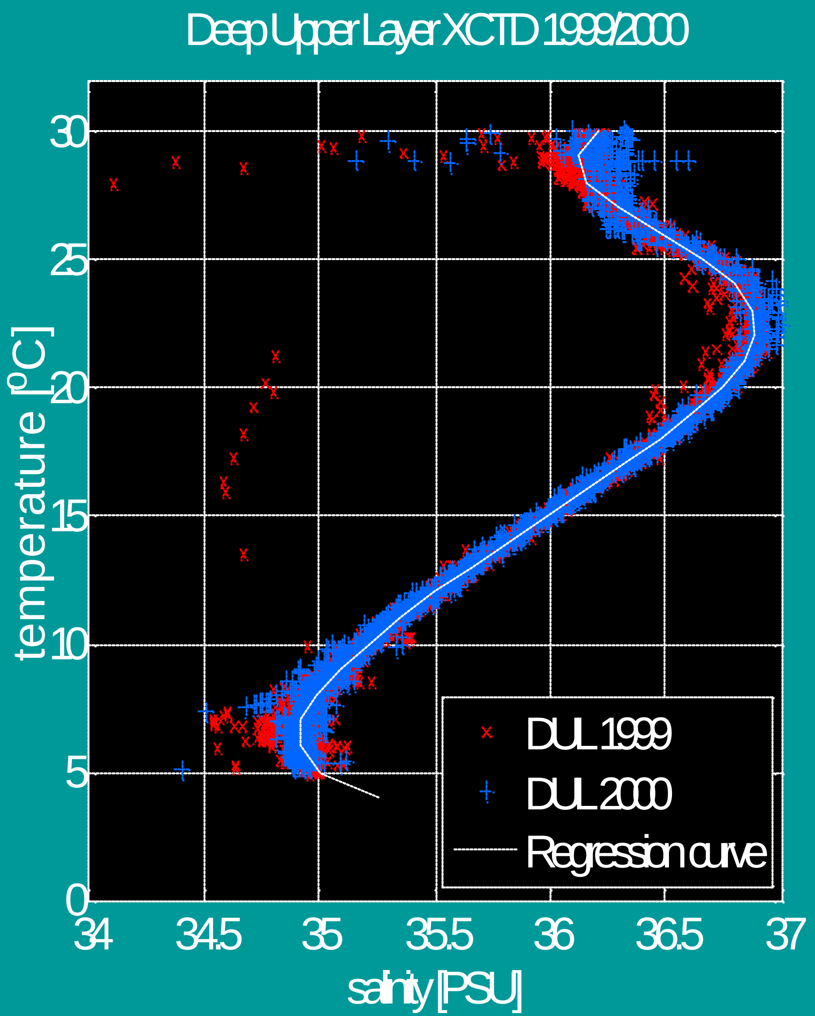

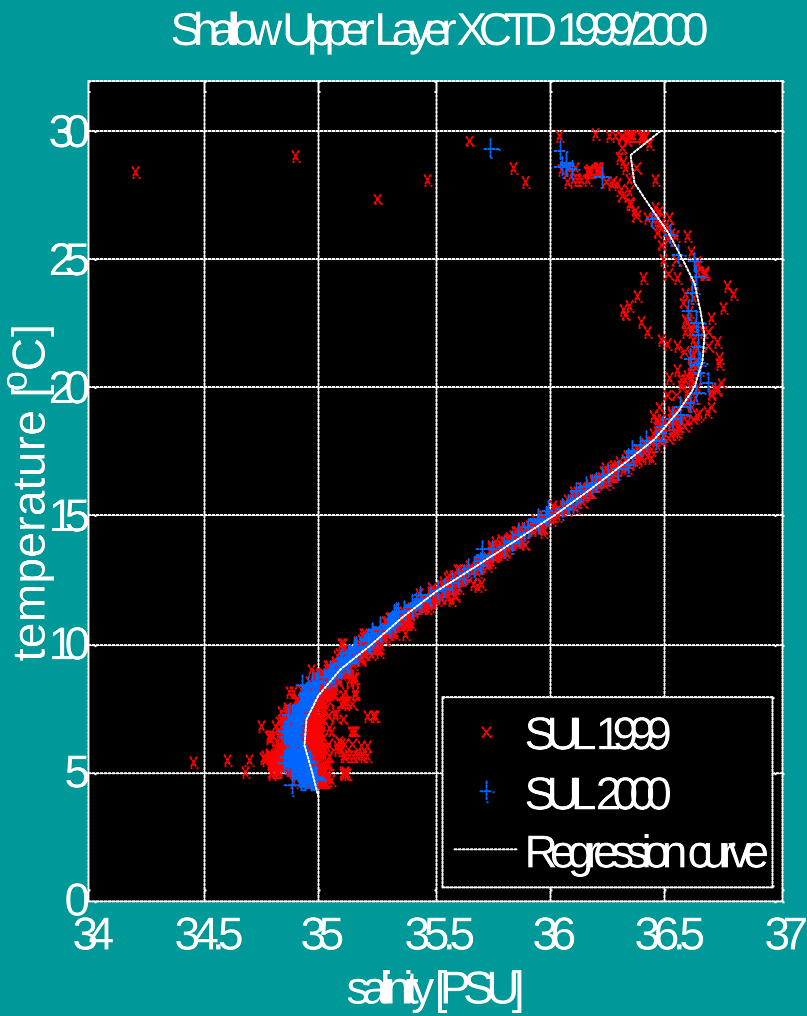

Salinity estimate: validation

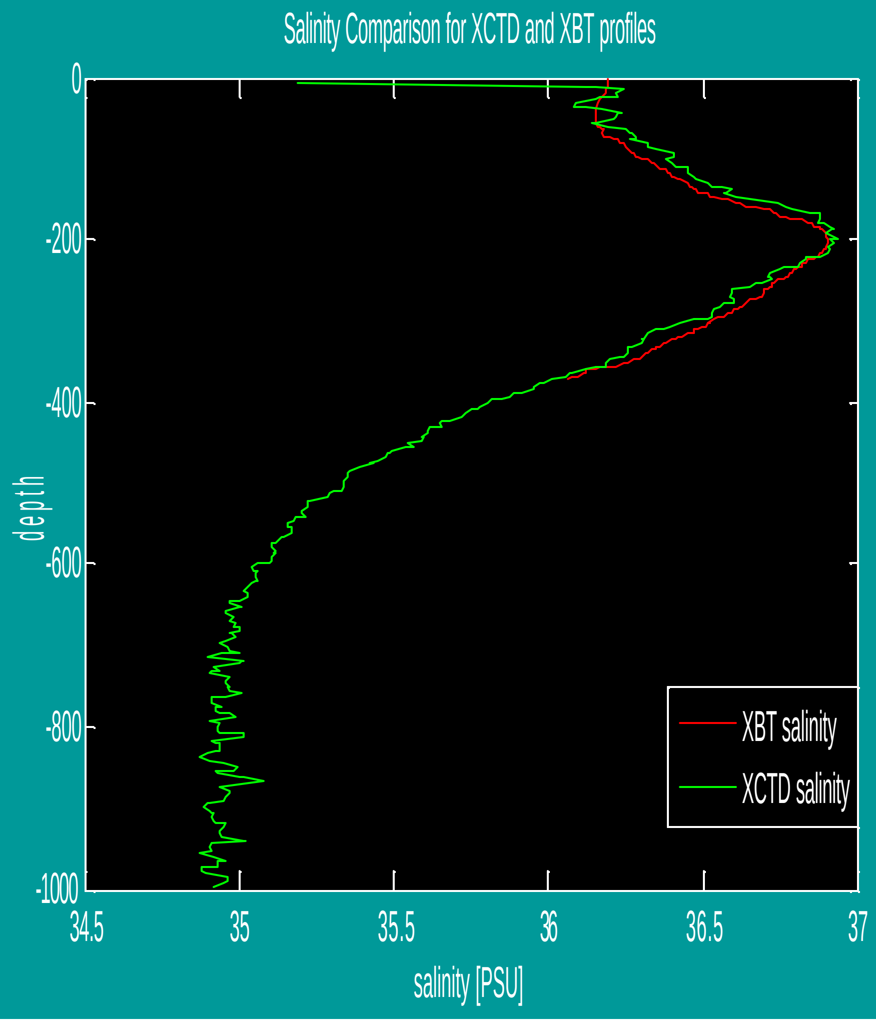

- XCTD profile:
  latitude -90.350
  longitude 27.433
- XBT profile:
  latitude -89.683
  longitude 27.367

DATA ANALYSIS

1. XCTD temperature and salinity profiles are used to find salinity-temperature relationship
2. salinity-temperature relationship is used to derive salinity for XBT and XCP data
3. Ocean water density is computed

OCEAN WATER DENSITY

- Ocean water density is derived from temperature and salinity using the equation of state which is defined as:

$$?(S, t, p) = \frac{?(S, t, 0)}{1 - p / K(S, t, p)}$$

$?$=density [kg/m^3] S=salinity [PSU]

t=temperature [°C] p=pressure [bars]

DATA ANALYSIS

1. XCTD temperature and salinity profiles are used to find salinity-temperature relationship
2. salinity-temperature relationship is used to derive salinity for XBT and XCP data
3. Ocean water density is computed
4. Upper layer heat content Q is calculated

Heat content

$$Q = C_p \,?_{0}^{d_{26}} ?(z)\,[\,T\,(z)–26\,]\,dz$$

Q=Heat Content [MJ/m^2] ?=density [kg/m^{3}] Z=depth [m]

C_p=Specific Heat [MJ°C^{-1}/kg] T=temperature [°C] d_{26}=26° isotherm [m]

- This equation was used to determine the Upper Ocean Heat Content Q from the measured data.
- Salinity vs. depth plots were used to compare both results in order to determine the reliability of the data provided by the TOPEX and AVHRR satellites.

DATA ANALYSIS

1. XCTD temperature and salinity profiles are used to find salinity-temperature relationship
2. salinity-temperature relationship is used to derive salinity for XBT and XCP data
3. Ocean water density is computed
4. Upper layer heat content Q is calculated
5. Comparison with satellite Q using 2-layer model

Heat content from satellite data

- 26°C isotherm d_{26} is determined from altimeter data

- Heat content is estimated using 2-layer model:

$$Q = C_p \, ?_0 \, G \, (d_{26})^2$$

where

- $?_0$ *= average oceanic density =1026 g/cm*^{3}
- G = water temperature gradient from AVHRR sea surface temperature and historic hydrographic data

Heat Content:

comparison in-situ / satellite data

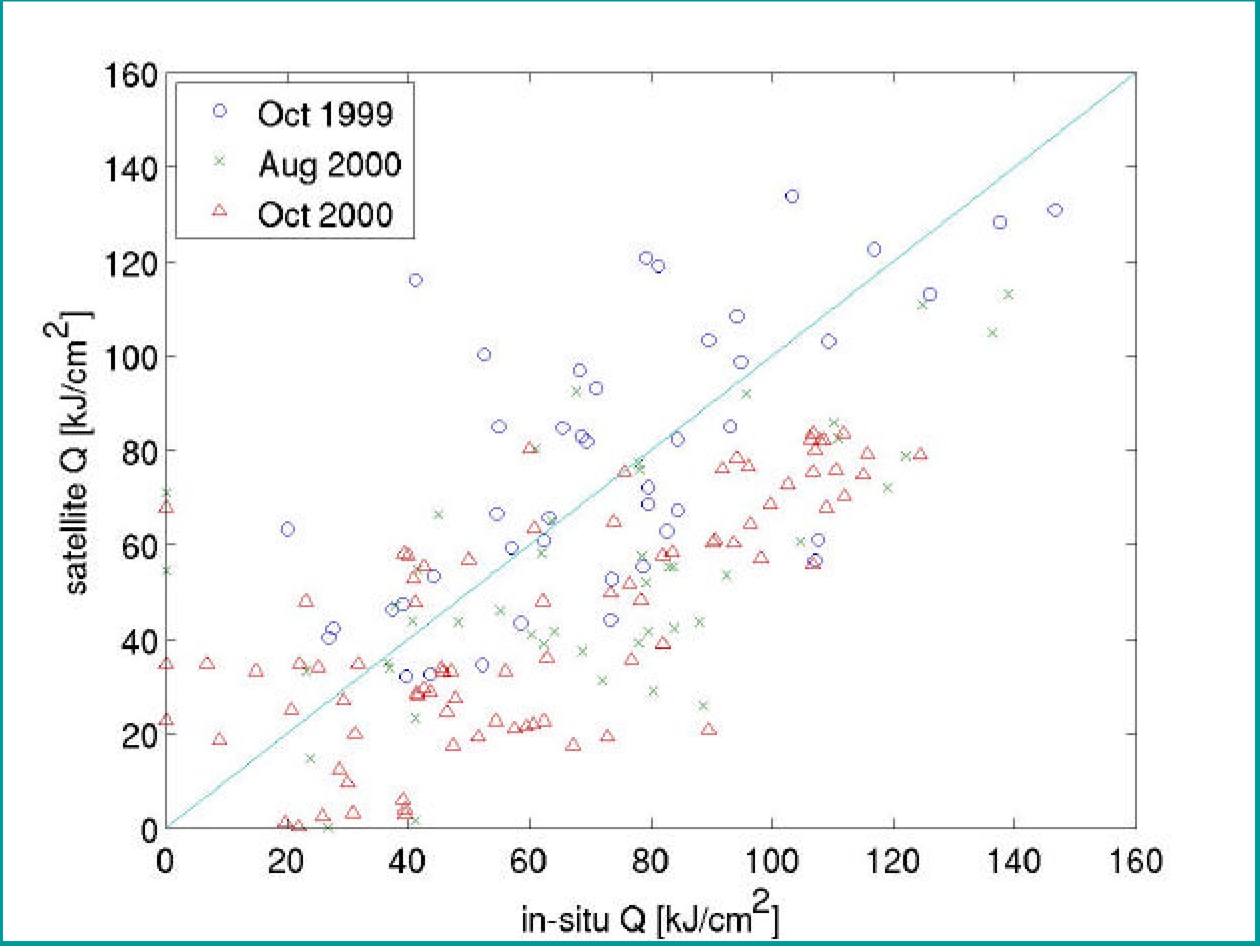

26°C Isotherm:

comparison in-situ / satellite data

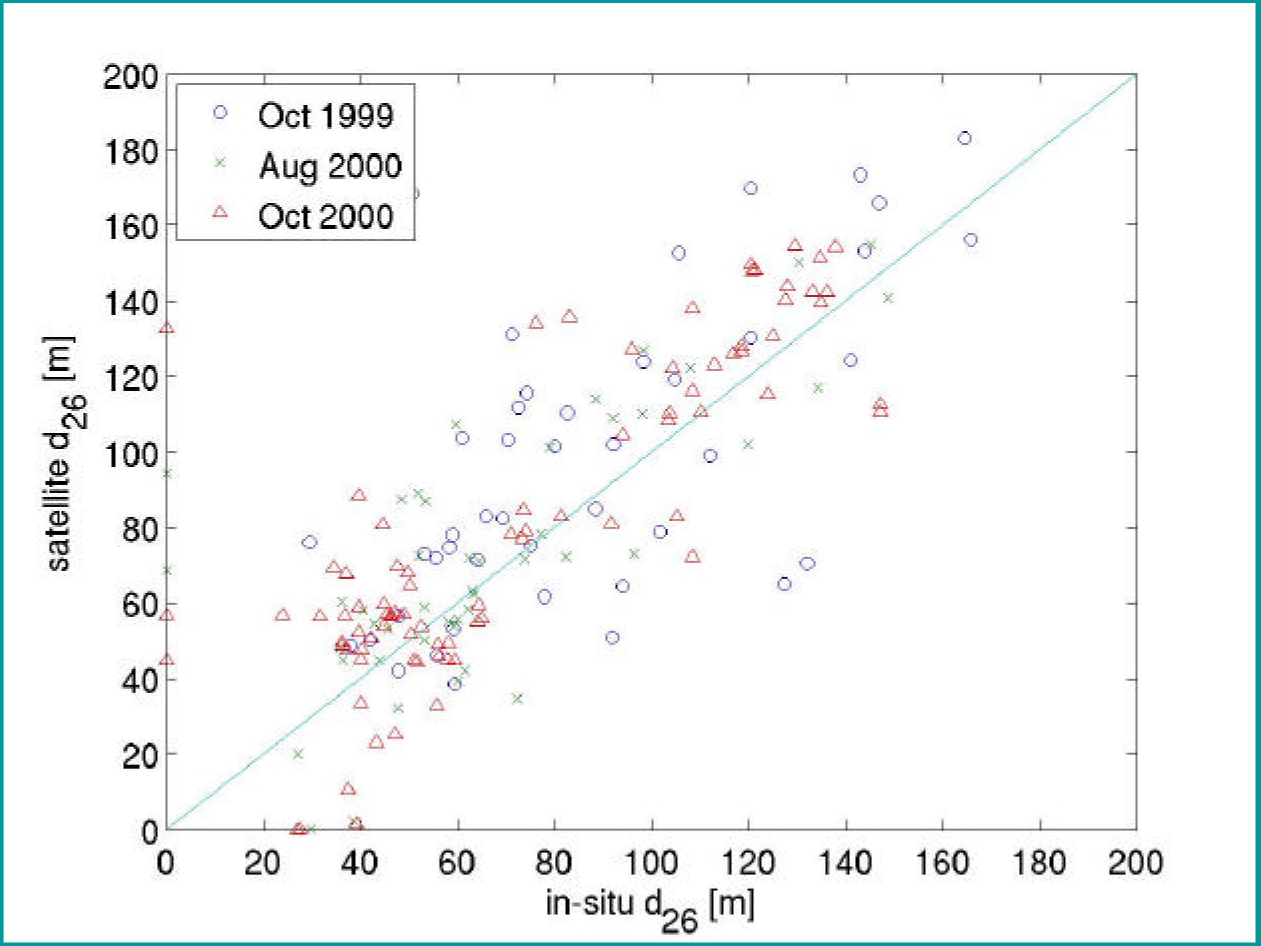

Q COMPARISON
in situ / satellite

October 1999

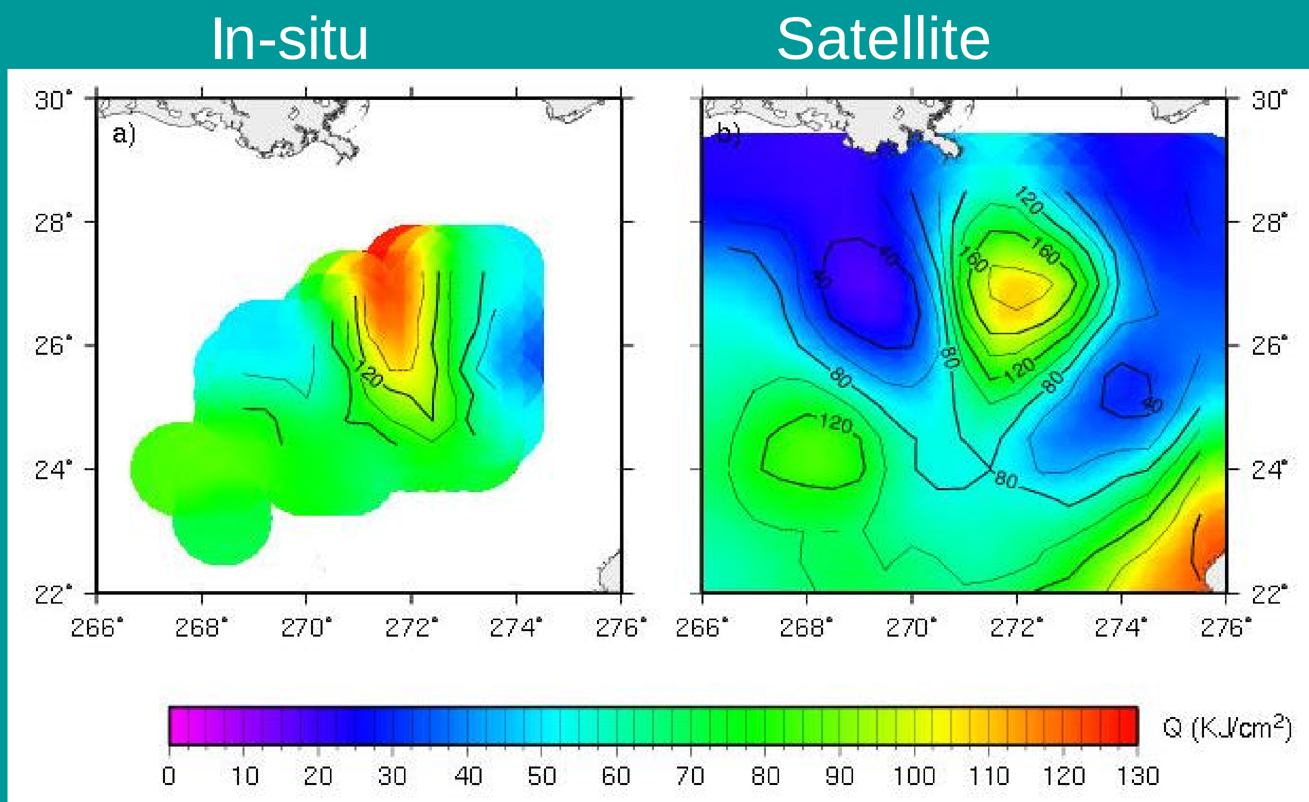

Q COMPARISON
in situ / satellite

August 2000

In-situ Satellite

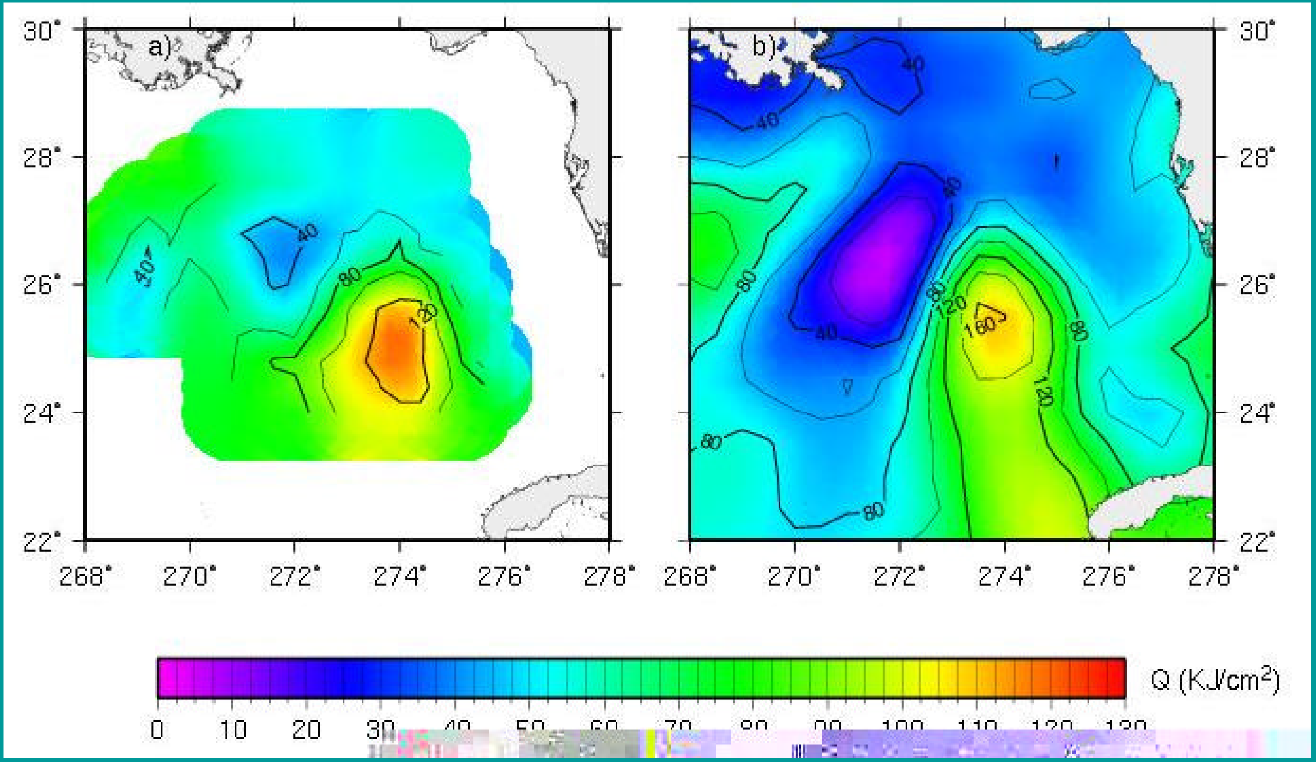

Q COMPARISON
in situ / satellite

October 2000

In-situ Satellite

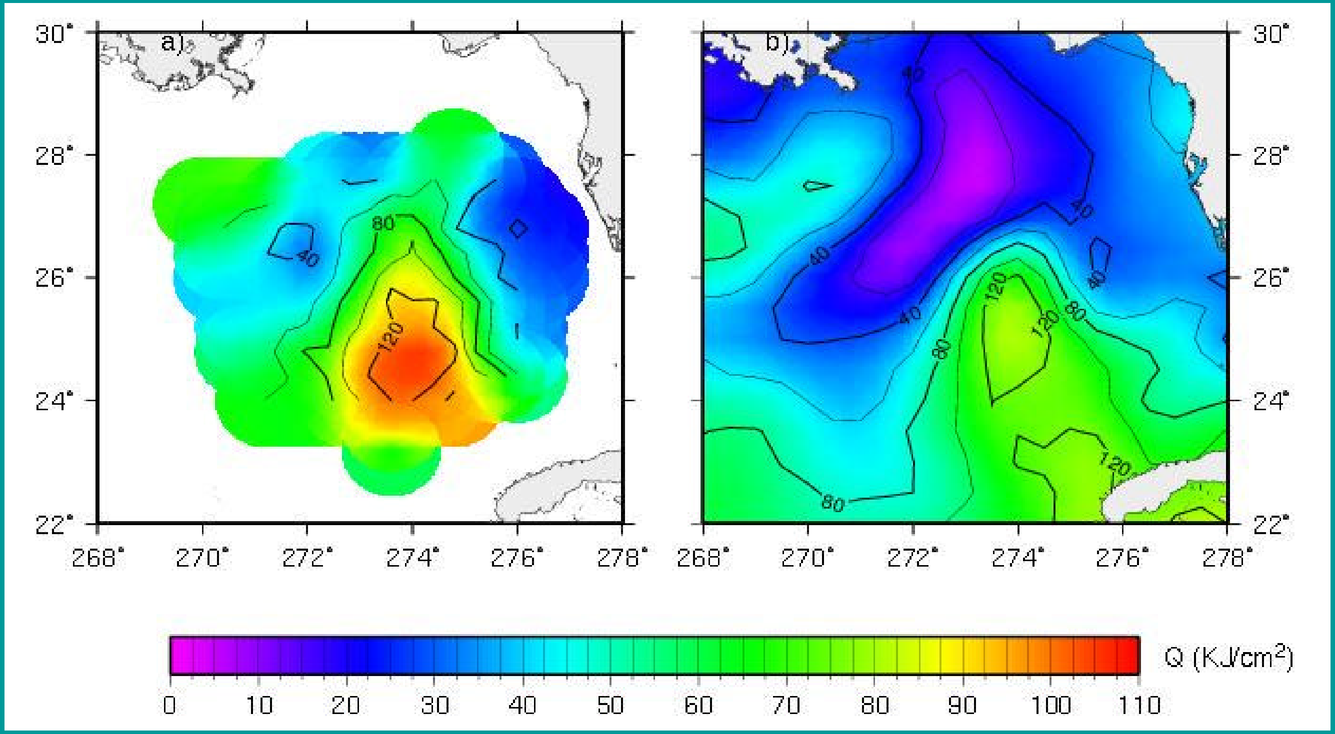

Conclusions

- Temperature and salinity profiles have been used to calculate 26°C isotherm d_{26} and upper ocean heat content Q
- Satellite data has been used to estimate Q with 2-layer model
- Satellite is underestimating heat content Q and slightly overestimating d_{26}
- 2-layer model is not satisfactory

  ? need to develop N-layer model

Acknowledgements

- Paolo de Matthaeis
- S. Daniel Jacob

  for his assistance with Data and Methodology
- David M. Le Vine, Emmanuel P. Dinnat and Saji Abraham

  for their useful advice and suggestions
- Per Gloersen
- Valerie Casasanto
- SI students

Modeled and Microwave Observations of Variation of Snow Depth on Greenland

Ashley Welty

North Carolina State University

Mentor: Dr. Per Gloersen

Goddard Space Flight Center

Greenland

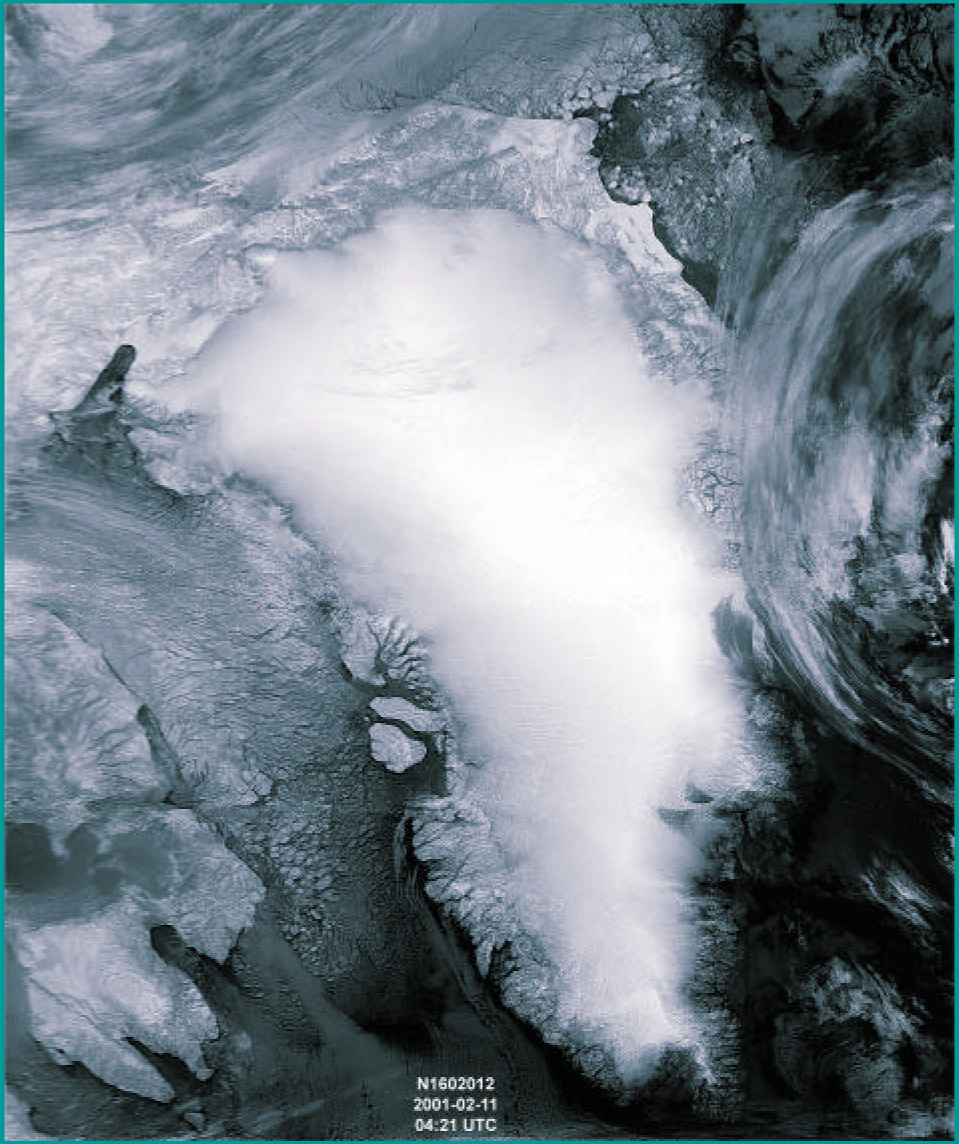

Data

- Dr. Edward Hanna created snow accumulation data that was sent to us.
- He used data from ERA-40 reanalysis.
  - time series of data that were generated by a weather prediction model run
- His data were validated by ice core accumulation datasets

Satellite Aqua

AMSR-E

Advanced Microwave Scanning Radiometer for EOS

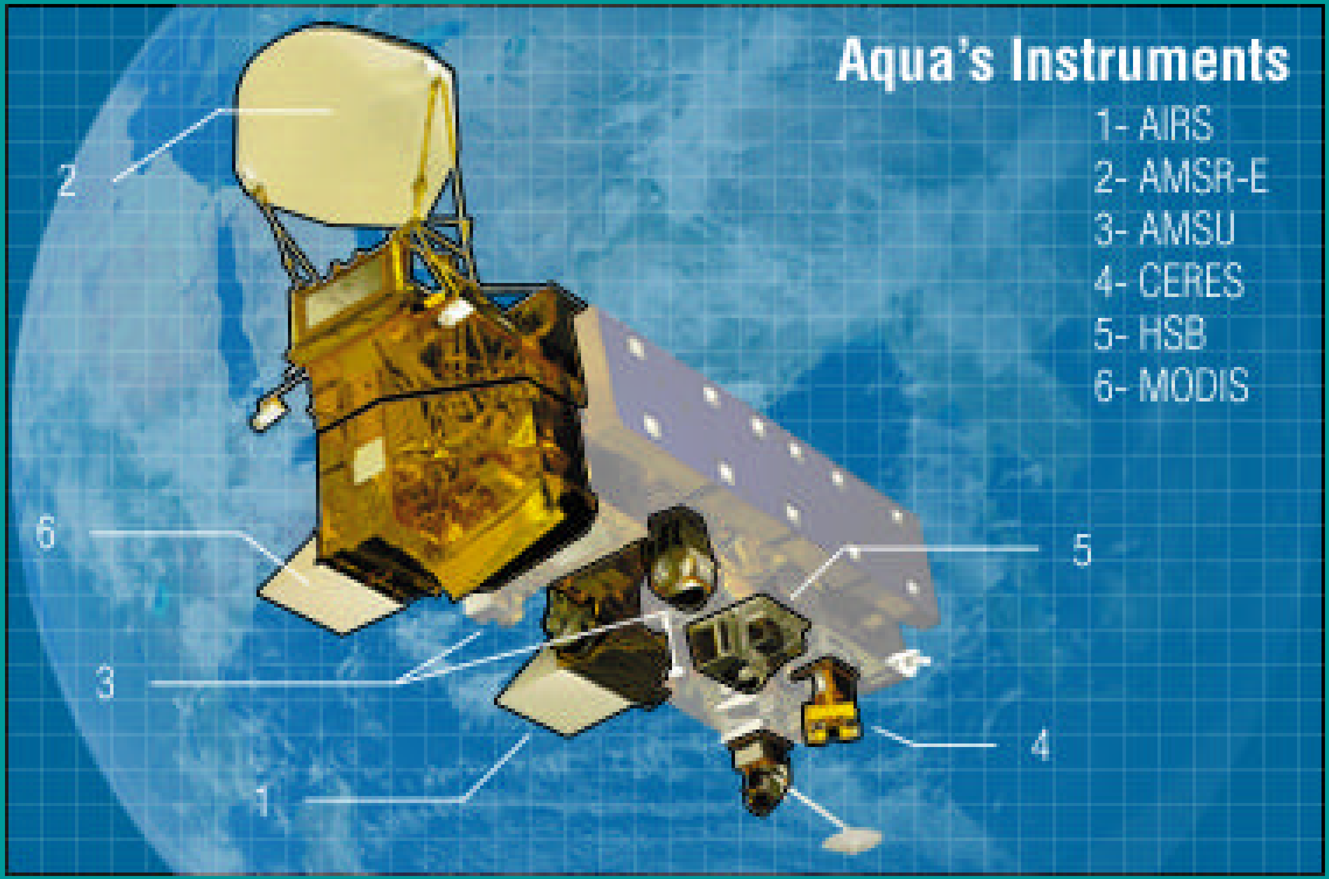

Why These Comparisons are Being Made

- Looked for consistency of Dr. Edward Hanna’s data
- Checked his interpolation scheme with that of microwave data

Dr. Hannah's Data

First Comparison

- Created MATLAB programs
- Had to discard about 2/3 of data
- Created data sets with 19GHz and 37GHz spectral brightness temperatures
- Compared snow accumulation and spectral gradient ratio

Results From Comparison of Snow Accumulation and Spectral Gradient Ratio with 19/37 GHz

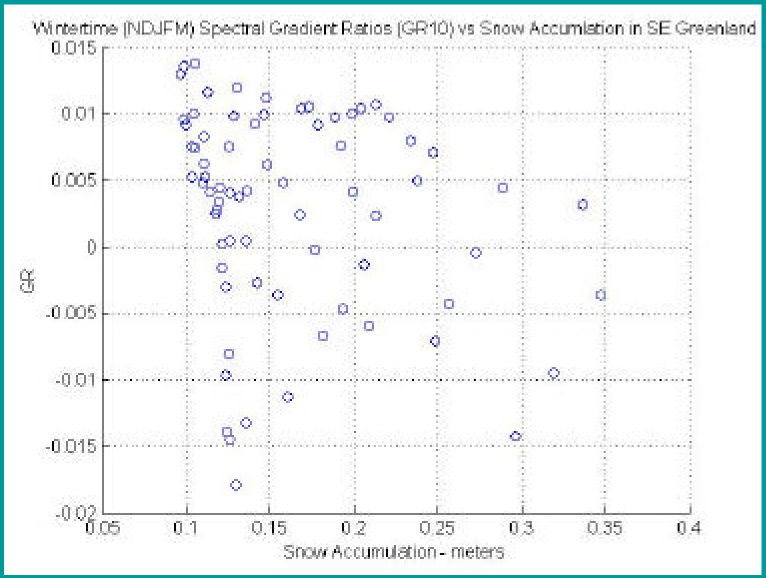

October 2003 – March 2004

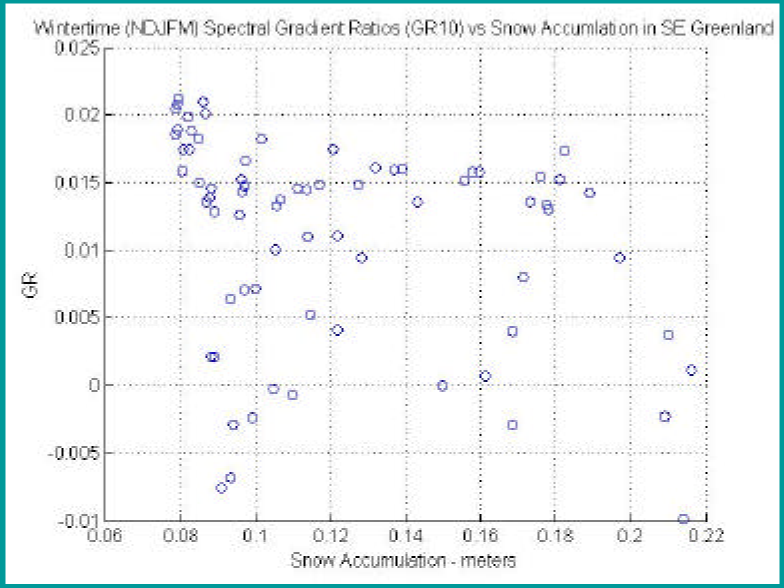

October 2004 – March 2005

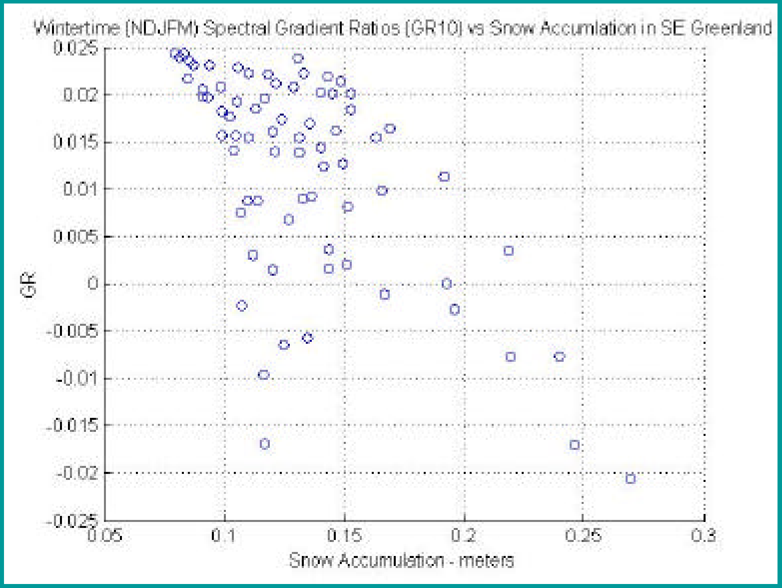

October 2005 – March 2006

Dr. Hanna’s Data

Second Comparison

- Used Dr. Hanna’s snow accumulation data again
- Created MATLAB programs
- Created data sets with 10GHz and 19GHz spectral brightness temperatures
- Compared snow accumulation and spectral gradient ratio

Results From Comparison of Snow Accumulation and Spectral Gradient Ratio with 10/19 GHz

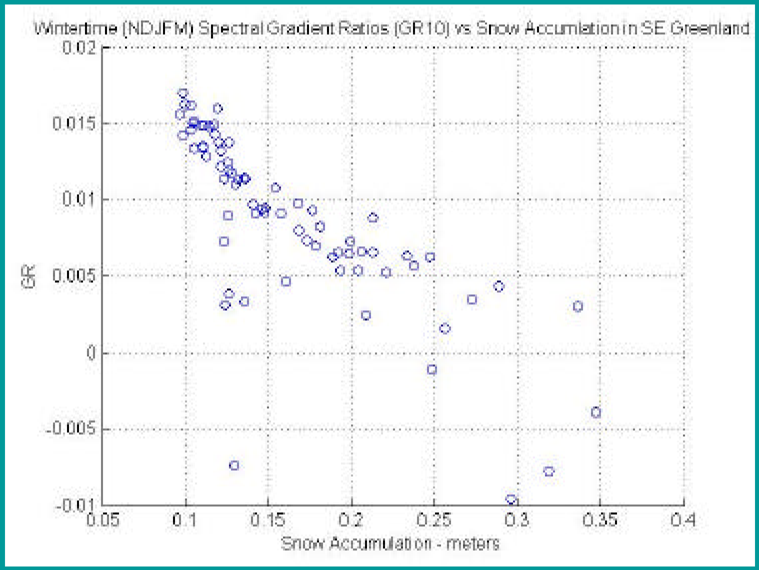

October 2003 – March 2004

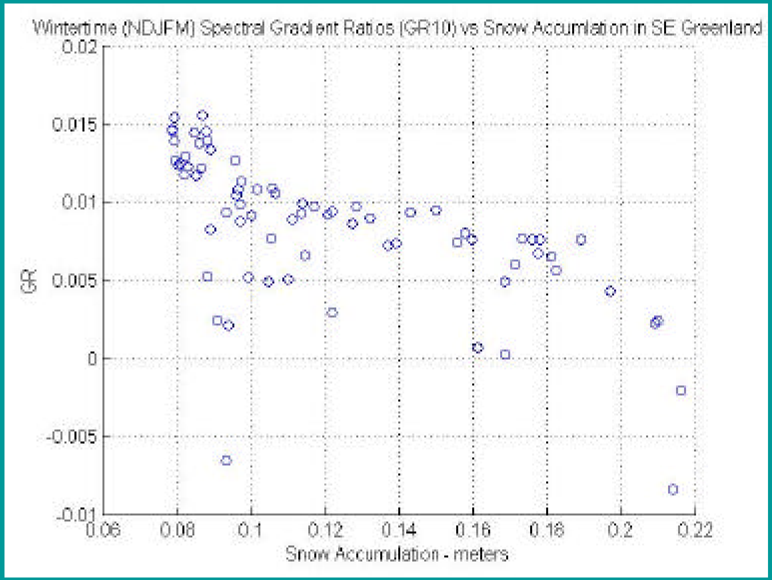

October 2004 – March 2005

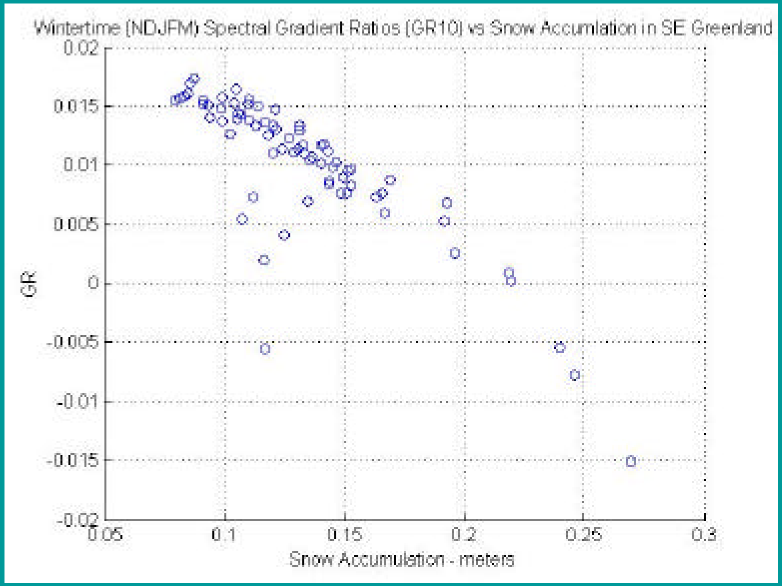

October 2005 – March 2006

Next Step

- Use altimeter data from ICESat/GLAS instrument and compare the data to the snow accumulation data from Dr. Hanna

Geoscience Laser Altimeter System

Conclusions

Unfortunately there were no definite conclusions that could be made due to different reasons such as:

a. We were not able to compare snow accumulation data with altimeter data from ICESat.

b. The data was limited to southeastern Greenland.

References

- Hanna, E., J. McConnell, S. Das, J. Cappelen & A. Stephens (2006) Observed and modeled Greenland Ice Sheet snow accumulation, 1958-2003, and links with regional climate forcing. *Journal of Climate* 19, 244-358, doi: 10.1175/JCLI3615.1.

Thank You

Dr. Per Gloersen

Steve Fiegles

Kristine Barbieri